This document contains the responses to the referees' comment on the manuscript version 3, followed by a version 4 manuscript (starts in page 8). The reviewers' comments and questions are in bold. For each comment / question, the authors' reply / answer is in black, and the corresponding modifications in the manuscript version 3 are marked in blue colour. The line index mentioned in the response correspond to the line number in manuscript version 4 (without markups)

(1) Author's response to Anonymous Referee #1

Thank you very much for your comments. The following are the responses to your specific comments.

Summary

This manuscript uses a case study to illustrate the derivation of the aerosol single scattering albedo (SSA) using observations from the OMI sensor of a large biomass-burning event in south Chile in 2017.
UV remote sensing of aerosols has not received the same level of attention as other sensors (such as MODIS/VIIRS) and studies like this one are a welcome addition to the general body of knowledge regarding the measurement of aerosol absorption from space. The paper is well laid out and its novelty resides in the combination of sensors utilized, its focus on single scattering albedo and aerosol height retrievals (as opposed to AOD and SSA) and its application using OMI observations. Overall, I think this paper can be published in its present form after some clarifications and corrections are included (mostly technicallso, I second the Editor's comments that the Satheesh et al and the Gassó and Torres papers should be consider in this analysis plus the lack of mentioning of the recent SSA studies using OMI done by Jethva and Torres.

Thanks for your advice. We already have added the literatures you mentioned to the manuscript.

Satheesh et al. (2009) is referred at the following locations:
'But this aerosol absorption over near-UV is highly sensitive to the assumption on aerosol layer height. Satheesh et al. (2009) therefore used the τ from MODerate-resolution Imaging Spectroradiometer (MODIS), which is independent of aerosol layer height, to constrain the OMAERUV retrieval.' (Line 44-46)

'Besides, the MODIS retrieved τ is free from the uncertainty triggered by assumed aerosol profile (Satheesh et al., 2009).' (Line 193-194)

Gassó and Torres (2016) is referred at the following locations:
'This OMI-MODIS joint retrieval was also evaluated by Gassó and Torres (2016). They found under less absorbing condition, the hybrid method is sensitive to the variations in the input τ, which is used to select the retrieved pair of aerosol layer and ω_0.' (Line 48-50)

'It is noted that the observed aerosol vertical distribution is limited for the Chile wildfires. Previous research suggested AAI cannot be quantitatively used without τ or z_{aer} information (Gassó and Torres, 2016).' (Line 268-269)

Jethva and Torres (2011) is referred at the following locations:
'We thus find a much weaker wavelength dependence than the value in Jethva and Torres (2011) study, where a 20% difference between the two UV wavelengths was applied to OMAERUV algorithm to achieve the result that 70% of the retrieved ω_0 differ less than $\pm$0.03 from the ω_0 from the AERONET measurements.' (Line 329-331)

'From the sensitivity study of Jethva and Torres (2011), a stronger spectral dependence of n_i between 354 and 388 nm would allow simulations to reach a higher AAI while keeping n_i at a relatively low level. In our study, this means to retrieve a higher ω_0 at 550 nm.' (Line 338-340)

Details

L325-326: the explanation provided does not make much sense to me. If there is little sensitivity to deltaZ , why the claim that there is an amplification of absorption in the layer?. My interpretation is that if there is an amplification of absorption, the AAI increases which means there is sensitivity to deltaZ. Please, revise the sentence.

Sorry for the misunderstanding. We just wanted to claim that Δz has an effect on AAI value though it is very limited. We have rephrased into: 'The reason could be that a larger Δz indicates the coming sunlight has a higher possibility to be absorbed by aerosols, slightly enhancing the aerosol absorption. Although the sensitivity exists, the impact is only up to 5%, which is negligible for practical purposes.' (Line 139-141)

Line 332-333: A similar conclusion was reached by Colarco et al (2017) when analyzing the sensitivity of OMI UVAI . Colarco, P. R., Gassó, S., Ahn, C., Buchard, V., da Silva, A. M., and Torres, O.: Simulation of the Ozone Monitoring Instrulment aerosol index using the NASA Goddard Earth Observing System aerosol reanalysis products, Atmos. Meas. Tech., 10, 4121-4134, https://doi.org/10.5194/amt-10-4121-2017, 2017.

Thank you for your advice. We have added to the manuscript: 'As a result, the AAI decreases significantly due to smaller $\Delta I_{\lambda 1}$, in agreement with a previous study (de Graaf et al., 2005; Colarco et al., 2017).' (Line 147-148)

Lines 343-347: It should be mentioned that while the sensitivity is exists, in this case, it is very small; color range in the respective figure is from 0 to 1% which is negligible for practical purposes.
There might be a misunderstanding here. We assume you are referring to Fig.6. The figure shows the normalized parameter, namely the value is divided by the maximum among all the cases in the comparison group. In terms of percentage, the difference due to different measuring geometry can be up to 20% (i.e. (1 – 0.8) * 100%), which is not negligible. This dependence on measuring geometry can also be explained from the view of AAI's definition. AAI is directly calculated from the measuring radiance, which is a parameter relies on the directions of incident lights and measuring angles. That is exactly the reason we have to use the same measuring geometry as OMI satellite to simulate the AAI.

However, this suggestion can be applied to the sensitivity to the Δz. As shown in Fig.4, the difference due to different Δz is only up to 5% (i.e. (1 – 0.95) * 100%).

Section 3.1.1 Include the time difference between GOME-2 and OMI overpasses the respective type of orbits (ascending/descending)
We have added it to the manuscript: 'Note the GOME-2 and OMI have different equator crossing time (9:30 LT descending node for GOME-2 and 13:45 LT ascending node for OMI) that may affect the inter-comparison of the two satellite measurements.' (Line 174-175)

Line 378: please remove this sentence unless you can make a more convincing case. The data set used in this study is not good enough for making assessments of the MODIS SSA assumption (which certainly needs to be addressed). You need at least well-collocated CALIPSO and Aeronet data. This does not mean that the comments regarding MODIS biases should be removed. The results are suggestive at most and it should be included.
Thank you for your correction. We simply have rephrased into: 'In addition, the τ measured by OMI and AERONET are compared with MODIS.' (Line 197)

Line 444: what is a " ground pixel"? in this context it seems like the word pixel is enough.
We have changed accordingly. 'It should be noted that for all pixels in the plume we assume the same aerosol microphysical properties as well as the same aerosol layer height.' (Line 275-276)

Line 540: This method does not "retrieve an aerosol profile", it retrieves an average aerosol height. Please correct this case and other that are included in the paper.
Sorry for the misunderstanding. We have rephrased them into proper statements.

Figure 2: I see very little value in including a single-phase function in the figure. At reference to a paper should be enough and publication charges will be saved. Alternatively, you may want include additional phase functions to point out differences between aerosol models.
To your question, the phase function is actually range from 0 to 180 degree with 1degree resolution as the continuous line in Fig.2, the marker just indicates the scattering angle we are interested.
Since in this study our focus is on how the AAI response to a specific phase function and the measuring geometry rather than how the aerosol microphysical parameters determine the phase function, the discussion in the sensitivity studies is exclusively on the default case. We prefer to mention other phase functions in the Appendix A as shown in Fig.A1 to A3 (also attached below).

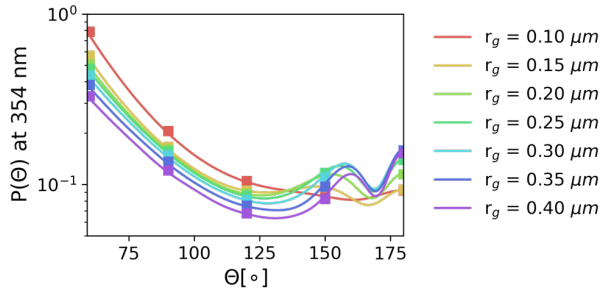

Figure.A1: Phase function p(Θ) at 354 nm of the parameterized Mie scattering aerosol in sensitivity analysis as a function of r_g (with n_r = 1.5 and n_i = 0.06). The markers in the plot correspond to values when Θ=60°, 90°, 120°, 150°, 180°.

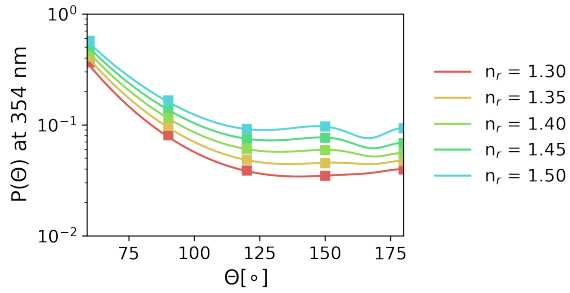

Figure.A2: Phase function p(Θ) at 354 nm of the parameterized Mie scattering aerosol in sensitivity analysis as a function of n_r (with r_g = 0.15 µm and n_i = 0.06). The markers in the plot correspond to values when Θ=60°, 90°, 120°, 150°, 180°.

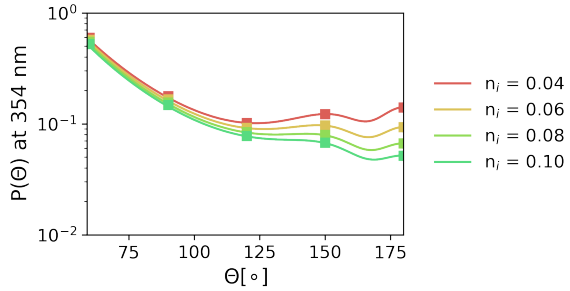

Figure.A3: Phase function p(Θ) at 354 nm of the parameterized Mie scattering aerosol in sensitivity analysis as a function of n_i (with r_g = 0.15 µm and n_r = 1.5). The markers in the plot correspond to values when Θ=60°, 90°, 120°, 150°, 180°.

Figure 5: a) and b) seem to be inverted
Thank you for the correction. We have changed accordingly.

Figure 6a: Put the same ticks in both x and y axis.
Thank you for the correction. We have changed accordingly.

Figure 6: caption does not include reference or explanation of figure 6b.
Thank you for the correction. We have changed the figure caption into: 'Figure.6 AAI sensitivity to θ and θ_0 at φ=180°. The black dashed contour in (a) indicates the Θ=60°, 90°, 120°, 150°. The white dashed line in (a) indicates the cross sections, with its corresponding normalized AAI, $\Delta I_{\lambda 1}$ and $I_{\lambda 1}^{obs}$ in (b).' (Line 657-658)

Figure 7: since the colorbar is not the standard colorbar used in the official CALIPSO quicklooks, can you clarify if the dark red are cloud? The contrast between in smoke and cloud appears to be between orange and red but a clarification will be appreciated.
We have clarified the caption accordingly: 'Figure.7 CALIOP backscatter coefficient β at 532 nm. The solid and dashed line indicate the retrieved z_{aer} and Δz, respectively. The red to black dots indicate clouds and the orange dots indicate aerosol layers, respectively.' (Line 676-677)

Figure 8 Caption: nowhere in the caption mentions the word AI. Is this the parameter displayed?
We have added accordingly: 'Figure.8 AAI from OMI observations (a–d) and DISAMAR simulations (e–h) of the Chile wildfires on 26, 27, 29 and 30 January 2017. The black and red cross symbols are the AERONET station and the main fire sources (Pichilemu W34.39° S72.00° and Consititución S35.33°, W72.42°), respectively. The grey dashed line indicates the CALIOP paths in the region of interest, where the paths used to validate the plume height are marked by black dashed line. The scatter plots (i–l) present the OMI observations against DISAMAR simulations for only qualified data (red dot) and all data (blue dot), respectively.' (Line 687-691)

(2) Author's response to Anonymous Referee #3
Thank you very much for your comments to our manuscript. The following are the responses to your specific comments.

This manuscript presents a technique to retrieve aerosol SSA from satellite data by simulating near UV AAI and constraining AOD. This is similar to and draws from the same philosophical lines as the study of Satheesh et al., 2009. The authors have chosen to retrieve SSA at 550 nm by using MODIS-AOD at 550 nm from the simulated AAI. This makes the UV-Vis spectral dependence of aerosols under investigation a key parameter. Since the simulation of AAI is driven by aerosol microphysics, complex refractive index from the nearest AERONET site which determines this spectral dependence. This raises a flag on its representativeness on the simulation and in-turn the retrieved properties far away from the site (at least for the case presented here – smoke plume travels up to 3000 km away from source fires and AERONET site). I think the authors should include some discussion in the manuscript about this representativeness and reliability of technique for studying such long-range transport of aerosols.

Thank you for the advice. In the manuscript, we have put emphasis on the fact that the location of the AERONET site is not in the source area, while little attention was paid on the spatial representativeness of the AERONET data. We only briefly mentioned the location difference between AERONET and the plume detected by the satellite. Here we added discussion on the spatial representativeness of the AERONET:

In section 4 Results and discussion:

'Last but not least, the spatial representation of the in situ instrument also concerns. Santese et al. (2007) showed that the selected AERONET aerosol parameters can be representative of a 300×300 km^2 southeast Italy area. For the Chile wildfires with the most remote pixel over 3000 km away from the continent, the measurements at AERONET cannot fully represent the plume detected by satellites.' (Line 348-351)

In section 5 Conclusions:

'the insufficient spatial representativeness of a single AERONET site;' (Line 395)

'It is also reliable to retrieve aerosol absorption for each individual pixel with constraint of the aerosol layer height product. The problem due to the poor spatial representativeness of in situ measurement can then be eased by comparing with the nearby satellite pixels.' (Line 404-407)

Few general points (in no specific order) the author should take care of, before the paper is ready for a final publication.

1) The purpose of the study mentioned in L 73 – 74, should also be presented in the abstract before they say "In the first part of this study.....and later we present...." with the reference wavelength of the SSA retrieval.

We have added the purpose accordingly: 'In this study, we attempt to quantify the aerosol absorption by retrieving the single scattering albedo (ω_0) at 550 nm from the satellite measured AAI in near-UV channel.' (Line 10-11)

2) Line 17 : This sentence sounds like it is the instrument's deficiency. It is not. Please make it clear. Something like "The CALIOP overpasses over the region failed to capture the complete evolution...."

Thank you for the correction. We have rephrased into: 'The Cloud and Aerosol Lidar with Orthogonal Polarization (CALIOP) overpasses failed to capture the complete evolution of the smoke plume over the research region, therefore the aerosol profile is parameterized.' (Line 17-19)

3) Line 21 : replace 'observations' with 'satellite observations'

Thank you for the correction. We have rephrased into: 'The results show that the AAI simulated by DISAMAR is consistent with satellite observations.' (Line 21-22)

4) Line 69 – 71 : Poorly phrased. Please re-write it.

Sorry for the misunderstanding. We have rephrased into: 'This study is inspired by previous research to quantify the aerosol absorption from AAI. We use the near-UV AAI provided by OMI on-board Aura, the successor of TOMS, to derive the aerosol properties of the central Chile (Pichilemu 34.39°S, 72.00°W and Consititución 35.33°S, 72.42°W) wildfires in January 2017. The series of fires were triggered by a combination of long-term drought and high temperature, and was regarded as the worst wildfire season in the national history (The Guardian, 2017).' (Line 68-72)

5) Line 108 :'linearly' should be 'linear'.

Thank you for the correction. We have rephrased into: 'with only fine mode particles and weak linear wavelength dependence of the complex refractive index (n_r and n_i).' (Line 109 -110)

6) Line 207 – 209 : Poorly phrased. Please re-write it.
Sorry for the misunderstanding. We have rephrased into: 'Note that the AERONET level 1.5 dataset is not quality-assured. In addition, the location of this AERONET site is in downtown of Santiago City and close to major roads, where the presence of scattering urban aerosols may bias the measurements of the plume.'(Line 213-215)

7) Line 234 – 235 : I am not sure what the authors are saying here. Firstly, the Santiago_Beauchef site has near-UV AERONET measurements. Secondly, the aerosol complex refractive index is provided in their Inversion product that is always only for 440, 675, 880 and 1020 nm. So, what does "site only covers the visible band" and "absence of observations" mean there ?
Sorry for the misunderstanding. 'only covers the visible band' refers to that the site only has sky radiance measurements since visible band. In other word, the inversion product of this site is only available in visible and longer wavelength range. 'absence of observations' therefore indicates the absence of observations of microphysical parameter in UV band. We have rephrased into a clearer way: 'The AERONET instrument at this site only cover the visible and infrared band (440 nm to 1020 nm) for sky radiance measurements, i.e. no aerosol inversion products at UV band. Due to the absence of observations, assumptions have to be made on the spectral dependence of aerosol properties to obtain their values in the near-UV band.' (Line 240-242)

8) Line 286 : Please mention the wavelength of SSA retrieval.
Thank you for the correction. We have added the wavelength at which the SSA is retrieved to the manuscript: 'By applying the methodology described in the previous section, we quantitatively retrieved the aerosol profile and ω_0 at 550 nm of the Chile 2017 wildfires by AAI simulation.' (Line 295-296)

9) Line 295 : What do mean by "may even fail to capture the elevated plume" ?
As shown in Fig.8(a), the CALIOP overpass we selected (the black dashed line) is on the east side of the plume, while the elevated plume detected by OMI was blown away from the continent to the open ocean. From Fig.7(a), one can also see that the CALIOP overpass only captures the smoke at the source (near surface rather than elevated into sky). We mentioned this in order to emphasize that OMI and CALIOP did not always measure the same target due to spatial coverage and measuring time difference. To make it clearer, we have rephrased it into: 'It is noted that due to the spatial coverage and the measuring time difference, CALIOP are not able to represent the entire plume captured by the OMI.' (Line 303-304)

10) Line 305, 307 : It should be '... for 26 January ....'.
Thank you for the correction. We have rephrased into:
'Except for 26 January, the median of simulated AAI in other cases is in good agreement with the measurements, with relative differences within $\pm$6%.' (Line 315-316)
'The majority of the simulated AAI for 26 January is negatively biased, which is reflected by the small slope without an intercept correction in Fig.8 (i)' (Line 317-318)

11) Line 306 : low RMSE ? Not really. For a quantity like AAI which is varying from 0 – 4, an RMSE of 0.5 or 0.6 is not low. Further the measures RMSE and correlation alone cannot confirm an agreement or disagreement between model and observations. Probably one could try using a T-test and say at what confidence level the agreement is statistically significant, I am not sure if your sample size allows for it ?
Thank you for your correction. To some extent, a RMSE of 0.5 for AAI is not low but just acceptable, considering the assumption of homogenous aerosol properties over the entire plume and the lack of aerosol profile information. The sample size is provided in Table 2. The sample size for this event is indeed limited. But we appreciate your advice and may apply statistical tests in future cases where more sample points available.
We have rephrased into: 'The RMSE is only acceptable reflects that part of the plume cannot be fit by the assumptions in the forward simulation.' (Line 316-317)

12) In Table 2, please also provide RMSE for the SSA to be consistent with the AAI report.

As we assumed the homogeneous properties of the plume, i.e. all pixels in the plume have the same SSA. The retrieved SSA is an average level for the entire plume and is compared to the AERONET measurement. In Table 2, we already have provided the absolute and relative difference between retrieved and measured SSA, respectively.

13) Please provide the sample size (number of pixels) for which statistics are derived in the Table 2 and also in figure 8 (i – l).
Thank you for the reminding. We have added in Table.2.

14) Line 313 : Is this 'accounting' or 'contributing' ?
Thank you for the correction. We have rephrased into: 'There are many sources contributing to this discrepancy in ω_0.' (Line 323)

15) Line 319 – 321 : I think, the authors should also report absolute difference in SSA with the AERONET before drawing parallels with the study mentioned here. It is confusing to compare percent difference in ni and absolute difference in SSA.
Sorry for the confusion. To be clear, the percent in this part is not the relative difference of imaginary refractive index, but the difference of the imaginary refractive index between two wavelengths, i.e. 354 and 388 nm. This relative difference between the two wavelength indicates the spectral dependence of the imaginary refractive index in the near-UV channel. This dependence further determines the relation between the near-UV AAI and the visible SSA: the larger this spectral dependence, the higher SSA can be retrieved at the same AAI level, and the other way around for weaker spectral dependence. We have rephrased into: 'This would also affect the spectral dependence of complex refractive index used to constrain the radiative transfer calculation.' (Line 325-326).
The following part then discusses how this wavelength dependence affects the AAI simulation and SSA retrieval.

16) The spectral dependence retrieved in the study should also be compared with the in- situ measurements and other studies on biomass burning in the literature and include in the discussion (L 320 – 330).
Thank you for the advice. We have added the following content in the discussion: 'We thus find a much weaker wavelength dependence than the value in Jethva and Torres (2011) study, where a 20% difference between the two UV wavelengths was applied to OMAERUV algorithm to achieve the result that 70% of the retrieved ω_0 differ less than $\pm$0.03 from the ω_0 from the AERONET measurements. This 20% spectral dependence adopted in their work is associated with findings of Hoffer et al. (2006). They conducted in situ measurements on humic-like substances (HULIS) of Amazonia biomass burning aerosols and found that around 35% - 50% light absorption at 300 nm, whereas only around 15% at 400 nm. In terms of the absorbing Ångström exponent (AÅE), a 20% increase at 354 nm with respect to the value at 388 nm is equivalent to an AÅE value between 2.5 and 3, depending on the aerosol models of OMAERUV. According to Kirchstetter et al. (2004), the AÅE of urban pollution is near unit and biomass burning aerosols ranges is approximately 2 between 300 nm to 1 μm. Bergstrom et al. (2007) also confirmed this conclusion from several field programs (SAFARI 2000, ACE Asia, PRIDE, TARFOX, INTEX-A). From the sensitivity study of Jethva and Torres (2011), z stronger spectral dependence of n_i between 354 and 388 nm would allow simulations to reach a higher AAI while keeping n_i at a relatively low level. In our study, this means to retrieve a higher ω_0 at 550 nm.' (Line 329-340)

17) Line 374 : "The retrieved SSA is out of typical uncertainty...." this statement does not make sense and should be removed or re-phrase appropriately. At least for the case presented here the authors did not come up with a quantitative estimate of the uncertainty in SSA and clearly it is difficult if not impossible because of the multiple error sources.
Thanks for the correction, we have removed this sentence.

Quantifying the single scattering albedo for the January 2017 Chile wildfires from simulations of the OMI absorbing aerosol index

Jiyunting Sun[1,2], J. Pepijn Veefkind[1,2], Peter van Velthoven[1], Pieternel F. Levelt[1,2]

[1]Royal Netherlands Meteorological Institute, De Bilt, 3731 GA, the Netherlands
[2]Department of Geoscience and Remote Sensing (GRS), Civil Engineering and Geosciences, Delft University of Technology, Delft, 2628 CD, the Netherlands

Correspondence to: Jiyunting Sun (jiyunting.sun@knmi.nl)

Abstract. The absorbing aerosol index (AAI) is a qualitative parameter directly calculated from satellite measured reflectance. Its sensitivity to absorbing aerosols in combination with a long-term data record since the late 1970's makes it an important parameter for climate research. In this study, we attempt to quantify the aerosol absorption by retrieving the single scattering albedo (ω_0) at 550 nm from the satellite measured AAI in near-UV channel. In the first part of this study, AAI sensitivity studies are presented exclusively for biomass burning aerosols. Later on, this study employs a radiative transfer model (DISAMAR) to simulate the AAI measured by the Ozone Monitoring Instrument (OMI) in order to derive ω_0 at 550 nm. Inputs for the radiative transfer calculations are satellite measurement geometry and surface conditions from OMI, aerosol optical thickness (τ) from the MODerate-resolution Imaging Spectroradiometer (MODIS), and aerosol micro-physical parameters from the AErosol RObotic NETwork (AERONET), respectively. This approach is applied to the Chile wildfires for the period from 26 to 30 January 2017, when the OMI observed AAI of this event reached its peak. The Cloud and Aerosol Lidar with Orthogonal Polarization (CALIOP) overpasses failed to capture the complete evolution of the smoke plume over the research region, therefore the aerosol profile is parameterized. The simulated plume ascends to an altitude of 4.5-4.9 km, which is in good agreement with available CALIOP backscatter coefficient measurements. Due to the data may contain the pixels outside the plume, an outlier detection criterion is applied. The results show that the AAI simulated by DISAMAR is consistent with satellite observations. The correlation coefficients fall into the range between 0.85 and 0.95. The retrieved mean ω_0 at 550 nm for the entire plume over the research period from 26-30 January 2017 varies from 0.81 to 0.87, whereas the nearest AERONET station reported values in the range from 0.89 to 0.92. The difference in geolocation of the AERONET site and the plume, the assumption of homogeneous and static plume properties, the lack of the aerosol profile information, and the uncertainties in the inputs for radiative transfer calculation are primarily responsible for this discrepancy.

1 Introduction

Biomass burning aerosols are generated from combustion of carbon-containing fuels, either by natural or anthropogenic processes (Bond et al., 2004; IPCC, 2014). They are of great concern from the climate perspective (Kaufman and Boucher, 2002; IPCC, 2007; Koch and Del Genio, 2010; Huang et al., 2013; IPCC, 2014). The reported radiative forcing of black carbon (BC) produced by fossil fuel and biofuel is around 0.4 Wm^{-2} (0.05 – 0.80 Wm^{-2}) (Ramanathan and Carmichael, 2008; Bond et al., 2013; Huang et al., 2013), but this estimate is highly uncertain. Accurate measurements of the aerosol single scattering albedo (ω_0) on a global scale can reduce the uncertainty in aerosol radiative forcing assessments (Hu et al., 2007). ω_0 is defined as the ratio of the aerosol scattering over the extinction. Currently ω_0 is mainly measured by ground-based instruments (Dubovik et al., 1998; Eck et al., 2003; Petters et al., 2003; Kassianov et al., 2005; Corr et al., 2009; Yin et al., 2015). Satellite sensors, such as the POLarization and Directionality of the Earth's Reflectances (POLDER), can retrieve ω_0 from a combination of multi-angular, multi-spectral observations of the polarized radiation. By measuring the anisotropy of the reflected radiance for each pixel, POLDER is expected to determine the reflected solar flux more accurately (Leroy et al.,

Formatted ... [1]
Formatted ... [2]
Formatted ... [3]
Formatted ... [4]
Formatted ... [5]
Formatted ... [6]
Deleted: The absorbing aerosol index (AAI) based on the near ... [7]
Formatted ... [8]
Deleted: a series of …AI sensitivity analys…tudiesis ... [9]
Formatted ... [10]
Deleted: is
Formatted ... [11]
Deleted: on
Formatted ... [12]
Deleted: applies
Formatted ... [13]
Deleted: and …n order to derive the aerosol single scattering ... [14]
Formatted ... [15]
Deleted: The …i ... [16]
Formatted ... [17]
Deleted: relatively small data size of
Formatted ... [18]
Commented [Sj1]: Because the data in this case is sensitive to ... [21]
Deleted: this case
Formatted ... [19]
Deleted: has to be
Formatted ... [20]
Formatted ... [22]
Commented [JV2]: Add a range instead of a single number?
Commented [Sj3R2]: Changed.
Deleted: are over
Formatted ... [23]
Formatted ... [24]
Formatted ... [25]
Deleted: is
Formatted ... [26]
Deleted: approximately
Deleted: in the range
Formatted ... [27]
Deleted: 0.84,
Formatted ... [28]
Deleted: . The
Formatted ... [29]
Deleted: slightly smaller than the value of 0.90 measured ... [30]
Deleted: relative distance…ifference in geolocation between ... [31]
Formatted ... [32]
Deleted: Except for the observational errors, the impact of ... [33]
Deleted: They consist of fine particles (aerodynamic diameter ... [34]
Formatted ... [35]
Deleted: also …f great concern from the the ... [36]
Formatted ... [37]
Deleted: …of climate. They contain absorbing aerosols, which ... [38]
Formatted ... [39]
Deleted:), one type of absorbing aerosol, black carbon (BC), ca ... [40]
Formatted ... [41]
Deleted: (Huang et al., 2013… or by enhancing the absorption of ... [42]
Formatted ... [43]
Deleted: ¶ ... [44]
Formatted ... [45]
Deleted: ….ut But ... [46]
Deleted: ,…defined as the ratio of the aerosol scattering over the ... [47]
Formatted ... [48]
Deleted: Many implementations have been done for
Formatted ... [49]

1997). Unfortunately, there is no continuous temporal coverage of ω_0 because the first two POLDER missions ended prematurely due to technical problems, and the third POLDER mission only covered the period 2004-2014. Instead, satellite derived ω_0 is usually retrieved simultaneously with the aerosol optical thickness (τ) based on the pre-defined aerosol properties, such as the near-UV aerosol product (OMAERUV) of the Ozone Monitoring Instrument (OMI) (Torres et al., 2005; Torres et al., 2007). But this aerosol absorption over near-UV is highly sensitive to the assumption on aerosol layer height. Satheesh et al. (2009) therefore used the τ from MODerate-resolution Imaging Spectroradiometer (MODIS), which is independent of aerosol layer height, to constrain the OMAERUV retrieval. Their validation showed that compared with operational OMAERUV algorithm, the retrieved aerosol height by the hybrid method is in a better agreement with air-borne measurements, implying a potential improvement in aerosol absorption retrieval. This OMI-MODIS joint retrieval was also evaluated by Gassó and Torres (2016). They found that under less absorbing conditions, the hybrid method is sensitive to the variations in the input τ, which is used to select the retrieved pair of aerosol layer and ω_0.

Herman et al. (1997) first defined the near Ultra-Violet (UV) absorbing aerosol index (AAI), which provides an alternative methodology to retrieve ω_0 from satellite observations. The near-UV AAI, usually derived from the spectral range between 340 and 390 nm, is a qualitative measure of absorbing aerosols that was first provided by the Total Ozone Mapping Spectrometer (TOMS) on-board Nimbus-7 in 1979. Since then several instruments have contributed to the AAI data record, that now spans nearly four decades. This long data record is an important motivation for us to derive quantitative aerosol absorption information in the near-UV channel.

The most important advantage of the satellite retrieved AAI is that it does not depend on a-prior aerosol types, which are major uncertainties in aerosol parameter retrievals, such as τ. Ginoux et al. (2004) suggested that comparing model simulations with AAI from TOMS allows a better control of discrepancies because the only error source is from models. Further advantages of AAI are the low reflectivity of the Earth's surface and the absence of significant molecular absorption over the near-UV range. Using this band can ensure the aerosol absorption is one of the major contributors to the total signal. Moreover, the near-UV AAI is by definition highly sensitive to aerosol absorption. Previous studies have proven the potential of the near-UV AAI from TOMS in absorbing aerosol properties retrieval. Torres et al. (1998) provided the theoretical basis of an inversion method to derive τ and ω_0 from backscattered radiation. This method was validated by ground-based observations during the Southern African Regional Science Initiative (SAFARI) 2000 measurement campaign. The agreement of τ and ω_0 reaches $\pm$30% and $\pm$0.03, respectively (Torres et al., 2005). Hu et al. (2007) retrieved global columnar ω_0 based on the AAI from TOMS with an average uncertainty of 15%.

This study is inspired by previous research to quantify the aerosol absorption from AAI. We use the near-UV AAI provided by OMI on-board Aura, the successor of TOMS, to derive the aerosol properties of the central Chile (Pichilemu 34.39°S, 72.00°W and Consititución 35.33°S, 72.42°W) wildfires in January 2017. The series of fires were triggered by a combination of long-term drought and high temperature, and were regarded as the worst wildfire season in the national history (The Guardian, 2017). The fires led to evacuations of the affected areas and massive losses of the local forestry industry (pine and eucalyptus forests) (NASA.gov, 2017). The smoke plume was transported away from the source regions towards the tropical area in the Pacific Ocean by north-westward winds (Fig.1). In this study, we quantitatively retrieve the ω_0 of this smoke by simulating the near-UV AAI of OMI with the radiative transfer model Determining Instrument Specifications and Analysing Methods for Atmospheric Retrieval (DISAMAR). The aerosol inputs of DISAMAR includes the τ retrieved from MODIS on-board the NASA EOS Aqua satellite, and information on aerosol micro-physical parameters provided by AERONET. In the next section, we provide a brief introduction on the near-UV AAI and its sensitivity to various parameters. The methodology is described in section 3. In section 4, retrieved results and uncertainty analysis of Chile 2017 wildfires are discussed, followed by main conclusions in section 5.

Formatted ... [50]
Deleted: ω_0 is defined as the ratio of the radiation scattered by ... [51]
Formatted ... [52]
Deleted: As a result, ω_0 is usually retrieved by forward simulations ... [53]
Deleted: instruments
Deleted: improved
Formatted ... [54]
Deleted:
Formatted ... [55]
Formatted ... [56]
Formatted ... [57]
Deleted: that constrains
Formatted ... [58]
Deleted: forward model simulations with the absorbing aerosol ... [59]
Formatted ... [60]
Deleted: more than 35 years
Formatted ... [61]
Deleted: improving …s to methods to ... [62]
Formatted ... [63]
Deleted: from
Formatted ... [64]
Deleted: foremost …ost important advantage of the satellite ... [65]
Formatted ... [66]
Deleted: assumptions on aerosol types, which significantly reduce ... [67]
Formatted ... [68]
Deleted: ….Ginoux et al. (2004) suggested that comparing model ... [69]
Formatted ... [70]
Deleted: the near-UV channel range
Formatted ... [71]
Deleted: , the sensitivity of τ in the visible band to ω_0 is lower ... [72]
Deleted: ω_0
Formatted ... [73]
Formatted ... [74]
Deleted:
Formatted ... [75]
Formatted ... [76]
Deleted: Empirical models were also developed to build ... [77]
Formatted ... [78]
Deleted: , that…e uses…the near-UV AAI provided by the Ozone ... [79]
Formatted ... [80]
Deleted: Triggered by
Formatted ... [81]
Deleted: , this series of fires occurring in central Chile (Pichilemu ... [82]
Formatted ... [83]
Deleted: ,
Deleted: caused
Deleted:
Deleted: from
Formatted ... [84]
Deleted: the MODerate-resolution Imaging Spectroradiometer ... [85]
Formatted ... [86]
Deleted: ¶

2 AAI sensitivity studies based on DISAMAR

In this section, we first introduce the near-UV AAI. In the sensitivity analysis, we show that the AAI depends not only on aerosol parameters, but also on the surface conditions and the observation geometry. The sensitivity analysis in this study is only designed for biomass burning aerosols.

2.1 Near-UV AAI definition

The concept of the near-UV AAI was first conceived to detect UV-absorbing aerosols from the spectral contrast provided by TOMS observations, known as the residue method (Herman et al., 1997). The basic idea of the residue method is that in a pure Rayleigh atmosphere, the reflectance (or equivalently the radiance (I_λ)) decreases strongly with the wavelength. The presence of absorbing aerosols will reduce this spectral dependence of I_λ. The change in this wavelength dependence is summarized as the AAI, which is calculated from the I_λ at the wavelength pair λ_1 and λ_2 ($\lambda_1 < \lambda_2$):

$$\mathrm{AAI} = -100\left(log_{10}\left(\frac{I_{\lambda 1}}{I_{\lambda 2}}\right)^{obs} - log_{10}\left(\frac{I_{\lambda 1}}{I_{\lambda 2}}\right)^{Ray}\right). \quad (1)$$

The *obs* and *Ray* denote the I_λ is measured by satellite and calculated using a Rayleigh atmosphere, respectively. The longer wavelength λ_2 is treated as reference wavelength where the surface albedo (a_s) is determined by fitting the observed radiance, i.e. $I^{Ray}_{\lambda 2}(a_s) = I^{obs}_{\lambda 2}$. This is done using an atmosphere containing only molecular scattering bounded by a Lambertian surface. The spectral dependence of the surface albedo is neglected thus $I^{Ray}_{\lambda 1}$ is calculated using the same value for a_s. Defining $\Delta I_{\lambda 1} = I^{Ray}_{\lambda 1} - I^{obs}_{\lambda 1}$, Eq.(1) can be rewritten as:

$$\mathrm{AAI} = 100 log_{10}\left(\frac{\Delta I_{\lambda 1}}{I^{obs}_{\lambda 1}} + 1\right) \quad (2)$$

It is advantageous to use Eq.(2) because the AAI can be simply interpreted as the ratio between the simulated and observed radiance at λ_1.

2.2 Near-UV AAI sensitivity studies

In this section, we present results from sensitivity studies performed by the radiative transfer model DISAMAR. DISAMAR can perform simulations of the forward I_λ spectrum in a wide spectral coverage (270 nm to 2.4 μm) and model scattering and absorption by gases, aerosols and clouds, as well as reflection by the surface (De Haan, 2011). It uses either the Doubling-Adding method or the Layer Based Orders of Scattering (LABOS) for the radiative transfer calculations. In this study the latter one is employed, because it is less computationally intensive (De Haan et al., 1987; De Haan, 2011). DISAMAR allows to apply several aerosol scattering approximations. Here we assume Mie scattering aerosols. The parameters to describe Mie particles and their corresponding values are listed in Table 1. Considering the Chile wildfires plumes, which were dominated by biomass burning aerosols, these sensitivity studies are specifically performed for parameterized smoke aerosols, with only fine mode particles and weak linear wavelength dependence of the complex refractive index (n_r and n_i). The default values refer to observations of the daily average on January 27 of the AERONET station Santiago_Beauchef (33.46°S, 70.66°W). We obtain the size distribution function and complex refractive index at 440, 675, 880 and 1018 nm from AERONET, and apply a linear interpolation / extrapolation to derive the complex refractive index over the spectrum from 340 to 675 nm, with spectral resolutions of 2 nm. Then DISAMAR uses above information to calculate the aerosol phase function P(Θ) and ω_0 over the full spectrum (340 to 675 nm). The corresponding P(Θ) at 354 nm for default case (r_g = 0.15 μm, n_r = 1.5 and n_i = 0.06) is presented in Fig.2. P(Θ) for other cases are provided in the Appendix A (Fig.A1, A2 and A3). DISAMAR requires τ to be defined at reference wavelength 550 nm. Surface parameters include a spectrally flat a_s and the surface pressure P_s. The aerosol profile is parameterized as a single layer box shape, with its bottom

Formatted ... [87]
Formatted ... [88]
Deleted: for …n a pure Rayleigh atmosphere, where …he ... [90]
Formatted ... [89]
Formatted ... [91]
Deleted: dependency
Formatted ... [92]
Formatted ... [93]
Deleted: from
Formatted ... [94]
Deleted: the
Deleted: observed
Deleted: measurement
Deleted: the model …alculated using a Rayleigh atmosphere I ... [95]
Deleted: ¶
Formatted ... [96]
Formatted ... [97]
Formatted ... [98]
Deleted: The aerosol effect is assumed at λ_2 is negligible, so that ... [99]
Formatted ... [100]
Formatted ... [101]
Formatted ... [102]
Deleted: Consequently, …E….(1) can be equivalently transformed ... [103]
Deleted: rephrased
Deleted: the difference between $I^{obs}_{\lambda 1}$ and $I^{Ray}_{\lambda 1}$ normalized by the ... [104]
Formatted ... [105]
Formatted ... [106]
Formatted ... [107]
Formatted ... [108]
Deleted: The advantage
Deleted: of
Formatted ... [110]
Deleted: writing the AAI using equation 2
Formatted ... [109]
Formatted ... [111]
Deleted: is that ….
Formatted ... [112]
Deleted: ¶
Formatted ... [113]
Deleted: The sensitivity studies are
Deleted: with
Formatted ... [114]
Deleted: It …ISAMAR can perform simulates …imulations of the ... [115]
Deleted: s
Deleted: various …cattering and absorption atmospheric ... [116]
Formatted ... [117]
Deleted: DISAMAR …t uses either the Doubling-Adding method ... [118]
Deleted: used
Formatted ... [119]
Formatted ... [120]
Deleted: Given size distribution function (r_g), complex refractive ... [121]
Deleted: that …hich mainly produced ... [122]
Deleted: ly…wavelength dependence dependency ... [123]
Formatted ... [124]
Deleted: in
Commented [JV4]: Which period?
Commented [Sj5R4]: Added.
Formatted ... [125]
Formatted ... [126]
Deleted:
Formatted ... [127]
Deleted: and t
Formatted ... [128]
Deleted:
Formatted ... [129]
Deleted: should
Formatted ... [130]
Deleted: influences

at z_{aer}-$\Delta z/2$ and top at z_{aer}+$\Delta z/2$, where z_{aer} and Δz are the geometric central height and the geometric thickness of the aerosol layer, respectively. The whole sensitivity analysis is performed for cloud-free conditions. The wavelength pair of OMI (354 and 388 nm) is applied to compute the AAI. To make different sensitivities studies comparable, the AAI calculated in this section is normalized by the maximum value in each sensitivity study. Note that sensitivity study always use the default settings listed in Table 1 unless different values are explicitly mentioned.

Aerosol optical properties are determined by micro-physics, such as the real and imaginary part of the complex refractive index (n_r and n_i), and the particle size (r_g). Fig.3 shows how is the variation of the AAI, $\Delta I_{\lambda 1}$, $I_{\lambda 1}^{obs}$ as well as of the optical properties (ω_0 and the asymmetry factor g) associated with the complex refractive and the particle size. The asymmetry factor g is the averaged cosine of the scattering angle Θ, weighted by P(Θ). Fig. 3 shows that the effect of the complex refractive index is dual. As shown in Fig.3 (a), an increase in the real part of refractive index n_r directly enhances the magnitude of $I_{\lambda 1}^{obs}$, whereas $\Delta I_{\lambda 1}$ reduces. This results in low values of the AAI, which correspond to a high ω_0 (Fig.3 (b)). Under the condition that measurement angle is Θ=150°, the declining g implies that more light is scattered in the line-of-sight of the detector, thus the higher $I_{\lambda 1}^{obs}$. Conversely, the imaginary part of refractive index n_i, which is directly associated with ω_0, has an opposite influence, see Fig.3 (c) and (d). The particle size distribution has a more complicated influence on the AAI. As shown in Fig.3 (e), the AAI first decreases and then increases, when r_g is varying from 0.1 to 0.4 μm. The AAI primarily follows the behaviour of $\Delta I_{\lambda 1}$, whereas ω_0 is continuously decreasing and g is continuously increasing.

In addition to the micro-physics, the concentration and vertical distribution of aerosols also have a strong influence on the wavelength dependence of the radiance $\Delta I_{\lambda 1}$. As shown in Fig.4 (a), the AAI is positively correlated with τ_a. The AAI is highly sensitive to the aerosol vertical distribution (Herman et al., 1997; Torres et al., 1998; de Graaf et al., 2005). As the aerosol layer ascends (Fig.4 (b)), more molecular scattering beneath the aerosol layer is shielded, which reduces $I_{\lambda 1}^{obs}$ while increases $\Delta I_{\lambda 1}$. The relation between the AAI and z_{aer} is almost linear. Fig.4 (c) shows that at the same altitude, the AAI slightly increases with the geometrical thickness of the aerosol layer. The reason could be that a larger Δz indicates the coming sunlight has a higher possibility to be absorbed by aerosols, slightly enhancing the aerosol absorption. Although the sensitivity exists, the impact is only up to 5%, which is negligible for practical purposes.

The calculated AAI does not only depend on the aerosols themselves, but also on ambient parameters such as surface and clouds. Although the near-UV AAI is capable to distinguish absorbing and non-absorbing agents (Herman et al., 1997) and even to retrieve aerosol information over clouds (Torres et al., 2012), the uncertainty triggered by clouds is relatively high and therefore cloudy conditions are excluded in this study. Surface conditions are parameterized by P_s and a_s. It can be seen in Fig.5 (a) that a decrease in P_s, or equivalently an elevated terrain height, leads to less Rayleigh scattering shielded between the surface and the aerosol layer. As a result, the AAI decreases significantly due to smaller $\Delta I_{\lambda 1}$, in agreement with a previous study (de Graaf et al., 2005; Colarco et al., 2017). According to de Graaf et al. (2005), increasing a_s has two counteracting effects. On the one hand, it increases the amount of directly reflected radiation at the top of the atmosphere, namely a larger $I_{\lambda 1}^{obs}$, on the other hand it enhances the role of absorption by the aerosol layer rather than the surface, namely a larger $\Delta I_{\lambda 1}$. Which effect of a_s is dominant depends on P_s (Fig.5 (b)). When the aerosol layer is relative to the sea level (P_s = 1013 hPa), the first effect dominates. However, a brighter surface compensates the loss of molecular scattering shielded by the aerosols when the terrain height rises (P_s = 813 hPa), which makes the absorbing layer more detectable.

The AAI also depends on the Sun-satellite geometry. Here we provide the AAI as a function of the measurement geometry for the default case with the relative azimuth angle $\Delta\varphi = 180^\circ$. As presented in Fig.6 (a), the AAI becomes very sensitive to the geometries for zenith angles larger than 60°, which confirms previous research (Herman et al., 1997; Torres et al., 1998; de Graaf et al., 2005). This is mainly due to the significant growth of P(Θ) when Θ becomes smaller (Fig.2). Thus, it is suggested that the OMI measurement with θ_0 larger than this value should be removed due to large variations in the AAI. To analyse the radiance behaviour as previously, we plotted the $I_{\lambda 1}^{obs}$ and $\Delta I_{\lambda 1}$ as a function of Θ along the cross section,

Deleted: make it
Formatted ... [131]
Deleted: among
Formatted ... [132]
Deleted: each …ensitivity study always uses…the default settings [133]
Formatted ... [134]
Deleted: ,
Formatted ... [135]
Deleted: ¶
Formatted ... [136]
Deleted: .
Formatted ... [137]
Formatted ... [138]
Formatted ... [139]
Deleted: , as a function of
Formatted ... [140]
Deleted: T
Deleted: effect
Formatted ... [141]
Deleted:
Formatted ... [142]
Formatted ... [143]
Formatted ... [144]
Deleted: large
Formatted ... [145]
Deleted: The asymmetry factor g is the averaged cosine of the ... [146]
Formatted ... [147]
Deleted:
Formatted ... [148]
Deleted: geometry
Formatted ... [149]
Formatted ... [150]
Deleted: (…ig.3 (c) and (d))… ¶ ... [151]
Deleted: varied
Formatted ... [152]
Formatted ... [153]
Deleted: ¶
Deleted: As shown in Fig.3 (e) and (f), even with a decreasing ... [154]
Formatted ... [155]
Formatted ... [156]
Deleted: T
Commented [Sj6]: Deleted.
Deleted: y
Formatted ... [157]
Formatted ... [158]
Deleted: as its definition (Eq.(1))
Formatted ... [159]
Formatted ... [160]
Deleted: it
Formatted ... [161]
Deleted: an
Deleted: possible …eason could be that a larger Δz indicates a ... [162]
Formatted ... [163]
Deleted: the absorbing layer
Formatted ... [164]
Deleted: amplifying
Formatted ... [165]
Deleted: of the aerosol layer… Although the sensitivity exists, the ... [166]
Formatted ... [167]
Formatted ... [168]
Deleted: ,
Formatted ... [169]
Deleted: the
Formatted ... [170]
Deleted: are not
Formatted ... [171]
Deleted: in
Formatted ... [172]

respectively (Fig.6 (b)). It is noted that $I_{\lambda 1}^{obs}$ increases when Θ is larger than 90°, whereas the P(Θ) decreases at this range (Fig.2). The reason could be that the Rayleigh scattering has an increasing contribution to the radiance at those measurement angles (backscattering).

3 Methodology and datasets

In this section, we first present the datasets used and their pre-processing, followed by the strategy to retrieve the aerosol ω_0 while constraining the simulated near UV AAI with the observed one.

3.1 Datasets

3.1.1 OMI and GOME-2 absorbing aerosol index

The TOMS near-UV AAI retrieval has been proven a robust algorithm and applied to successive sensors, such as OMI on-board Aura and GOME-2 on-board MetOp-A/B. GOME-2 has higher spectral resolution (0.2-0.4 nm) than TOMS, but the spatial resolution is rather coarse (80×40 km^2). In this study, GOME-2 measured AAI at wavelength pair 340 and 380 nm (http://archive.eumetsat.int) is only used as an independent dataset to assess the potential bias of the OMI measurements. OMI combines advantages of both TOMS and GOME-2. It covers wavelengths from 264 to 504 nm with a spectral resolution of approximately 0.5 nm and has a much higher spatial resolution than GOME-2 of 13×24 km^2 (Levelt et al., 2006). Note the GOME-2 and OMI have different equator crossing time (9:30 LT descending node for GOME-2 and 13:45 LT ascending node for OMI) that may affect the inter-comparison of the two satellite measurements.

Since OMI was launched in 2004, the AAI retrieved from this instrument has been widely used in various applications. Kaskaoutis et al. (2010) employed the OMI measured AAI for regional research of the aerosol temporal and spatial distribution in Greece. Torres et al. (2012) utilized the advantage of near-UV AAI to detect aerosols over clouds. The OMI observed AAI was even used to evaluate the impact of surface dust loading on human health (Deroubaix et al., 2013). Buchar et al. (2015) validated the NASA MERRA aerosol reanalysis with the AAI retrieved from OMI.

In this study, the OMI level 2 product OMAERO (https://disc.gsfc.nasa.gov) is used to provide AAI retrieved at the wavelength pair of 354 and 388 nm, and the corresponding viewing geometry and the surface condition when the measurements took place. The samples are included in the radiative transfer simulation only if θ_0 is smaller than 60°, and if satellite pixels are not contaminated by sun-glint, clouds, row anomalies of the instrument, etc. The simulation is only applied to pixels inside the biomass burning plume, which is defined as AAI values larger than 1 for both OMI and GOME-2.

3.1.2 MODIS and OMI aerosol optical thickness

MODIS on-board Aqua/Terra is a sensor that was specifically designed for atmosphere and climate research. The combination of two satellites ensures daily global coverage. The spatial resolution ranges from 250 m to 1 km and it has 36 spectral bands in the wavelength range between 400 nm and 14.4 μm (Remer et al., 2005). MODIS employs separated algorithms for aerosol retrieval over oceans and land (Tanré et al., 1997; Kaufman and Tanré, 1998; Hsu et al., 2004; Remer et al., 2005). Currently the τ provided by MODIS is one of the most reliable datasets (Lee et al., 2009), with an estimated uncertainty of only 3-5% over ocean and 5-15% over land (Remer st al., 2005). Besides, the MODIS retrieved τ is free from the uncertainty triggered by assumed aerosol profile (Satheesh et al., 2009). As mentioned before, DISAMAR requires τ at 550 nm. This study uses cloud-filtered τ at 550 nm from the Collection 6 level 2 product MYD04 as the input for radiative transfer calculation (https://ladsweb.modaps.eosdis.nasa.gov).

In addition, the τ measured by OMI and AERONET are compared with MODIS. The OMAERO τ retrieval uses multi-spectral fitting techniques. The retrieved τ is reported in good accordance with AERONET and is highly correlated with

Formatted ... [187]
Commented [Sj9]: I reconsider the reason, and also set up a ... [193]
Deleted: corresponding to the selected Θ does not strictly follow ... [188]
Deleted: This
Deleted: the reason that the length of the light path through the ... [191]
Formatted ... [189]
Formatted ... [190]
Formatted ... [192]
Formatted ... [194]
Deleted: involved
Commented [JV10]: I propose to delete this part
Commented [Sj11R10]: Deleted.
Deleted: Although the DISAMAR can calculate wavelength ... [197]
Formatted ... [195]
Deleted: ith additional constraint of the near-UV AAI from OMI
Formatted ... [196]
Formatted ... [198]
Formatted ... [199]
Deleted: 4
Formatted ... [200]
Formatted ... [201]
Formatted ... [202]
Formatted ... [203]
Deleted: http://dx.doi.org/10.5067/aura/omi/data2001
Formatted ... [204]
Deleted: by
Formatted ... [205]
Deleted: measurement
Formatted ... [206]
Deleted: s
Deleted: are
Formatted ... [207]
Deleted: ground
Formatted ... [208]
Deleted: ground
Deleted: plume …ixels inside the biomass burning plume, which is ... [209]
Formatted ... [210]
Deleted: defined for both OMI and GOME-2 retrieved
Deleted: ,… ... [211]
Formatted ... [212]
Deleted: ,
Formatted ... [213]
Deleted: and AERONET
Deleted: a …aily global coverage per 1 to 2 days… The spatial ... [214]
Formatted ... [215]
Deleted: the spectrum ranges from…t has 36 spectral bands in the ... [216]
Formatted ... [217]
Deleted: , respectively
Formatted ... [218]
Deleted:
Formatted ... [219]
Commented [JV13]: add collection number
Commented [Sj14R13]: Added
Formatted ... [220]
Formatted ... [221]
Deleted: treated as a reference dataset to evaluate potential biases ... [222]
Formatted ... [223]

MODIS (Torres et al., 2007), with a correlation of 0.66 over land and 0.79 over the oceans (Curier et al., 2008), although it suffers from cloud contamination due to the relatively coarse spatial resolution of OMI. Due to the wavelength difference, the τ measured by OMI at 442 nm has to be transferred to 550 nm using the Ångström exponent (ÅE) 440 – 675 nm taken from AERONET near the time when OMI flies over the selected site. The AERONET dataset used in this study is introduced in the next section.

3.1.3 AERONET aerosol properties

AERONET is an aerosol monitoring network of ground-based sun photometers. With standardized instruments, calibration, processing and distribution, AERONET provides a long-term global database for aerosol research and air-borne and space-borne measurement validation. The system takes two basic measurements. The τ and ÅE are retrieved from the direct solar irradiance measurements; the r_g, $P(\Theta)$ (Nakajima et al., 1983; Nakajima et al., 1996), ω_0 (Dubovik et al., 1998), n_r and n_i (Dubovik and King, 2000) are derived from multiple-angular measurements of sky radiance.

The AERONET site nearest to the fire sources of 2017 Chile wildfires is the Santiago_Beauchef (33.46°S, 70.66°W) (https://aeronet.gsfc.nasa.gov). The dataset in use is version 2 level 1.5 product. To minimize the influence of temporal difference, the parameters of AERONET measured closest to the time of the OMI overpass of the site are used to simulate the optical properties of Mie scattering aerosols in DISAMAR. Note that the AERONET level 1.5 dataset is not quality-assured. In addition, the location of this AERONET site is in downtown of Santiago City and close to major roads, where the presence of scattering urban aerosols may bias the measurements of the plume.

The AERONET retrieved τ and ω_0 are used to evaluate the MODIS τ and retrieved ω_0, respectively. The AERONET measured τ is transferred to 550 nm using the ÅE in range 440 – 675 nm while the ω_0 at 550 nm is linearly interpolated by values between 440 and 675 nm.

The AERONET inversion product needs to be processed into the inputs required by DISAMAR. Firstly, a conversion from the volume size distribution $V(r_v, \sigma_v)$ provided by AERONET to the number size distribution $N(r_g, \sigma_g)$ used in DISAMAR is required:

$$N(r_g, \sigma_g) = V(r_v, \sigma_v)\frac{3}{4\pi r_g^3}e^{-4.5\sigma_n^2}, \quad (4)$$

The following relation between the geometric and volumetric mean radii (r_g and r_v) and standard deviations (σ_g and σ_v) is assumed:

$$r_g = r_v e^{-3\sigma_g^2}, \quad (5)$$

$$\sigma_g = \sigma_v, \quad (6)$$

The fine and coarse mode particle size are derived by finding the two peaks of the log-normal distribution function provided by AERONET. The complex refractive index is assumed the same for both modes. Since bi-modal aerosol is not applicable in DISAMAR yet, we first calculate optical properties of two modes individually, then we externally combine the optical properties of two modes into a bi-modal aerosol with a fraction:

$$w_f = \frac{N_f(r_{g,f},\sigma_{g,f})}{N_f(r_{g,f},\sigma_{g,f})+N_c(r_{g,c},\sigma_{g,c})}, \quad (7)$$

$$w_c = 1 - w_f, \quad (8)$$

Then the weights for calculating the total ω_0 of the mixed aerosol are:

$$w_{\sigma,f} = \frac{w_f\sigma_f}{w_f\sigma_f+w_c\sigma_c}, \quad (9)$$

Formatted ... [224]
Deleted: .
Formatted ... [225]
Deleted: at
Formatted ... [226]
Deleted: The τ retrieved from AERONET also has to be converted to 550 nm to make them comparable.
Formatted ... [227]
Formatted: Font: 10 pt, English (US)
Formatted: English (US)
Deleted: micro-physical parameters
Formatted: Font: 10 pt, English (US)
Formatted ... [228]
Deleted: The
Formatted ... [229]
Deleted: used as inputs for radiative transfer calculation
Formatted ... [230]
Deleted: nearest
Formatted ... [231]
Deleted:
Formatted ... [232]
Deleted: inversion …roduct. To minimize the influence of temporal difference, the micro-physical …arameters of AERONET measured nea…losestr ... [233]
Formatted ... [234]
Deleted: when …f the OMI was flying over ... [235]
Deleted: It is notable
Formatted ... [236]
Deleted: ,
Formatted: Font: 10 pt, English (US)
Deleted: and
Formatted ... [237]
Deleted: . These facts
Deleted: , which
Formatted ... [238]
Formatted: Font: 10 pt, English (US)
Deleted: measurements
Formatted ... [239]
Formatted ... [240]
Formatted ... [241]
Formatted ... [242]
Deleted: separately from AERONET
Deleted: ….wW… first use DISAMAR to ... [243]
Deleted: , and the optical properties of …nto a bi-modal aerosols…with a fraction in DISAMAR are calculated by externally mixing the derived modes with a fraction ... [244]
Formatted ... [245]
Formatted ... [246]
Formatted ... [247]
Formatted ... [248]

$$w_{\sigma,c} = 1 - w_{\sigma,f}, \quad (10)$$

Where the σ_f and σ_c are the extinction cross section of the fine and coarse aerosols. The expansion coefficients of the mixed aerosol is weighed by the ω_0 of the fine and coarse aerosols ($\omega_{0,f}$ and $\omega_{0,c}$), respectively:

$$w_{\omega_0,f} = \frac{w_f \sigma_f \omega_{0,f}}{w_f \sigma_f \omega_{0,f} + w_c \sigma_c \omega_{0,c}}, \quad (11)$$

$$w_{\omega_0,c} = 1 - w_{\omega_0,f}, \quad (12)$$

The AERONET instrument at this site only cover the visible and infrared band (440 nm to 1018 nm) for sky radiance measurements, i.e. no aerosol inversion products at UV band. Due to the absence of observations, assumptions have to be made on the spectral dependence of aerosol properties to obtain their values in the near-UV band. The properties of biomass burning aerosol depend on the type of fuel, the procedure producing the smoke, the age of the smoke, and also the atmospheric conditions (Reid et al., 2005). Using measurements to constrain the input aerosol refractive index can reduce the uncertainties due to a-priori knowledge. Our treatment on the complex refractive index is as following: (1) take the complex refractive index at visible band (440 to 675 nm) from AERONET measurements; (2) linearly extrapolate the complex refractive index to near-UV band. The real part n_r for radiative transfer calculation is obtained in this step. A slight wavelength dependence of n_r is found from the measurements (Fig.9 (a)); (3) for the imaginary part n_i, we multiply it (for the entire wavelength from UV to visible) with a scaling factor as we set it as a free parameter. By varying the value of the scaling factor, both the magnitude and the wavelength dependence of n_i can change to meet the requirement of retrieval (Fig.9 (b)).

3.1.4 CALIOP backscattering coefficient

The CALIOP on-board CALIPSO, which was launched in 2006, provides high-resolution profiles of aerosols and clouds. It has three channels with one measuring the backscattering intensity at 1064 nm and the rest measuring orthogonally polarized components at 532 nm backscattering intensity (Winker and Omar, 2006). Due to the limited spatial coverage, CALIOP did not observe the Chile wildfires plume for all the cases where the OMI observation available. We only use the total attenuated backscatter at 532 nm from level 1B Version 4.10 Standard data to evaluate the parameterized aerosol profiles (https://eosweb.larc.nasa.gov/project/calipso).

3.2 Methodology

In this study, we employ the radiative transfer model DISAMAR to simulate the near-UV AAI from OMI and to derive the ω_0 for a specific case, i.e. the Chile wildfires in January 2017. We select the period from 26 to 30 January 2017 (28 January is excluded due to lack of data) when the AAI value reached its peak.

The forward simulation consists of two major steps. First, DISAMR calculates the Mie aerosol optical properties with aerosol micro-physical information taken from AERONET measurements (r_g, n_r and n_i). As mentioned in Section 3.1.3, we set the spectral-dependent imaginary part n_i as a free parameter to vary ω_0. Then, DISAMAR operates radiative transfer calculation with the calculated aerosol optical properties for the corresponding aerosol and environmental conditions of OMI.

It is noted that the observed aerosol vertical distribution is limited for the Chile wildfires. Previous research suggested AAI cannot be quantitatively used without τ or z_{aer} information (Gassó and Torres, 2016). Instead, we implement the same parameterization as in the sensitivity study to obtain the aerosol layer height. Since the AAI dependence on Δz is minor (Fig.4 (c)), and to reduce the computational cost, Δz is set a constant of 2 km based on the information from the CALIOP measurements of backscattering coefficient (β) at 532 nm (Fig.7). The z_{aer}, to which the AAI is highly sensitive, is treated as an unknown variable to be retrieved together with ω_0.

Formatted ... [249]
Formatted: Font: 10 pt, English (US)
Formatted ... [250]
Formatted ... [251]
Formatted ... [252]
Deleted: TSecondly, the measuring wavelengthspectral bands of the AERONET instrument at this site only covers the visible band. To constrain the spectral dependency of optical properties values inin the near-UV band, , n_r and $n_i$complex refractive index n_r and n_i are linearly extrapolated using available data between 440 and 675 nm. Finally, the AERONET retrieved ω_0 is also linearly interpolated toat 550 nm nm due to discrete sampling bands.
Formatted: Font: 10 pt, English (US)
Formatted: Left
Formatted ... [253]
Deleted: i
Deleted: s
Formatted: Font: 10 pt, English (US)
Deleted: In this study, w
Deleted:
Formatted: Font: 10 pt, English (US)
Deleted: for which
Formatted: Font: 10 pt, English (US)
Deleted: we have
Formatted: Font: 10 pt, English (US)
Formatted: English (US)
Formatted ... [254]
Deleted: Except for the measurement geometry and surface conditions, the aerosol inputs used in the radiative transfer calculation should be independent of OMI measurements. The aerosol information consists of the cloud free column τ retrieved from MODIS,
Formatted: Font: 10 pt, English (US)
Deleted: and the aerosol micro-physical parameters (r_g, n_r and n_i) retrieved from AERONET. For the real part of the refractive index n_r we use the spectrally interpolated/extrapolated values from AERONET, whereas for the imaginary part n_i we scale the AERONET derived values to vary ω_0. ¶
Formatted: Font: 10 pt, English (US)
Deleted: T
Formatted: Font: 10 pt, English (US)
Deleted: information
Formatted ... [255]
Deleted: profile
Deleted: dependency
Formatted ... [256]
Formatted ... [257]

Consequently, with various combinations of z_{aer} and ω_0, a lookup table (LUT) of the calculated AAI is constructed with DISAMAR. It should be noted that for all pixels in the plume we assume the same aerosol microphysical properties as well as the same aerosol layer height. Pixels outside the plume may have had significantly different properties and this will affect the results. As shown in Fig.8, the distribution of OMI measurements is sparse in space, which implies that the dataset is quite sensitive to geographical outliers that may cause the heterogeneous properties of the plume. Consequently, we apply a data quality control procedure before retrieving ω_0. First, we manually remove the pixels that are geographically isolated from the main plume. Furthermore, we remove the potential outliers based on statistical tool. We filter the dataset using an outlier detection based on the interquartile range (IQR) of the AAI difference between DISAMAR simulations and OMI measurements. According to Tukey's fences (Tukey, 1977), an AAI difference falling outside range between Q1-1.5 IQR and Q3+1.5 IQR may be regarded as an outlier and removed, where Q1 and Q3 are the first and third quartiles of the AAI difference, and the IQR is the range between Q1 and Q3. Only the data passing the outlier detection criterion is used to calculate the cost function (Eq.(13)):

$$\mathrm{RMSE} = \sqrt{\frac{\sum_i^n \left(AAI_{DSM,i}^{qualified} - AAI_{OMI,i}\right)^2}{n}}, \quad (13)$$

Here AAI_i indicates the AAI for ith satellite pixel of the selected OMI data; subscripts *DSM* and *OMI* indicate DISAMAR simulation and OMI observation, respectively. The combination of z_{aer} and ω_0 that leads to the minimum residue is used to simulate the AAI.

Finally, the simulated AAI is compared with OMI observations. We also employ the independent data from GOME-2 as a reference to identify the potential bias of OMI. Similarly, the τ retrieved from OMI and AERONET serves as a reference to that of MODIS. The estimated aerosol layer height and ω_0 at 550 nm are evaluated with independent observations from CALIOP and AERONET, respectively.

4 Results and discussion

By applying the methodology described in the previous section, we quantitatively retrieved the aerosol layer height and ω_0 at 550 nm of the Chile 2017 wildfires by AAI simulation. The OMI measurements of the plume are displayed in Fig.8 (a) – (d). The presented satellite pixels are with AAI value larger than 1, and are free of cloud contamination, sun-glint and row anomaly of the instrument. Fortunately, the remaining data is still able to capture the main plume features. It can be clearly seen that from 26 to 30 January, the plume produced by wildfires in the central Chile was transported by the south-easterly trade wind from the continent towards the lower latitude region of the Pacific Ocean. The plume travelled over a distance of 3000 km during the period.

The vertical movement of the plume is given by CALIOP backscattering coefficient measurements (β) at 532 nm (Fig.7). The CALIOP paths closest to the plume are marked by a black dashed line in Fig.7. It is noted that due to the spatial coverage and the measuring time difference, CALIOP are not able to represent the entire plume detected by OMI. The aerosol layer captured by CALIOP is distributed from 2 km to 6 km, with an average height at approximately 4-5 km. The ascent of the plume was driven by the heat generated by the fires and sunlight absorption, as well as the atmospheric vertical motions.

Fig.8 (e) – (h) show the AAI simulation selected by the data quality control mentioned in Section 3.2. The spatial distribution of the simulated AAI shows similar patterns as the OMI observations. Some data points that are geographically isolated from the plume, e.g. in case 26 and 30 January, differ strongly from what are observed inside the plume. Including these outliers in the optimization could bias the retrieved aerosol properties. This can also be seen in Fig.8 (i) – (l), where the

Deleted: ¶
Deleted: W
Formatted ... [259]
Deleted: ω_0
Formatted ... [258]
Formatted ... [260]
Deleted: ground …ixels in the plume we assume the same aerosol ... [261]
Formatted ... [262]
Deleted: Besides
Formatted ... [263]
Deleted: data size of the pre-processed
Formatted ... [264]
Deleted: is relatively small and the sample distribution …s rather ... [265]
Formatted ... [266]
Deleted: is
Formatted ... [267]
Commented [JV18]: What do you mean here
Commented [Sj19R18]: It means the number of observations ... [269]
Formatted ... [268]
Deleted:
Formatted ... [270]
Deleted: ¶
Formatted ... [271]
Deleted: w
Formatted ... [272]
Commented [JV20]: We first fit, then apply the outlier, then ... [273]
Commented [Sj21R20]: I implied that by the scatter plots in ... [275]
Formatted ... [274]
Formatted ... [276]
Formatted ... [277]
Deleted: ground
Formatted ... [278]
Deleted: on MetOp-A/B …s a reference to evaluate ... [279]
Formatted ... [280]
Deleted: profile
Formatted ... [281]
Formatted ... [282]
Deleted: In this study
Formatted ... [283]
Deleted: profile
Formatted ... [284]
Deleted: ground
Formatted ... [285]
Deleted: and
Formatted ... [286]
Deleted: from …f the …loud contamination, the …un-glint effect ... [287]
Formatted ... [288]
Deleted: But i
Formatted ... [289]
Deleted: probably did not always measure the plume feature, and ... [290]
Formatted ... [291]
Deleted: plume, e.g. on 26 January.
Formatted ... [292]
Deleted: ascending
Formatted ... [293]

points passing the data quality control described in Section 3.2 are highlighted in red color. By removing the outliers, the average spatial correlation coefficient reaches 0.90.

Table 2 lists the statistics of the qualified AAI data, in terms of the median, relative difference and RMSE. The median of measured AAI ranges from 2 to 4 during the research period. Except for 26 January, the median of simulated AAI in other cases is in good agreement with the measurements, with relative differences within ±6%. The RMSE is only acceptable reflects that part of the plume cannot be fit by the assumptions in the forward simulation. The majority of the simulated AAI for 26 January is negatively biased, which is reflected by the small slope without an intercept correction in Fig.8 (i). A systematic bias in the inputs might cause this result. In terms of ω_0, both the AERONET measured and the AAI retrieved aerosol absorption become weaker with time (Table 2). Although the simulated and observed AAI are in good agreement, the difference in ω_0 is significant. The mean of the retrieved ω_0 at 550 nm for the whole period is 0.84, contrast to the AERONET measurements with a mean value of 0.90.

There are many sources contributing to this discrepancy in ω_0. First of all, the nearest site Santiago Beauchef is not exactly in the primary biomass burning regions as mentioned in section 3.1.3. The AERONET site is located in downtown, where reflective urban or industrial aerosols may have been mixed with the smoke and enhanced the ω_0. This would also affect the spectral dependence of complex refractive index used to constrain the radiative transfer calculation. According to Table 2, the retrieved n_i reveals that the difference between 354 and 388 nm is less than 5%. This small spectral dependence of n_i is mainly determined by AERONET measurements in the visible band (dashed lines), whereas the effect of the scaling factor is minor in this case (Fig.9 (b)). We thus find a much weaker wavelength dependence than the value in Jethva and Torres (2011) study, where a 20% difference between the two UV wavelengths was applied to OMAERUV algorithm to achieve the result that 70% of the retrieved ω_0 differ less than ±0.03 from the ω_0 from the AERONET measurements. This 20% spectral dependence adopted in their work is associated with findings of Hoffer et al. (2006). They conducted in situ measurements on humic-like substances (HULIS) of Amazonia biomass burning aerosols and found that around 35% - 50% light absorption occurred at 300 nm, whereas only around 15% at 400 nm. In terms of the absorbing Ångström exponent (AÅE), a 20% increase at 354 nm with respect to the value at 388 nm is equivalent to an AÅE value between 2.5 and 3, depending on the aerosol models of OMAERUV. According to Kirchstetter et al. (2004), the AÅE of urban pollution is near unit and biomass burning aerosols ranges is approximately 2 between 300 nm to 1 μm. Bergstrom et al. (2007) also confirmed this conclusion from several field programs (SAFARI 2000, ACE Asia, PRIDE, TARFOX, INTEX-A). From the sensitivity study of Jethva and Torres (2011), a stronger spectral dependence of n_i between 354 and 388 nm would allow simulations to reach a higher AAI while keeping n_i at a relatively low level. In our study, this means to retrieve a higher ω_0 at 550 nm. The presence of non-absorbing aerosols weakens the spectral dependence (particularly in the UV spectral range) and the linear extension would overestimate the aerosol absorption in the visible band. Furthermore, the AERONET inversion product is not error-free. The uncertainty of size distribution retrieval is minor for biomass burning aerosols (Dubovik et al., 2000), but under optically thick circumstances, even when retrievals are quality-assured (i.e. level 2 data), the reported accuracy of complex refractive index is 0.04 for n_r and 30%-50% for n_i, respectively (Dubovik et al., 2002). It is also reported that AERONET tends to underestimate the absorption of biomass burning aerosols compared with in situ measurements (Dubovik et al., 2002; Reid et al., 2004). The uncertainty of ω_0 is 0.03 under high aerosol loading ($\tau_{440} > 0.5$) and 0.05-0.07 under low aerosol loading (Dubovik et al., 2002; Holben et al., 2006). Last but not least, the spatial representation of the in situ instrument also concerns. Santese et al. (2007) showed that the selected AERONET aerosol parameters can be representative of a 300×300 km^2 southeast Italy area. For the Chile wildfires with the most remote pixel over 3000 km away from the continent, the measurements at AERONET cannot fully represent the plume detected by satellites.

Apart from AERONET itself, information from other datasets could also bias our estimate of aerosol absorption. Among all the inputs, the parameterization of a one-layer box-shape aerosol profile could be the largest error source. Although the influence of Δz on the AAI is limited (Fig.4 (c)), the AAI calculation highly depends on z_{aer} (Fig.4 (b)). As shown in Table 2,

Deleted: u
Deleted: for
Formatted ... [294]
Deleted: .
Deleted: low …MSE is only acceptable reflects that part of the ... [297]
Formatted ... [295]
Deleted: T
Formatted ... [296]
Formatted ... [298]
Deleted: of
Formatted ... [299]
Deleted: ¶
Formatted ... [300]
Deleted: , which reflects is in correspondence with the smoke ... [301]
Deleted: . T
Formatted ... [303]
Deleted: he mean
Formatted ... [304]
Deleted: while
Formatted ... [302]
Formatted ... [305]
Deleted: provide
Formatted ... [306]
Formatted ... [307]
Formatted ... [308]
Deleted: . This difference might be due to the fact that the selected ... [309]
Formatted ... [310]
Moved down [2]: it is also reported that AERONET tends to
Deleted: Last but not least
Deleted: Also,
Deleted: micro-physics parameters retrieved from …ERONET ... [312]
Formatted ... [311]
Formatted ... [313]
Commented [JV22]: Should these be left in? The AERONET ... [315]
Commented [Sj23R22]: Just mention that AERONET ... [317]
Deleted: .
Formatted ... [314]
Formatted ... [316]
Deleted: U
Formatted ... [318]
Moved (insertion) [2]
Deleted: i… is also reported that AERONET tends to ... [319]
Formatted ... [320]
Deleted: while only
Formatted ... [321]
Deleted: ¶
Formatted ... [322]
Deleted: Although
Formatted ... [323]
Deleted: could overestimate the ω_0
Formatted ... [324]
Deleted: the
Formatted ... [325]
Deleted:
Formatted ... [326]
Deleted: due to the lack of observations
Deleted: s… Although the influence of Δz on the AAI is small ... [327]
Formatted ... [328]

the estimated plume altitude varies from 4.5 to 4.9 km. As the black solid line indicated in Fig.7, the retrieved z_{aer} can approximately capture the measured geometric vertical location of the plume. The z_{aer} on 26 January seems overestimated because of the temporal and spatial difference. Concretely, CALIOP sampled the plume near the sources and close to the surface, while the plume observed by OMI had been already elevated and transported to the open ocean. The lack of information on the real plume height makes it challenging to determine whether the plume height is responsible for the systematic bias in Fig.8 (i). Except for 26 January, z_{aer} is in good agreement with what CALIOP observed. Although the retrieved aerosol layer heights are convincing to some extent, one should keep in mind that CALIOP and OMI observations are not exactly co-located. Besides, the parameterized aerosol profile may fail to represent the spatial variation of the plume. Therefore, the uncertainty cannot be directly determined due to the lack of validation data.

Among the four days for which we retrieved ω_0, the value for 27 January is significantly lower than others. For this day the agreement with CALIOP is reasonable and also the CALIOP track is not far away from the OMI measurement. We therefore explore the effect of observational biases in AAI and τ on the retrieved ω_0. We investigate the potential bias of these two datasets by plotting the histogram of the AAI measurement difference between GOME-2 and OMI (Fig.10 (a)), against the τ measurement difference between MODIS and OMI (Fig.10 (b), both are converted into 550 nm). It is clear that on 27 January, the AAI from OMI seems to be overestimated compared to GOME-2. Although the difference in wavelength pair choice for AAI retrieval, measurement conditions, etc., could contribute to the AAI discrepancy between GOME-2 and OMI, exploring the difference between the two datasets is beyond the scope of this study. In aspect of input aerosol concentration, the τ from MODIS could be potentially underestimated. Fitting a higher AAI with a lower input τ leads to an overestimation in aerosol absorption. Here, we analytically quantify the impact of τ for this specific case by systematically enhancing the τ of MODIS with a constant variation ($\Delta\tau$) added to all pixels, with the AAI level and the aerosol layer height remain unchanged. Fig.10 (c) presents how the AAI RMSE and the estimated ω_0 respond to the enhanced τ. It can be clearly seen that an increase in overall τ level by 0.07 raises ω_0 to 0.84 and optimizes the AAI simulation to a RMSE less than 0.45. If we apply this τ adaption, the retrieved ω_0 of 27 January becomes more consistent with the other days.

Apart from the observational errors in AERONET, OMI and MODIS data, the assumption that the plume features are homogeneous could also result in the discrepancy between AAI retrieved and AERONET measured ω_0. In reality, the plume altitude, the optical properties and even the chemical compositions could vary in space and time, while our simulations cannot take into account those effects.

5 Conclusions

Biomass burning is a major source of absorbing aerosols, making a significant contribution to climate warming. Quantitatively characterizing the absorption by biomass burning aerosols is therefore important to reduce the uncertainty in assessments of global radiative forcing. Facing the lack of long-term ω_0 records, this study explores an approach to retrieve ω_0 based on reflectivity in the near-UV channel measured by OMI. Although AAI is not a geophysical parameter and depends on many factors, its independence from pre-defined aerosol types, its high sensitivity to aerosol absorption as well as its long-term data record, makes it an attractive parameter to aerosol research.

We test the retrieval of ω_0 for the wildfires happening in central Chile in January 2017. After filtering the data from outliers, high spatial correlation coefficients (0.85 to 0.95) reach between the simulated and observed AAI. The retrieved aerosol layer heights indicate the plume was elevated to height of 4.5-4.9 km during the research period. These results are in agreement with CALIOP measurements. This average of the retrieved ω_0 at 550 nm is approximately 0.84, which is 0.06 lower than that of AERONET retrieval. The sources for discrepancy includes: the location of the AERONET site that may bias the measured ω_0 and the spectral dependence of complex refractive index; the simplified parameterization of the aerosol profile; the insufficient spatial representativeness of a single AERONET site; the observational errors in the input aerosol

Deleted: accurately
Formatted ... [329]
Deleted: the main reason
Formatted ... [330]
Deleted: However, One should keep in mind that a
Formatted ... [331]
Deleted: profiles
Formatted ... [332]
Deleted: retrieved
Formatted ... [333]
Deleted: T
Deleted: observations
Formatted ... [334]
Deleted: From
Deleted: for the …ther day ... [336]
Formatted ... [335]
Formatted ... [337]
Deleted: potentia
Formatted ... [338]
Deleted: l
Deleted: ¶ ... [340]
Formatted ... [339]
Deleted: 9
Formatted ... [341]
Deleted: 9
Formatted ... [342]
Moved (insertion) [1]
Deleted: However…Although , …t…e difference in wavelength ... [343]
Formatted ... [344]
Deleted: also be responsible for
Deleted: . E… exploring the difference between the two datasets is ... [346]
Formatted ... [345]
Formatted ... [347]
Deleted: while
Formatted ... [348]
Deleted:
Formatted ... [349]
Deleted: But one should keep in mind that
Moved up [1]: However, the difference in wavelength pair choice
Deleted: .
Deleted: Hereby
Formatted ... [350]
Deleted: sample points
Formatted ... [351]
Deleted: profile
Formatted ... [352]
Deleted: 9
Formatted ... [353]
Deleted: estimated
Formatted ... [354]
Deleted: ,
Deleted: will be
Formatted ... [355]
Deleted: cases
Deleted: and static plume
Deleted: neglect
Formatted ... [356]
Deleted: such as BC
Formatted ... [357]
Deleted: , posing
Formatted ... [358]
Deleted: on
Formatted ... [359]
Deleted:
Formatted ... [360]
Deleted: provides
Deleted: parameters
Formatted ... [361]

micro-physics, τ, as well as AAI; and the assumption of homogeneous and static plume properties, which ignores the plume evolution over space and time. We quantitatively analyze the uncertainty of τ for a specific case (27 January) when the estimated aerosol layer height is in good agreement with the CALIOP measurements. An improvement in retrieved ω_0 can be seen by adapting the magnitude of aerosol concentration.

This study proves the potential of utilizing OMI measured AAI to quantitatively characterize aerosol optical properties like ω_0. Currently, it is challenging to retrieve and validate results without reliable aerosol profile information. In the future, the availability of daily global aerosol layer height data, e.g. the L2 aerosol layer height product of TROPOspheric Monitoring Instrument on-board Sentinel-5 Precursor (TROPOMI) that is underdevelopment (Sanders and de Haan, 2016), are expected to provide a stronger constraint on the forward calculation and to reduce the uncertainty in the retrieved aerosol properties. It is also reliable to retrieve aerosol absorption for each individual pixel with constraint of the aerosol layer height product. The problem due to the poor spatial representativeness of in situ measurement can then be eased by comparing with the retrievals of nearby satellite pixels. Perhaps, more sophisticated assumptions on spectral-dependent aerosol absorption (e.g. steeper gradient of n_i in UV than visible band) have to be made and evaluated by other observational aerosol properties in UV spectral range, e.g. AERONET measured τ in UV band, instead of only depending on measured refractive index in visible band.

Acknowledgements

This work was performed in the framework of the KNMI Multi-Annual Strategic Research (MSO). The authors thank to NASA's GES-DISC, LAADS DAAC and ASDC for free online access of OMI, MODIS and CALIOP data. The authors also thank to the Centre for Climate Resilience Research (CR)2 at University of Chile (CONICYT/FONDAP/15110009) providing the data of the Santiago, Beauchef AERONET station.

References

Bergstrom, R. W., Pilewskie, P., Russell, P. B., Redemann, J., Bond, T. C., Quinn, P. K. and Sierau, B.: Spectral absorption properties of atmospheric aerosols, Atmos. Chem. Phys., 7(23), 5937–5943, doi:10.5194/acp-7-5937-2007, 2007.

Bond, T. C., Streets, D. G., Yarber, K. F., Nelson, S. M., Woo, J. H. and Klimont, Z.: A technology-based global inventory of black and organic carbon emissions from combustion, J. Geophys. Res. D Atmos., 109, D14203, doi:10.1029/2003JD003697, 2004.

Bond, T. C., Doherty, S. J., Fahey, D. W., Forster, P. M., Berntsen, T., Deangelo, B. J., Flanner, M. G., Ghan, S., Kärcher, B., Koch, D., Kinne, S., Kondo, Y., Quinn, P. K., Sarofim, M. C., Schultz, M. G., Schulz, M., Venkataraman, C., Zhang, H., Zhang, S., Bellouin, N., Guttikunda, S. K., Hopke, P. K., Jacobson, M. Z., Kaiser, J. W., Klimont, Z., Lohmann, U., Schwarz, J. P., Shindell, D., Storelvmo, T., Warren, S. G. and Zender, C. S.: Bounding the role of black carbon in the climate system: A scientific assessment, J. Geophys. Res. Atmos., 118, 5380–5552, doi:10.1002/jgrd.50171, 2013.

Buchard, V., Silva, A. M., Colarco, P. R., Darmenov, A., Randles, C. A., Govindaraju, R., Torres, O. and Goddard, N.: Using the OMI aerosol index and absorption aerosol optical depth to evaluate the NASA MERRA Aerosol Reanalysis, Atmos. Chem. Phys., 15, 5743–5760, doi:10.5194/acp-15-5743-2015, 2015.

Colarco, P. R., Gassó, S., Ahn, C., Buchard, V., Dasilva, A. M. and Torres, O.: Simulation of the Ozone Monitoring Instrument aerosol index using the NASA Goddard Earth Observing System aerosol reanalysis products, Atmos. Meas. Tech., 10(11), 4121–4134, doi:10.5194/amt-10-4121-2017, 2017.

Corr, C. A., Krotkov, N., Madronich, S., Slusser, J. R., Holben, B., Gao, W., Flynn, J., Lefer, B., Kreidenweis, S. M., Collins, F., Sciences, E., County, B., Division, A. C., Resource, N., Collins, F., Branch, B. S. and Sciences, A.: Retrieval of aerosol single scattering albedo at ultraviolet wavelengths at the T1 site during MILAGRO, Atmos. Chem. Phys., 9, 5813–

Deleted: AAI and
Formatted: Font: 10 pt, English (US)
Formatted: English (US)
Deleted: the aerosol micro-physics
Formatted: Font: 10 pt, English (US)
Deleted: s
Formatted: Font: 10 pt, English (US)
Deleted: profile
Formatted: Font: 10 pt, English (US)
Formatted: Font: 10 pt, English (US)
Formatted: Font color: Text 1
Formatted: Font color: Text 1, (Asian) Chinese (China)
Formatted: Font color: Text 1
Formatted: Font color: Text 1
Formatted: Font color: Text 1
Formatted: Font color: Text 1
Formatted: Font color: Text 1
Formatted: Font color: Text 1
Deleted: This study proves the potential of utilizing OMI measured AAI to quantitatively characterize aerosol optical properties like ω0. Even without direct observation of aerosol profiles, this parameter can also be retrieved with quite good confidence. However, apart ... [376]
Formatted: Font: 10 pt, Font color: Text 1, English (US)
Formatted: Font color: Text 1, English (UK)
Deleted: work, a chemistry transport model is needed to describe ... [377]
Formatted: Font: 10 pt, English (US)
Formatted: English (US)
Formatted: Font: 10 pt, English (US)
Formatted: English (US)
Deleted:
Formatted: Font: 10 pt, English (US)
Formatted: English (US)
Formatted: Font: 10 pt, English (US)
Formatted: English (US)
Formatted: English (US)
Deleted: ¶
Formatted: Font: 10 pt, English (US)
Formatted ... [378]
Formatted: Left, Line spacing: 1.5 lines
Formatted: Left
Deleted: Adler, G., Flores, J. M., Abo Riziq, A., Borrmann, S. ... [379]
Formatted: Font: 10 pt, English (US)
Formatted: Font: 10 pt, English (US), Not Highlight
Formatted: Font: 10 pt, English (US)
Deleted: ??
Formatted: Font: 10 pt, English (US)
Formatted: Font: 10 pt, English (US)
Formatted: Left, Line spacing: 1.5 lines
Formatted ... [380]
Formatted: Left
Formatted: Font: 10 pt, English (US)

5827, 2009.

Curier, R. L., Veefkind, J. P., Braak, R., Veihelmann, B., Torres, O. and de Leeuw, G.: Retrieval of aerosol optical properties from OMI radiances using a multiwavelength algorithm: Application to western Europe, J. Geophys. Res. Atmos., 113, D17S90, doi:10.1029/2007JD008738, 2008.

Deroubaix, A., Martiny, N., Chiapello, I. and Marticorena, B.: Remote Sensing of Environment Suitability of OMI aerosol index to re fl ect mineral dust surface conditions : Preliminary application for studying the link with meningitis epidemics in the Sahel, Remote Sens. Environ., 133, 116–127, doi:10.1016/j.rse.2013.02.009, 2013.

de Graaf, M., Stammes, P., Torres, O. and Koelemeijer, R. B. A.: Absorbing Aerosol Index: Sensitivity analysis, application to GOME and comparison with TOMS, J. Geophys. Res. D Atmos., 110, D01201, doi:10.1029/2004JD005178, 2005.

de Haan, J. F.: DISAMAR Algorithm description and background information, De Bilt, 2011.

de Haan, Johan F., Bosma, P.B and Hovenier, J. W.: The adding method for multiple scattering of polarized light, Astron. Astrophys., 183, 371–391, 1987.

Dubovik, O., Holben, B., Eck, T. F., Smirnov, A., Kaufman, Y. J., King, M. D., Tanré, D., Slutsker, I., Sciences, G. E. and Directorate, E. S.: Variability of Absorption and Optical Properties of Key Aerosol Types Observed in Worldwide Locations, J. Atmos. Sci., 59(3), 590–608, doi:10.1175/1520-0469(2002)059<0590:VOAAOP>2.0.CO;2, 2002.

Dubovik, O., Holben, B. N., Kaufman, Y. J., Yamasoe, M., Smirnov, A., Tanré, D. and Slutsker, I.: Single-scattering albedo of smoke retrieved from the sky radiance and solar transmittance measured from ground, J. Geophys. Res., 103, 31903–31923, doi:10.1029/98JD02276, 1998.

Dubovik, O. and King, M. D.: A flexible inversion algorithm for retrieval of aerosol optical properties from Sun and sky radiance measurements, J. Geophys. Res., 105, 20637–20969, doi:10.1029/2000JD900282, 2000.

Dubovik, O., Smirnov, A., Holben, B. N., King, M. D., Kaufman, Y. J., Eck, T. F. and Slutsker, I.: Accuracy assessments of aerosol optical properties retrieved from Aerosol Robotic Network (AERONET) Sun and sky radiance measurements, J. Geophys. Res., 105, 9791–9806, doi:10.1029/2000JD900040, 2000.

Eck, T. F., Holben, B. N., Ward, D. E., Mukelabai, M. M., Dubovik, O., Smirnov, A., Schafer, J. S., Hsu, N. C., Piketh, S. J., Queface, A., Roux, J. Le, Swap, R. J. and Slutsker, I.: Variability of biomass burning aerosol optical characteristics in southern Africa during the SAFARI 2000 dry season campaign and a comparison of single scattering albedo estimates from radiometric measurements, J. Geophys. Res., 108, 8477, doi:10.1029/2002JD002321, 2003.

Eck, T. F., Holben, B. N., Reid, J. S., Mukelabai, M. M., Piketh, S. J., Torres, O., Jethva, H. T., Hyer, E. J., Ward, D. E., Dubovik, O., Sinyuk, A., Schafer, J. S., Giles, D. M., Sorokin, M., Smirnov, A. and Slutsker, I.: A seasonal trend of single scattering albedo in southern African biomass-burning particles : Implications for satellite products and estimates of emissions for the world ' s largest biomass-burning source, J. Geophys. Res., 118, 6414–6432, doi:10.1002/jgrd.50500, 2013.

Gassó, S. and Torres, O.: The role of cloud contamination, aerosol layer height and aerosol model in the assessment of the OMI near-UV retrievals over the ocean, Atmos. Meas. Tech., 9(7), 3031–3052, doi:10.5194/amt-9-3031-2016, 2016.

Ginoux, P., Prospero, J. M., Torres, O. and Chin, M.: Long-term simulation of global dust distribution with the GOCART model: Correlation with North Atlantic Oscillation, Environ. Model. Softw., 19, 113–128, doi:10.1016/S1364-8152(03)00114-2, 2004.

Herman, J. R., Bhartia, P. K., Torres, O., Hsu, C., Seftor, C. and Celarier, E.: Global distribution of UV-absorbing aerosols from Nimbus 7/TOMS data, J. Geophys. Res., 102, 16911–16992, doi:10.1029/96JD03680, 1997.

Holben, B. N., Eck, T. F., Slutsker, I., Smirnov, A., Sinyuk, A., Schafer, J., Giles, D., Dubovik, O. and Lille, U. S. T. De: AERONET's Version 2 .0 quality assurance criteria, Int. Soc. Opt. Photonics, 6408, 64080Q, 2006.

Hsu, N. C., Tsay, S. C., King, M. D. and Herman, J. R.: Aerosol properties over bright-reflecting source regions, IEEE Trans. Geosci. Remote Sens., 42, 557–569, doi:10.1109/TGRS.2004.824067, 2004.

Formatted: Font: 10 pt, English (US)

Formatted: Font: 10 pt, English (US)

Deleted: Eck, T. F., Holben, B. N., Reid, J. S., Mukelabai, M. M., Piketh, S. J., Torres, O., Jethva, H. T., Hyer, E. J., Ward, D. E., Dubovik, O., Sinyuk, A., Schafer, J. S., Giles, D. M., Sorokin, M., Smirnov, A. and Slutsker, I.: A seasonal trend of single scattering albedo in southern African biomass-burning particles : Implications for satellite products and estimates of emissions for the world ' s largest biomass-burning source, J. Geophys. Res., 118, 6414–6432, doi:10.1002/jgrd.50500, 2013.¶

Formatted: Font: 10 pt, English (US)

Formatted: Font: (Default) SimSun, (Asian) SimSun, 10 pt, (Asian) Chinese (China), (Other) English (US)

Formatted: Font: 10 pt, English (US)

Deleted: ¶

Formatted: Font: 10 pt, English (US)

Formatted: Left

Formatted: Font: 10 pt, English (US)

Deleted: Ginoux, P. and Torres, O.: Empirical TOMS index for dust aerosol: Applications to model validation and source characterization, J. Geophys. Res., 108, 4534, doi:10.1029/2003JD003470, 2003.¶

Formatted: Font: 10 pt, English (US)

Formatted: Font: 10 pt, English (US)

Formatted: Font: 10 pt, English (US)

Hu, R. M., Martin, R. V. and Fairlie, T. D.: Global retrieval of columnar aerosol single scattering albedo from space-based observations, J. Geophys. Res. Atmos., 112, D02204, doi:10.1029/2005JD006832, 2007.

Hoffer, A., Gelencsér, A., Guyon, P., Kiss, G., Schmid, O., Frank, G. P., Artaxo, P. and Andreae, M. O.: Optical properties of humic-like substances (HULIS) in biomass-burning aerosols, Atmos. Chem. Phys., 6(11), 3563–3570, doi:10.5194/acp-6-3563-2006, 2006.

IPCC, 2007: Climate Change 2007: Synthesis Report. Contribution of Working Groups I, II and III to the Fourth Assessment Report of the Intergovernmental Panel on Climate Change [Core Writing Team, Pachauri, R.K and Reisinger, A. (eds.)]. IPCC, Geneva, Switzerland, 104 pp.

IPCC, 2014: Climate Change 2014: Synthesis Report. Contribution of Working Groups I, II and III to the Fifth Assessment Report of the Intergovernmental Panel on Climate Change [Core Writing Team, R.K. Pachauri and L.A. Meyer (eds.)]. IPCC, Geneva, Switzerland, 151 pp.

Jethva, H., Torres, O., Sciences, P. and Space, G.: Satellite-based evidence of wavelength-dependent aerosol absorption in biomass burning smoke inferred from Ozone Monitoring Instrument, , 10541–10551, doi:10.5194/acp-11-10541-2011, 2011.

Kaskaoutis, D.G.; Nastos, P.T.; Kosmopoulos, P.G.; Kambezidis, H.D.; Kharol, S.K.and Badarinath, K. V. S.: The Aura – OMI Aerosol Index distribution over Greece, Atmos. Res. J., 98, 28–39, doi:10.1016/j.atmosres.2010.03.018, 2010.

Kassianov, E. I., Barnard, J. C. and Ackerman, T. P.: Retrieval of aerosol microphysical properties using surface MultiFilter Rotating Shadowband Radiometer (MFRSR) data : Modeling and observations, J. Geophys. Res., 110, D09201, doi:10.1029/2004JD005337, 2005.

Kaufman, Y. J., Tanré, D. and Boucher, O.: A Satellite View of Aerosols in the Climate System, Nature, 419, 215–223, 2002.

Kirchstetter, T. W., Novakov, T. and Hobbs, P. V.: Evidence that the spectral dependence of light absorption by aerosols is affected by organic carbon, J. Geophys. Res. D Atmos., 109(21), 1–12, doi:10.1029/2004JD004999, 2004.

Koch, D. and Del Genio, A. D.: Black carbon semi-direct effects on cloud cover: Review and synthesis, Atmos. Chem. Phys., 10, 7685–7696, doi:10.5194/acp-10-7685-2010, 2010.

Lee, K. H., Li, Z., Kim, Y. J. and Kokhanovsky, A.: Atmospheric Aerosol Monitoring fromSatellite Observations: A History of Three Decades, in Atmospheric and Biological Environmental Monitoring, pp. 13–38., 2009.

Leroy, M., Deuzé, J. L., Bréon, F. M., Hautecoeur, O., Herman, M., Buriez, J. C., Tanré, D., Bouffiès, S., Chazette, P. and Roujean, J. L.: Retrieval of atmospheric properties and surface bidirectional reflectances over land from POLDER/ADEOS, J. Geophys. Res., 102, 17023-17037, doi:10.1029/96JD02662, 1997.

Levelt, P. F., Oord, G. H. J. Van Den, Dobber, M. R., Mälkki, A., Visser, H., Vries, J. De, Stammes, P., Lundell, J. O. V and Saari, H.: The Ozone Monitoring Instrument, IEEE Trans. Geosci. Remote Sens., 44, 1093–1101, 2006.\

Myhre, G., Shindell, D., Bréon, F. M., Collins, W., Fuglestvedt, J., Huang, J., ... & Nakajima, T.: Anthropogenic and Natural Radiative Forcing, Clim. Chang., 432, 658–740, 2013.

Nakajima, T., Tanaka, M. and Yamauchi, T.: Retrieval of the optical properties of aerosols from aureole and extinction data, Appl. Opt., 22, 2951–2959, 1983.

Nakajima, T., Tonna, G., Rao, R., Boi, P., Kaufman, Y. and Holben, B.: Use of sky brightness measurements from ground for remote sensing of particulate polydispersions, Appl. Opt., 35, 2672–2686, doi:10.1364/AO.35.002672, 1996.

NASA.gov: NASA's Terra Catches Fires in Central Chile, [online] Available from: https://www.nasa.gov/image-feature/goddard/2017/nasas-terra-catches-fires-in-central-chile (Accessed 1 May 2017), 2017.

Petters, J. L., Saxena, V. K., Slusser, J. R., Wenny, B. N. and Madronich, S.: Aerosol single scattering albedo retrieved from measurements of surface UV irradiance and a radiative transfer model, J. Geophys. Res., 108, 4288, doi:10.1029/2002JD002360, 2003.

Ramanathan, V. and Carmichael, G.: Global and regional climate changes due to black carbon, Nat. Geosci., 1, 221–227,

Formatted: Font: Not Bold, English (US), Do not check spelling or grammar

Formatted: Left, Line spacing: 1.5 lines

Deleted: ¶
Ialongo, I., Buchard, V., Brogniez, C., Casale, G. R. and Siani, A. M.: Aerosol Single Scattering Albedo retrieval in the UV range : an application to OMI satellite validation, Atmos. Chem. Phys., 10, 331–340, 2010.¶

Formatted: Font: 10 pt, English (US)

Formatted: Left, Don't adjust right indent when grid is defined, No widow/orphan control, Don't adjust space between Latin and Asian text, Don't adjust space between Asian text and numbers

Formatted: Left

Formatted: Font: 10 pt, English (US)

Formatted: Font: 10 pt, English (US)

Formatted: Font: 10 pt, English (US)

Deleted: Kaufman, Y. J.: Aerosol Optical Thickness and Atmospheric Path Radiance, J. Geophys. Res., 98, 2677–2692, doi:10.1029/92JD02427, 1993.¶
Kaufman, Y. J., Tanré, D., Remer, L. A., Vermote, E. F., Chu, A. and Holben, B. N.: Operational remote sensing of tropospheric aerosol over land from EOS moderate resolution imaging spectroradiometer, J. Geophys. Res., 102, 17051–17067, doi:10.1029/96JD03988, 1997.¶

Formatted: English (US)

Formatted: Left, Space Before: 0 pt, After: 0 pt, Line spacing: 1.5 lines

Deleted: ¶

Formatted: Font: 10 pt, English (US), Not Highlight

Formatted: Font: 10 pt, English (US)

Formatted: Left

Deleted: Lee, K. H., Li, Z., Wong, M. S., Xin, J., Wang, Y., Hao, W. and Zhao, F.: Aerosol single scattering albedo estimated across China from a combination of ground and satellite measurements, J. Geophys. Res., 112, D22S15, doi:10.1029/2007JD009077, 2007.¶

Formatted: Font: 10 pt, English (US)

Formatted: Font: 10 pt, English (US)

Formatted: Font: 10 pt, English (US)

Formatted: Font: 10 pt, English (US)

Formatted: Font: 10 pt, English (US)

Formatted: Font: 10 pt, English (US)

doi:10.1038/ngeo156, 2008.

Reid, J. S., Eck, T. F., Christopher, S. A., Koppmann, R., Dubovik, O., Eleuterio, D. P., Holben, B. N., Reid, E. A. and Zhang, J.: A review of biomass burning emissions part III: intensive optical properties of biomass burning particles, Atmos. Chem. Phys. Discuss., doi:10.5194/acpd-4-5201-2004, 2004.

Remer, L.A., Kaufman; Y.J., Tanré; D., Mattoo, S., Chu, D.A., Martins, J.V., Li, R.R., Ichiku, C., Levy, R.C., Kleidman, R.G., Eck, T.K., Vermote, E. and Holben, B. N.: The MODIS Aerosol Algorithm, Products, and Validation, J. Atmos. Sci., 62, 947–973, 2005.

Remer, L.A., Tanré, D. and Kaufman, Y. J.: Algorithm for remote sensing of tropospheric aerosol from MODIS:Collection 5 Product ID: MOD04/MYD04-C005., 1998.

Sanders, A.F.J. and de Haan, J.F: TROPOMI ATBD of the Aerosol Layer Height product, 2016.

Stein Zweers, D.C: TROPOMI ATBD of the UV aerosol index., 2016.

Santese, M., De Tomasi, F. and Perrone, M. R.: AERONET versus MODIS aerosol parameters at different spatial resolutions over southeast Italy, J. Geophys. Res. Atmos., 112(10), 1–12, doi:10.1029/2006JD007742, 2007.

Satheesh, S. K., Torres, O., Remer, L. A., Babu, S. S., Vinoj, V., Eck, T. F., Kleidman, R. G. and Holben, B. N.: Improved assessment of aerosol absorption using OMI-MODIS joint retrieval, J. Geophys. Res. Atmos., 114(5), 1–10, doi:10.1029/2008JD011024, 2009.

Tanr, D., J Kaufman, B. Y., Herman, M. and Mattoo, S.: Remote sensing of aerosol properties over oceans using the MODIS/EOS spectral radiances, J. Geophys. Res., 102, 16971–16988, doi:10.1029/96JD03437, 1997.

The Guardian: Chile battles devastating wildfires: 'We have never seen anything on this scale', [online] Available from: https://www.theguardian.com/world/2017/jan/25/chile-fire-firefighting-international-help?utm_source=Climate+News+Network&utm_campaign=afdf3cf10c-EMAIL_CAMPAIGN_2017_02_03&utm_medium=email&utm_term=0_1198ea8936-afdf3cf10c-38798061 (Accessed 25 Jan 2017), 2017.

Torres, O., Bhartia, P. K., Herman, J. R., Ahmad, Z. and Gleason, J.: Derivation of aerosol properties from satellite measurements of backscattered ultraviolet radiation: Theoretical basis, J. Geophys. Res. Atmos., 103, 17099–17110, doi:10.1029/98JD00900, 1998.

Torres, O., Bhartia, P. K., Sinyuk, A., Welton, E. J. and Holben, B.: Total Ozone Mapping Spectrometer measurements of aerosol absorption from space: Comparison to SAFARI 2000 ground-based observations, J. Geophys. Res. D Atmos., 110, D10S18, doi:10.1029/2004JD004611, 2005.

Torres, O., Tanskanen, A., Veihelmann, B., Ahn, C., Braak, R., Bhartia, P. K., Veefkind, P. and Levelt, P.: Aerosols and surface UV products from Ozone Monitoring Instrument observations : An overview, J. Geophys. Res., 112, D24S47, doi:10.1029/2007JD008809, 2007.

Torres, O., Jethva, H. and Bhartia, P. K.: Retrieval of Aerosol Optical Depth above Clouds from OMI Observations: Sensitivity Analysis and Case Studies, J. Atmos. Sci., 69, 1037–1053, doi:10.1175/JAS-D-11-0130.1, 2012.

Tukey, J.W.: Exploratory data analysis, Addison-Wesley Publishing Company, 1977.

Winker, D. M., Vaughan, M. A., Omar, A., Hu, Y., Powell, K. A., Liu, Z.;Hunt, W.H.;Young, S. A.: Overview of the CALIPSO Mission and CALIOP Data Processing Algorithms, Technol. J. Atmos. Ocean., 26, 2310–2323, doi:10.1175/2009JTECHA1281.1, 2009.

Yin, B., Min, Q. and Joseph, E.: Retrievals and uncertainty analysis of aerosol single scattering albedo from MFRSR measurements, J. Quant. Spectrosc. Radiat. Transf., 150, 95–106, doi:10.1016/j.jqsrt.2014.08.012, 2015.

Formatted: Font: 10 pt, English (US)

Formatted: Font: 10 pt, English (US)

Formatted: Font: 10 pt, English (US)

Formatted: Left, Line spacing: 1.5 lines

Formatted: Left

Deleted: ¶
D.C. Stein Zweers: TROPOMI ATBD of the UV aerosol index., 2016.

Formatted: Left, Space Before: 0 pt, After: 0 pt, Line spacing: 1.5 lines

Formatted: Left

Formatted: Font: 10 pt, English (US)

Deleted: ¶

Deleted: ¶

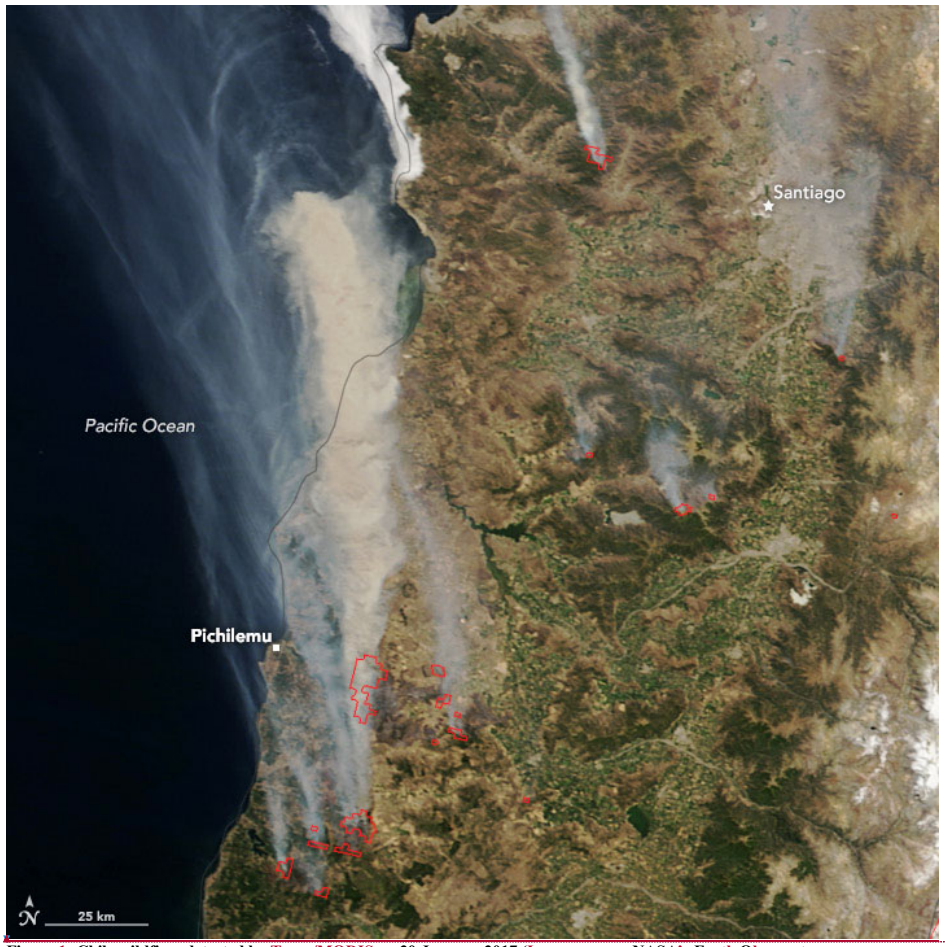

Figure 1: Chile wildfires detected by Terra/MODIS on 20 January 2017 (Image source: NASA's Earth Observatory https://earthobservatory.nasa.gov/IOTD/view.php?id=89496).

Deleted: ¶
¶
<object>¶

Formatted: Font: 10 pt

Formatted: Font: 10 pt, English (US)

Formatted: Font: 6.5 pt

Formatted: English (US)

Deleted: MODIS

Deleted: /Terra

Formatted: English (US)

Formatted: English (US), Check spelling and grammar

Deleted: 1

Deleted: https://earthobservatory.nasa.gov/IOTD/view.php?id=89496

Formatted: English (US)

Formatted: Default Paragraph Font, English (US)

Formatted: English (US)

Formatted: Font: 6.5 pt, English (US)

Formatted: Left

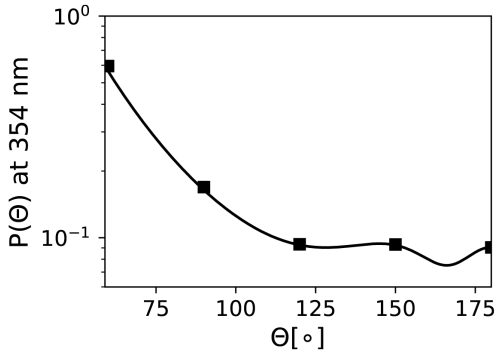

Figure 2: Phase function p(Θ) at 354 nm of the parameterized Mie scattering aerosol of default case (r_g = 0.15 μm, n_r = 1.5 and n_i = 0.06) in sensitivity analysis. The markers in the plot correspond to the value when Θ=60°, 90°, 120°, 150°, 180°.

Deleted: ¶

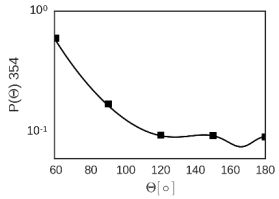

Deleted:

Formatted: Font: 10 pt, Bold

Formatted: Font: 6.5 pt

Formatted: Font: 6.5 pt, (Asian) Chinese (China), (Other) English (US)

Formatted: English (US)

Formatted: Font: 9 pt

Formatted: Font: 9 pt

Formatted: Font: 9 pt

Deleted: s

Formatted: English (US)

Formatted: Font: 10 pt, English (US)

Formatted: Left

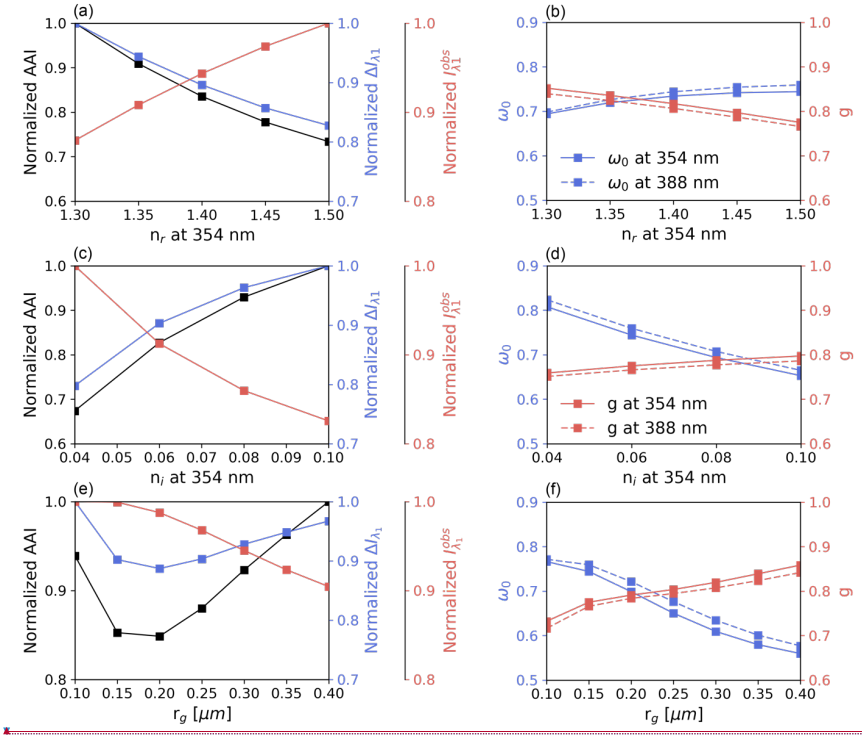

Figure 3: AAI sensitivity to micro-physical parameters: n_i (a, b), n_r (c, d), and r_g (e, f). The left panels (a, c and e) show the sensitivity of the normalized AAI (black), the normalized $\Delta I_{\lambda 1}$ (blue) and the normalized $I^{obs}_{\lambda 1}$ (red). The right panels (b, d and f) show ω_0 (blue) and g (red) at wavelength 354 (solid line) and 388 (dashed line) nm, respectively.

Deleted:

Formatted: Font: 10 pt

Formatted: Font: 10 pt, English (US)

Formatted: English (US)

Formatted: Caption, Add space between paragraphs of the same style

Formatted: English (US)

Formatted: English (US)

Formatted: English (US)

Formatted: English (US)

Formatted: English (US)

Formatted: English (US)

Formatted: English (US)

Formatted: Font: 10 pt, English (US)

Formatted: Left

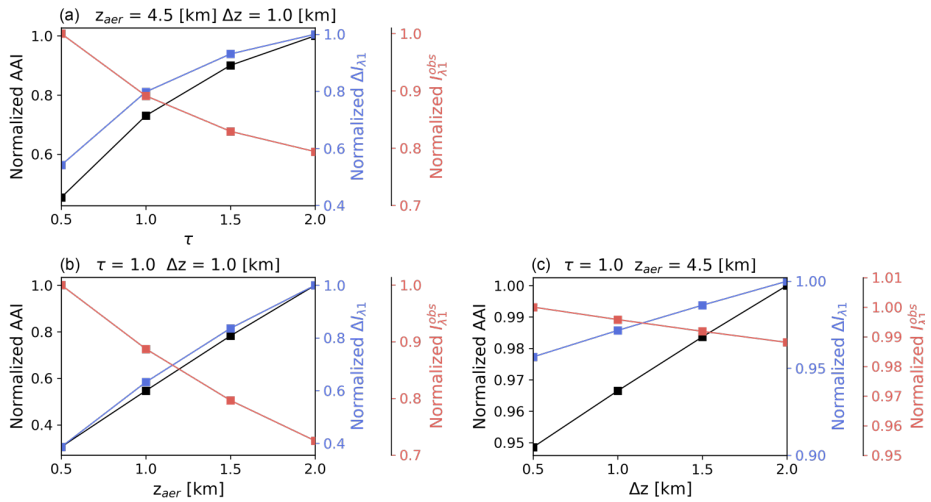

Figure 4: AAI sensitivity to macro-physical parameters: (a) τ at 550 nm, (b) z_{aer} and (c) Δz.

Deleted:

Formatted: Font: 10 pt

Formatted: Font: 10 pt, English (US)

Formatted: English (US)

Formatted: Font: 10 pt, English (US)

Formatted: Left

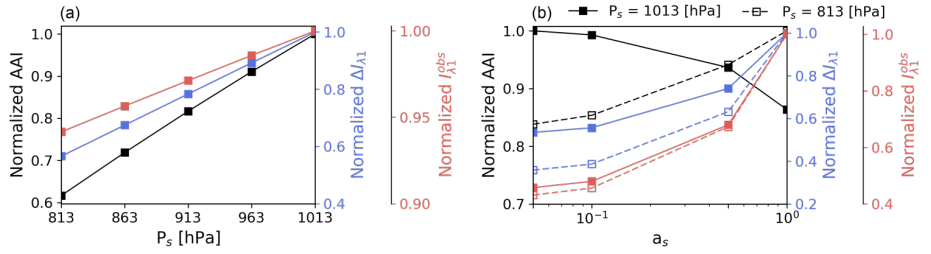

Figure.5 AAI sensitivity to surface parameters: P_s (a) and a_s (b). The solid line and dashed line in (b) indicates terrain height at sea level (P_s = 1013 hPa) and elevated terrain height (P_s = 813 hPa), respectively.

Deleted:

Formatted: Font: 10 pt

Formatted: Font: 10 pt, English (US)

Formatted: English (US)

Deleted: a

Formatted: English (US)

Deleted: P_s

Formatted: English (US)

Formatted: Font: 10 pt, English (US)

Formatted: Left

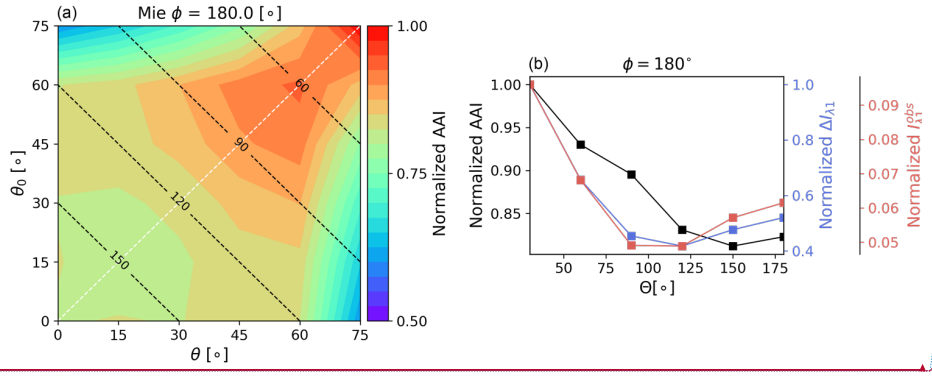

Figure.6 AAI sensitivity to θ and θ_0 at φ=180˚. The black dashed contour in (a) indicates the Θ=60°, 90°, 120°, 150°. The white dashed line in (a) indicates the cross sections, with its corresponding normalized AAI, $\Delta I_{\lambda 1}$ and $I_{\lambda 1}^{obs}$ in (b).

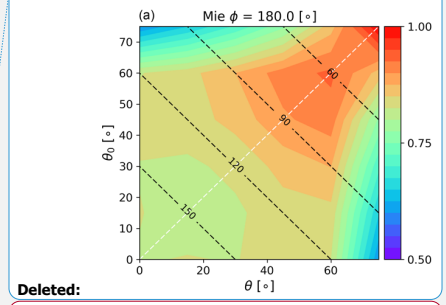

Deleted:

Formatted: Font: 10 pt, Bold

Formatted: Font: 10 pt, English (US)

Formatted: English (US)

Deleted: n.

Formatted: English (US)

Formatted: English (US)

Formatted: Font: 10 pt, English (US)

Formatted: Left

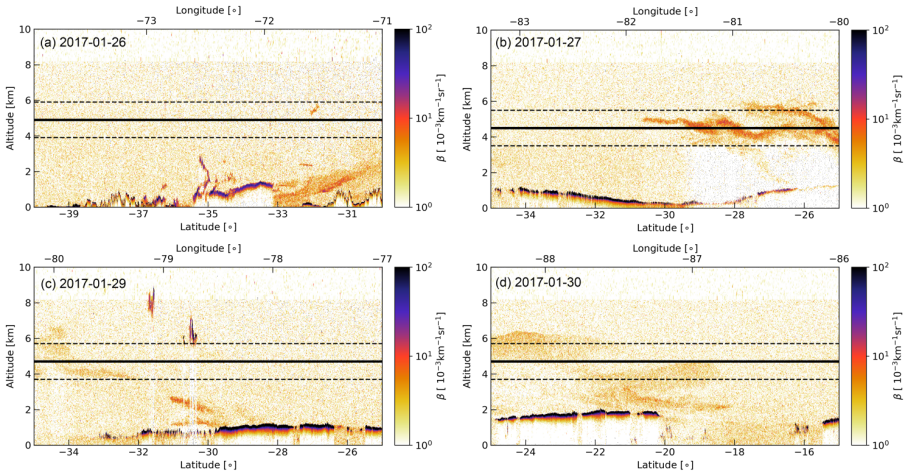

Figure.7 CALIOP backscatter coefficient β at 532 nm. The solid and dashed line indicate the retrieved z_{aer} and Δz, respectively. The red to black dots indicate clouds and the orange dots indicate aerosol layers, respectively.

Formatted: Font: 10 pt

Formatted: Font: 10 pt, English (US)

Formatted: English (US)

Formatted: English (US)

Formatted: Font: 10 pt, English (US)

Formatted: Left

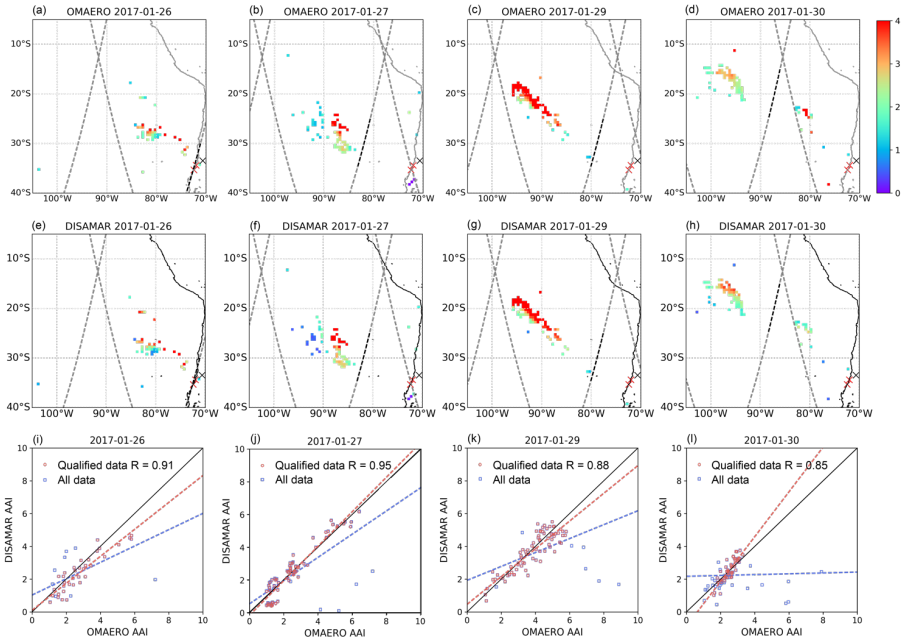

Figure.8 AAI from OMI observations (a–d) and DISAMAR simulations (e–h) of the Chile wildfires on 26, 27, 29 and 30 January 2017. The black and red cross symbols are the AERONET station and the main fire sources (Pichilemu W34.39° S72.00° and Consititución S35.33°, W72.42°), respectively. The grey dashed line indicates the CALIOP paths in the region of interest, where the paths used to validate the plume height are marked by black dashed line. The scatter plots (i–l) present the OMI observations against DISAMAR simulations for only qualified data (red dot) and all data (blue dot), respectively.

Formatted: Font: 10 pt
Formatted: Font: 10 pt, English (US)
Formatted: English (US)
Formatted: English (US)
Formatted: English (US)
Formatted: English (US)
Formatted: Font: 10 pt, English (US)
Formatted: Left

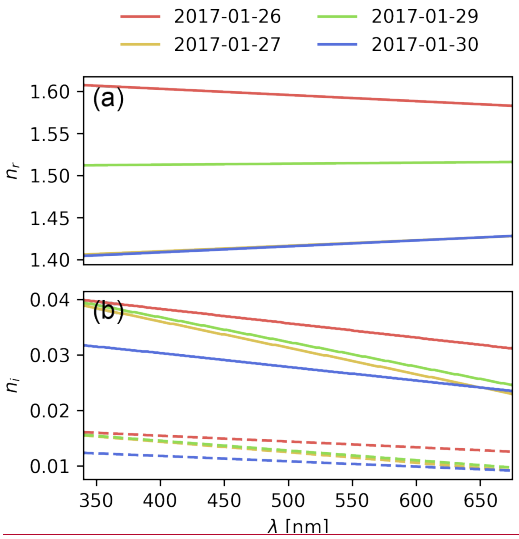

Figure.9 Retrieved complex refractive index for each case: (a) n_r and (b) n_i. The dashed line in lower panel is the wavelength dependent n_i measured by AERONET.

Formatted: Left

Formatted: Font: 10 pt, English (US)

Formatted: Font: 10 pt, English (US)

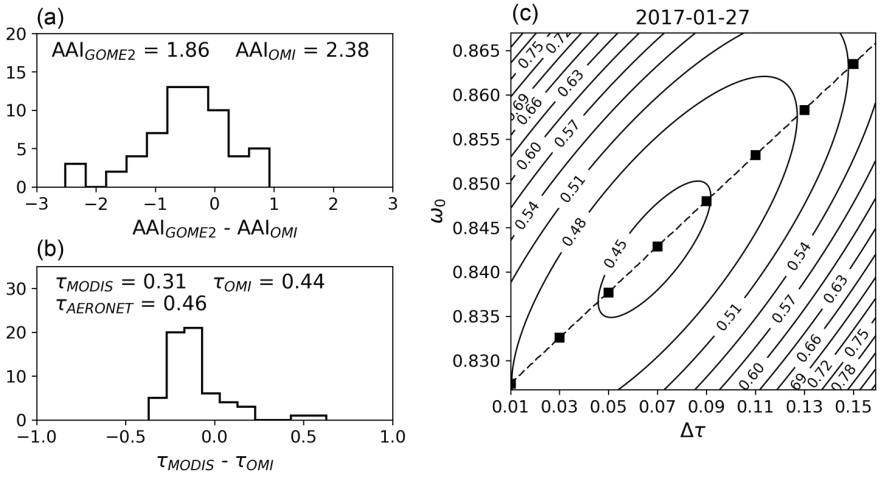

Figure.10 Histogram of (a) the AAI difference between GOME-2 and OMI, against (b) the τ difference at 550 nm between MODIS and OMI for 27 January. Contour of (c) the AAI RMSE as a function of variation in τ and ω_0 for 27 January. The dashed line is the best estimation for each pair of Δτ and ω_0.

Deleted: ¶

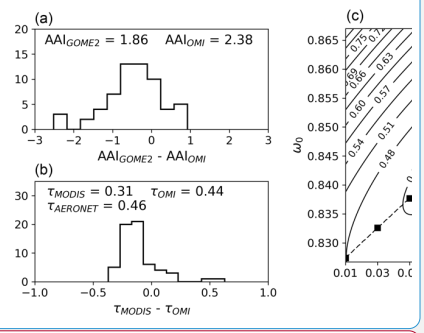

Formatted: Font: 10 pt

Formatted: Font: 10 pt, English (US)

Formatted: English (US)

Deleted: 9

Formatted: English (US)

Formatted: Font: 6.5 pt, English (US)

Formatted: Font: 10 pt, English (US)

Formatted: Normal

Formatted: English (US)

Formatted: Font: 10 pt, English (US)

Formatted: Font: 6.5 pt, English (US)

Table 1. Parameters used in sensitivity studies.

Parameters	Default value	Sensitivity range	Unit
Geometric mean radius (r_g)	0.15	0.1, 0.15, 0.2, 0.25, 0.3, 0.35, 0.4	μm
Geometric standard deviation (σ_g)	1.5	-	μm
Real refractive index (n_r) at 354 nm	1.5	1.3, 1.35, 1.4, 1.45, 1.5	-
Imaginary refractive index (n_i) at 354 nm	0.06	0.04, 0.06, 0.08, 0.1	-
Aerosol layer geometric central height (z_{aer})	4.5	2.5, 4.5, 6.5, 8.5	km
Aerosol layer geometric thickness (Δz)	1	0.5, 1, 1.5, 2	km
Aerosol optical thickness (τ) at 550 nm	1	0.5, 1, 1.5, 2	-
Surface albedo (a_s)	0.05	0.05, 0.1, 0.5, 1.0	-
Surface pressure (P_s)	1013	1013, 963, 913, 863, 813	hPa
Solar zenith angle (θ_0)	30	0, 15, 30, 45, 60, 75	°
Viewing zenith angle (θ)	0	0, 15, 30, 45, 60, 75	°
Relative azimuth angle ($\Delta\Phi = \varphi - \varphi_0$+180°	0	0, ±45, ±90, ±135, ±180	°

Deleted: analysis

Formatted ... [381]
Formatted ... [382]
Formatted ... [383]
Formatted ... [387]
Formatted ... [388]
Formatted ... [384]
Formatted ... [385]
Formatted ... [386]
Formatted ... [389]
Formatted ... [390]
Formatted ... [391]
Formatted ... [392]
Formatted ... [393]
Formatted ... [394]
Formatted ... [395]
Formatted ... [396]
Formatted ... [397]
Formatted ... [398]
Formatted ... [399]
Formatted ... [400]
Formatted ... [401]
Formatted ... [402]
Formatted ... [403]
Formatted ... [404]
Formatted ... [405]
Formatted ... [406]
Formatted ... [407]
Formatted ... [408]
Formatted ... [409]
Formatted ... [410]
Formatted ... [411]
Formatted ... [412]
Formatted ... [413]
Formatted ... [414]
Formatted ... [415]
Formatted ... [416]
Formatted ... [417]
Formatted ... [418]
Formatted ... [419]
Formatted Table ... [420]
Formatted ... [421]
Formatted ... [422]
Formatted ... [423]
Formatted ... [424]
Formatted ... [425]
Formatted ... [426]
Formatted ... [427]
Formatted ... [428]
Formatted ... [429]
Formatted ... [430]
Formatted ... [431]
Formatted ... [432]
Formatted ... [433]
Formatted ... [434]
Formatted ... [435]
Formatted ... [436]
Formatted ... [437]
Formatted ... [438]
Formatted ... [439]
Formatted ... [440]
Formatted ... [441]
Formatted ... [443]
Formatted ... [444]
Formatted ... [445]
Formatted ... [446]
Formatted ... [447]

Table.2 Summary of retrieved results (after applying IQR outlier detection).

Date		2017-01-26	2017-01-27	2017-01-29	2017-01-30
Number of pixels in the plume		44	70	82	75
AAI	AAI median (OMAERO)	2.52	2.38	4.05	2.61
	AAI median (DISAMAR)	2.17	2.48	3.81	2.49
	Relative difference (%)	-13.88	4.20	-5.93	-4.60
	RMSE	0.67	0.51	0.60	0.41
Aerosol profile parameters	z_{aer} [km]	4.9	4.5	4.7	4.7
	Δz [km]	2			
n_s	n_s at 354 nm	0.0395	0.0382	0.0388	0.0314
	n_s at 388 nm	0.0386	0.0366	0.0373	0.0306
	n_s difference between 354 and 388 nm	2.33%	4.37%	4.02%	2.61%
ω_0 at 550 nm	ω_0 (AERONET)	0.89	0.89	0.92	0.91
	ω_0 (DISAMAR)	0.83	0.81	0.87	0.85
	Relative difference (%)	-6.74	-8.99	-5.43	-6.59

Appendix A

Formatted: Font: Bold

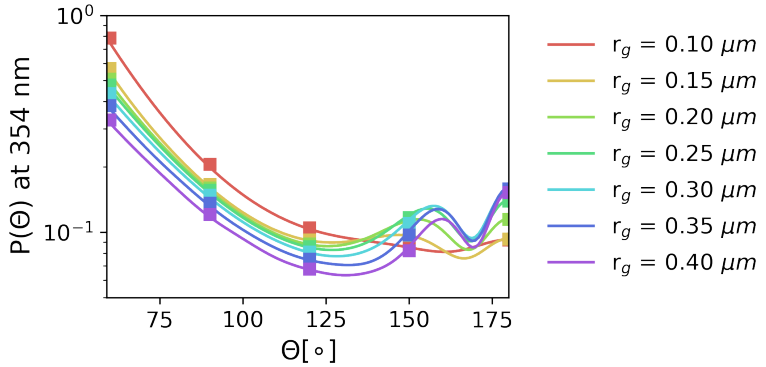

Figure.A1: Phase function p(Θ) at 354 nm of the parameterized Mie scattering aerosol in sensitivity studies as a function of r_g (with n_r = 1.5 and n_i = 0.06). The markers in the plot correspond to values when Θ=60°, 90°, 120°, 150°, 180°.

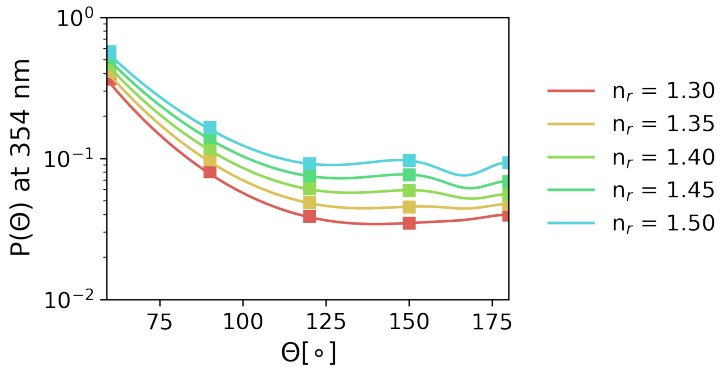

Figure.A2: Phase function p(Θ) at 354 nm of the parameterized Mie scattering aerosol in sensitivity studies as a function of n_r (with r_g = 0.15 µm and n_i = 0.06). The markers in the plot correspond to values when Θ=60°, 90°, 120°, 150°, 180°.

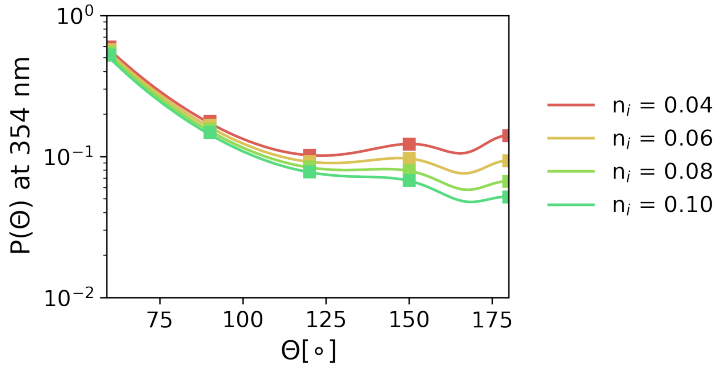

Figure.A3: Phase function p(Θ) at 354 nm of the parameterized Mie scattering aerosol in sensitivity studies as a function of n_i (with r_g = 0.15 µm and n_r = 1.5). The markers in the plot correspond to values when Θ=60°, 90°, 120°, 150°, 180°.

280

Formatted: Font: 10 pt, Bold, English (US)

Page 7: [1] Formatted **Sun ji** **8/10/18 6:00:00 PM**

English (UK)

Page 7: [2] Formatted **Sun ji** **6/11/18 1:55:00 PM**

Font: 12 pt, English (US)

Page 7: [3] Formatted **Sun ji** **6/11/18 1:55:00 PM**

Font: 10 pt, English (US)

Page 7: [4] Formatted **Sun ji** **5/15/18 10:32:00 PM**

Left

Page 7: [5] Formatted **Sun ji** **5/15/18 10:32:00 PM**

Left

Page 7: [6] Formatted **Sun ji** **6/11/18 1:55:00 PM**

English (US), Not Highlight

Page 7: [6] Formatted **Sun ji** **6/11/18 1:55:00 PM**

English (US), Not Highlight

Page 7: [6] Formatted **Sun ji** **6/11/18 1:55:00 PM**

English (US), Not Highlight

Page 7: [6] Formatted **Sun ji** **6/11/18 1:55:00 PM**

English (US), Not Highlight

Page 7: [6] Formatted **Sun ji** **6/11/18 1:55:00 PM**

English (US), Not Highlight

Page 7: [7] Deleted **Sun ji** **5/22/18 4:38:00 PM**

The absorbing aerosol index (AAI) based on the near Ultra-Violet (near-UV) remote sensing techniques is a qualitative parameter that allows to retrieve aerosol optical properties with confidence

Page 7: [8] Formatted **Sun ji** **6/11/18 1:55:00 PM**

Font: 10 pt, English (US)

Page 7: [8] Formatted **Sun ji** **6/11/18 1:55:00 PM**

Font: 10 pt, English (US)

Page 7: [9] Deleted **Sun ji** **8/10/18 2:14:00 PM**

a series of

Page 7: [9] Deleted **Sun ji** **8/10/18 2:14:00 PM**

a series of

Page 7: [9] Deleted **Sun ji** **8/10/18 2:14:00 PM**

a series of

Page 7: [10] Formatted **Sun ji** **6/11/18 1:55:00 PM**

Font: 10 pt, English (US)

Page 7: [11] Formatted **Sun ji** **6/11/18 1:55:00 PM**

Font: 10 pt, English (US)

Page 7: [12] Formatted **Sun ji** **6/11/18 1:55:00 PM**

Font: 10 pt, English (US)

Page 7: [13] Formatted **Sun ji** **6/11/18 1:55:00 PM**

Font: 10 pt, English (US)

Page 7: [14] Deleted **Sun ji** **5/8/18 11:59:00 AM**

and

Page 7: [14] Deleted **Sun ji** **5/8/18 11:59:00 AM**

and

Page 7: [14] Deleted **Sun ji** **5/8/18 11:59:00 AM**

and

Page 7: [15] Formatted **Sun ji** **6/11/18 1:55:00 PM**

Font: 10 pt, English (US)

Page 7: [16] Deleted **Sun ji** **8/10/18 1:31:00 PM**

The

Page 7: [16] Deleted **Sun ji** **8/10/18 1:31:00 PM**

The

Page 7: [17] Formatted **Sun ji** **6/11/18 1:55:00 PM**

Font: 10 pt, English (US)

Page 7: [17] Formatted **Sun ji** **6/11/18 1:55:00 PM**

Font: 10 pt, English (US)

Page 7: [17] Formatted **Sun ji** **6/11/18 1:55:00 PM**

Font: 10 pt, English (US)

Page 7: [17] Formatted **Sun ji** **6/11/18 1:55:00 PM**

Font: 10 pt, English (US)

Page 7: [18] Formatted **Sun ji** **6/11/18 1:55:00 PM**

English (US), Not Highlight

Page 7: [18] Formatted **Sun ji** **6/11/18 1:55:00 PM**

English (US), Not Highlight

Page 7: [19] Formatted **Sun ji** **6/11/18 1:55:00 PM**

Font: 10 pt, (Asian) Chinese (China), (Other) English (US)

Page 7: [20] Formatted **Sun ji** **6/11/18 1:55:00 PM**

Font: 10 pt, English (US)

Page 7: [21] Commented [Sj1] **Sun ji** **5/15/18 4:25:00 PM**

Because the data in this case is sensitive to outliers, we applied outlier detection to remove outlier first.

Page 7: [22] Formatted **Sun ji** **6/11/18 1:55:00 PM**

Font: 5.5 pt

Page 7: [22] Formatted **Sun ji** **6/11/18 1:55:00 PM**

Font: 5.5 pt

Page 7: [22] Formatted **Sun ji** **6/11/18 1:55:00 PM**

Font: 5.5 pt

Page 7: [22] Formatted **Sun ji** **6/11/18 1:55:00 PM**

Font: 5.5 pt

Page 7: [23] Formatted **Sun ji** **6/11/18 1:55:00 PM**

Font: 10 pt, English (US)

Page 7: [24] Formatted **Sun ji** **6/11/18 1:55:00 PM**

Font: 5.5 pt

Page 7: [25] Formatted **Sun ji** **6/11/18 1:55:00 PM**

Font: 10 pt, English (US)

Page 7: [25] Formatted **Sun ji** **6/11/18 1:55:00 PM**

Font: 10 pt, English (US)

Page 7: [25] Formatted **Sun ji** **6/11/18 1:55:00 PM**

Font: 10 pt, English (US)

Page 7: [25] Formatted **Sun ji** **6/11/18 1:55:00 PM**

Font: 10 pt, English (US)

Page 7: [26] Formatted **Sun ji** **6/11/18 1:55:00 PM**

Font: 10 pt, (Asian) Chinese (China), (Other) English (US)

Page 7: [27] Formatted **Sun ji** **6/11/18 1:55:00 PM**

English (US)

Page 7: [27] Formatted **Sun ji** **6/11/18 1:55:00 PM**

English (US)

Page 7: [28] Formatted **Sun ji** **6/11/18 1:55:00 PM**

English (US)

Page 7: [29] Formatted **Sun ji** **6/11/18 1:55:00 PM**

Font: 10 pt, English (US)

Page 7: [29] Formatted **Sun ji** **6/11/18 1:55:00 PM**

Font: 10 pt, English (US)

Page 7: [29] Formatted **Sun ji** **6/11/18 1:55:00 PM**

Font: 10 pt, English (US)

Page 7: [30] Deleted **JP Veefkind** **5/15/18 8:23:00 AM**

slightly smaller than the value of 0.90 measured independently by the AERONET instrument.

Page 7: [31] Deleted **Sun ji** **5/8/18 12:03:00 PM**

relative distance

Page 7: [31] Deleted **Sun ji** **5/8/18 12:03:00 PM**

relative distance

Page 7: [31] Deleted **Sun ji** **5/8/18 12:03:00 PM**

relative distance

Page 7: [32] Formatted **Sun ji** **6/11/18 1:55:00 PM**

Font: 10 pt, English (US)

Page 7: [32] Formatted **Sun ji** **6/11/18 1:55:00 PM**

Font: 10 pt, English (US)

Page 7: [33] Deleted **Sun ji** **5/8/18 12:07:00 PM**

Except for the observational errors, the impact of remaining error sources on ω_0 retrieval is difficult to quantify.

Page 7: [34] Deleted **Sun ji** **4/23/18 2:30:00 PM**

They consist of fine particles (aerodynamic diameter smaller than 2.5 μm) that have adverse impacts on the environment and human health (Bäumer et al., 2008; Adler et al., 2011). Biomass burning aerosols

Page 7: [35] Formatted **Sun ji** **6/11/18 1:55:00 PM**

Font: 10 pt, English (US)

Page 7: [35] Formatted **Sun ji** **6/11/18 1:55:00 PM**

Font: 10 pt, English (US)

Page 7: [35] Formatted **Sun ji** **6/11/18 1:55:00 PM**

Font: 10 pt, English (US)

Page 7: [35] Formatted **Sun ji** **6/11/18 1:55:00 PM**

Font: 10 pt, English (US)

Page 7: [36] Deleted **Sun ji** **4/23/18 2:28:00 PM**

also

Page 7: [36] Deleted **Sun ji** **4/23/18 2:28:00 PM**

also

Page 7: [37] Formatted **Sun ji** **6/11/18 1:55:00 PM**

Font: 10 pt, English (US)

Page 7: [37] Formatted **Sun ji** **6/11/18 1:55:00 PM**

Font: 10 pt, English (US)

Page 7: [38] Deleted **Sun ji** **8/10/18 1:44:00 PM**

Page 7: [38] Deleted **Sun ji** **8/10/18 1:44:00 PM**

Page 7: [39] Formatted **Sun ji** **6/11/18 1:55:00 PM**

Font: 10 pt, English (US)

Page 7: [39] Formatted **Sun ji** **6/11/18 1:55:00 PM**

Font: 10 pt, English (US)

Page 7: [39] Formatted **Sun ji** **6/11/18 1:55:00 PM**

Font: 10 pt, English (US)

Page 7: [40] Deleted **Sun ji** **4/23/18 2:09:00 PM**

), one type of absorbing aerosol, black carbon (BC), can be considered as the second important warming agent after carbon dioxide. Absorbing aerosols heat the atmosphere primarily by interaction with solar radiation. They directly absorb the incoming or reflected sunlight. They are also able to reduce the reflectivity of the planet by depositing on bright surfaces

Page 7: [41] Formatted	Sun ji	6/11/18 1:55:00 PM

Font: 10 pt, English (US)

Page 7: [42] Deleted	Sun ji	4/23/18 2:09:00 PM

(Huang et al., 2013

Page 7: [42] Deleted	Sun ji	4/23/18 2:09:00 PM

(Huang et al., 2013

Page 7: [43] Formatted	Sun ji	6/11/18 1:55:00 PM

Font: 10 pt, English (US)

Page 7: [43] Formatted	Sun ji	6/11/18 1:55:00 PM

Font: 10 pt, English (US)

Page 7: [43] Formatted	Sun ji	6/11/18 1:55:00 PM

Font: 10 pt, English (US)

Page 7: [43] Formatted	Sun ji	6/11/18 1:55:00 PM

Font: 10 pt, English (US)

Page 7: [43] Formatted	Sun ji	6/11/18 1:55:00 PM

Font: 10 pt, English (US)

Page 7: [43] Formatted	Sun ji	6/11/18 1:55:00 PM

Font: 10 pt, English (US)

Page 7: [43] Formatted	Sun ji	6/11/18 1:55:00 PM

Font: 10 pt, English (US)

Page 7: [44] Deleted	Sun ji	4/23/18 2:12:00 PM

Quantifying the climate effect of absorbing aerosols is therefore important.

Page 7: [44] Deleted	Sun ji	4/23/18 2:12:00 PM

Quantifying the climate effect of absorbing aerosols is therefore important.

Page 7: [45] Formatted	Sun ji	6/11/18 1:55:00 PM

Font: 10 pt, English (US)

Page 7: [45] Formatted	Sun ji	6/11/18 1:55:00 PM

Font: 10 pt, English (US)

Page 7: [45] Formatted	Sun ji	6/11/18 1:55:00 PM

Font: 10 pt, English (US)

Page 7: [45] Formatted **Sun ji** **6/11/18 1:55:00 PM**

Font: 10 pt, English (US)

Page 7: [46] Deleted **JP Veefkind** **5/14/18 11:53:00 AM**

.

Page 7: [46] Deleted **JP Veefkind** **5/14/18 11:53:00 AM**

.

Page 7: [47] Deleted **Sun ji** **5/22/18 5:41:00 PM**

,

Page 7: [47] Deleted **Sun ji** **5/22/18 5:41:00 PM**

,

Page 7: [48] Formatted **Sun ji** **6/11/18 1:55:00 PM**

Font: 10 pt, English (US)

Page 7: [48] Formatted **Sun ji** **6/11/18 1:55:00 PM**

Font: 10 pt, English (US)

Page 7: [48] Formatted **Sun ji** **6/11/18 1:55:00 PM**

Font: 10 pt, English (US)

Page 7: [48] Formatted **Sun ji** **6/11/18 1:55:00 PM**

Font: 10 pt, English (US)

Page 7: [48] Formatted **Sun ji** **6/11/18 1:55:00 PM**

Font: 10 pt, English (US)

Page 7: [49] Formatted **Sun ji** **6/11/18 1:55:00 PM**

English (US), Not Highlight

Page 7: [49] Formatted **Sun ji** **6/11/18 1:55:00 PM**

English (US), Not Highlight

Page 7: [49] Formatted **Sun ji** **6/11/18 1:55:00 PM**

English (US), Not Highlight

Page 7: [49] Formatted **Sun ji** **6/11/18 1:55:00 PM**

English (US), Not Highlight

Page 7: [49] Formatted **Sun ji** **6/11/18 1:55:00 PM**

English (US), Not Highlight

Page 7: [49] Formatted **Sun ji** **6/11/18 1:55:00 PM**

English (US), Not Highlight

Page 8: [50] Formatted **Sun ji** **6/11/18 1:55:00 PM**

English (US)

Page 8: [50] Formatted **Sun ji** **6/11/18 1:55:00 PM**

English (US)

Page 8: [50] Formatted **Sun ji** **6/11/18 1:55:00 PM**

English (US)

Page 8: [50] Formatted **Sun ji** **6/11/18 1:55:00 PM**

English (US)

Page 8: [51] Deleted **Sun ji** **5/22/18 11:30:00 AM**

ω_0 is defined as the ratio of the radiation scattered by aerosol particles to the total attenuation. Because aerosol compositions and properties are highly variable in space and time, measuring the global distribution of ω_0 relies on remote sensing techniques. The POLarization and Directionality of the Earth's Reflectances (POLDER) ω_0 from a combination of multi-angular, multi-spectral observations of the measures aerosol polarized phase function. This provides information directly related to ω_0 (Leroy et al., 1997). But However, there is no continuous temporal coverage because the first two instruments encountered technical hitches that prematurely ended the missions ended prematurely due to technical problems on the satellite level. The third POLDER instrument mission covered the period 2004-2014.

Page 8: [52] Formatted **Sun ji** **6/11/18 1:55:00 PM**

Font: 10 pt, (Asian) Chinese (China), (Other) English (US)

Page 8: [53] Deleted **Sun ji** **5/22/18 12:33:00 PM**

As a result, ω_0 is usually retrieved by forward simulations that are adapted to observational parameters. Many implementations have been done for ground-based network measurements (Dubovik et al., 1998; Eck et al., 2003; Petters et al., 2003; Kassianov et al., 2005; Corr et al., 2009; Yin et al., 2015), while relatively fewer applications to satellite instruments exist due to lack of validation (Lee et al., 2007; Ialongo et al., 2010; Eck et al., 2013). Moreover, a majority of those methods heavily depend on the aerosol optical thickness (τ), either in forward model simulations or in validation procedures. This makes the derived ω_0 subject to large uncertainties. The reason is that τ retrieval requires assumptions on aerosol types, and the commonly used τ that is retrieved in the visible band where the signal of bright surfaces is strong. Besides, the aerosol effect on radiance is inversely proportional to wavelength (Kaufman, 1993), and the sensitivity to ω_0 is not significant for most τ measurements in the visible and infrared band (Kaufman et al., 1997).

The

Page 8: [54] Formatted	Sun ji	6/11/18 1:55:00 PM

Font: 10 pt, (Asian) Chinese (China), (Other) English (US)

Page 8: [54] Formatted	Sun ji	6/11/18 1:55:00 PM

Font: 10 pt, (Asian) Chinese (China), (Other) English (US)

Page 8: [54] Formatted	Sun ji	6/11/18 1:55:00 PM

Font: 10 pt, (Asian) Chinese (China), (Other) English (US)

Page 8: [54] Formatted	Sun ji	6/11/18 1:55:00 PM

Font: 10 pt, (Asian) Chinese (China), (Other) English (US)

Page 8: [54] Formatted	Sun ji	6/11/18 1:55:00 PM

Font: 10 pt, (Asian) Chinese (China), (Other) English (US)

Page 8: [54] Formatted	Sun ji	6/11/18 1:55:00 PM

Font: 10 pt, (Asian) Chinese (China), (Other) English (US)

Page 8: [54] Formatted	Sun ji	6/11/18 1:55:00 PM

Font: 10 pt, (Asian) Chinese (China), (Other) English (US)

Page 8: [54] Formatted	Sun ji	6/11/18 1:55:00 PM

Font: 10 pt, (Asian) Chinese (China), (Other) English (US)

Page 8: [54] Formatted	Sun ji	6/11/18 1:55:00 PM

Font: 10 pt, (Asian) Chinese (China), (Other) English (US)

Page 8: [54] Formatted	Sun ji	6/11/18 1:55:00 PM

Font: 10 pt, (Asian) Chinese (China), (Other) English (US)

Page 8: [54] Formatted	Sun ji	6/11/18 1:55:00 PM

Font: 10 pt, (Asian) Chinese (China), (Other) English (US)

Page 8: [54] Formatted	Sun ji	6/11/18 1:55:00 PM

Font: 10 pt, (Asian) Chinese (China), (Other) English (US)

Page 8: [55] Formatted	Sun ji	6/11/18 1:55:00 PM

Font: 10 pt, English (US)

Page 8: [55] Formatted	Sun ji	6/11/18 1:55:00 PM

Font: 10 pt, English (US)

Page 8: [56] Formatted	Sun ji	6/11/18 1:55:00 PM

Font: 10 pt, English (US)

Page 8: [56] Formatted **Sun ji** **6/11/18 1:55:00 PM**

Font: 10 pt, English (US)

Page 8: [56] Formatted **Sun ji** **6/11/18 1:55:00 PM**

Font: 10 pt, English (US)

Page 8: [57] Formatted **Sun ji** **6/11/18 1:55:00 PM**

English (US), Not Highlight

Page 8: [57] Formatted **Sun ji** **6/11/18 1:55:00 PM**

English (US), Not Highlight

Page 8: [58] Formatted **Sun ji** **6/11/18 1:55:00 PM**

English (US), Not Highlight

Page 8: [58] Formatted **Sun ji** **6/11/18 1:55:00 PM**

English (US), Not Highlight

Page 8: [59] Deleted **Sun ji** **5/22/18 3:58:00 PM**

forward model simulations with the absorbing aerosol index (AAI) (Herman et al., 1997)

Page 8: [60] Formatted **Sun ji** **6/11/18 1:55:00 PM**

Font: 10 pt, English (US)

Page 8: [60] Formatted **Sun ji** **6/11/18 1:55:00 PM**

Font: 10 pt, English (US)

Page 8: [60] Formatted **Sun ji** **6/11/18 1:55:00 PM**

Font: 10 pt, English (US)

Page 8: [60] Formatted **Sun ji** **6/11/18 1:55:00 PM**

Font: 10 pt, English (US)

Page 8: [60] Formatted **Sun ji** **6/11/18 1:55:00 PM**

Font: 10 pt, English (US)

Page 8: [61] Formatted **Sun ji** **6/11/18 1:55:00 PM**

English (US)

Page 8: [61] Formatted **Sun ji** **6/11/18 1:55:00 PM**

English (US)

Page 8: [62] Deleted **Sun ji** **5/8/18 12:15:00 PM**

improving

Page 8: [62] Deleted **Sun ji** **5/8/18 12:15:00 PM**

improving

Page 8: [63] Formatted **Sun ji** **6/11/18 1:55:00 PM**

Font: 10 pt, English (US)

Page 8: [64] Formatted **Sun ji** **6/11/18 1:55:00 PM**

Font: 10 pt, English (US)

Page 8: [64] Formatted **Sun ji** **6/11/18 1:55:00 PM**

Font: 10 pt, English (US)

Page 8: [65] Deleted **Sun ji** **5/8/18 12:16:00 PM**

foremost

Page 8: [65] Deleted **Sun ji** **5/8/18 12:16:00 PM**

foremost

Page 8: [65] Deleted **Sun ji** **5/8/18 12:16:00 PM**

foremost

Page 8: [65] Deleted **Sun ji** **5/8/18 12:16:00 PM**

foremost

Page 8: [66] Formatted **Sun ji** **6/11/18 1:55:00 PM**

Font: 10 pt, English (US)

Page 8: [67] Deleted **Sun ji** **8/10/18 2:02:00 PM**

assumptions on aerosol types, which significantly reduce the retrieval uncertainty

Page 8: [68] Formatted **Sun ji** **6/11/18 1:55:00 PM**

Font: 10 pt, English (US)

Page 8: [68] Formatted **Sun ji** **6/11/18 1:55:00 PM**

Font: 10 pt, English (US)

Page 8: [68] Formatted **Sun ji** **6/11/18 1:55:00 PM**

Font: 10 pt, English (US)

Page 8: [68] Formatted **Sun ji** **6/11/18 1:55:00 PM**

Font: 10 pt, English (US)

Page 8: [68] Formatted **Sun ji** **6/11/18 1:55:00 PM**

Font: 10 pt, English (US)

Page 8: [68] Formatted **Sun ji** **6/11/18 1:55:00 PM**

Font: 10 pt, English (US)

Page 8: [68] Formatted **Sun ji** **6/11/18 1:55:00 PM**

Font: 10 pt, English (US)

Page 8: [69] Deleted **Sun ji** **4/23/18 6:58:00 PM**

.

Page 8: [69] Deleted **Sun ji** **4/23/18 6:58:00 PM**

.

Page 8: [70] Formatted **Sun ji** **6/11/18 1:55:00 PM**

Font: 10 pt, English (US)

Page 8: [70] Formatted **Sun ji** **6/11/18 1:55:00 PM**

Font: 10 pt, English (US)

Page 8: [71] Formatted **Sun ji** **6/11/18 1:55:00 PM**

English (US)

Page 8: [71] Formatted **Sun ji** **6/11/18 1:55:00 PM**

English (US)

Page 8: [71] Formatted **Sun ji** **6/11/18 1:55:00 PM**

English (US)

Page 8: [71] Formatted **Sun ji** **6/11/18 1:55:00 PM**

English (US)

Page 8: [72] Deleted **Sun ji** **4/23/18 7:02:00 PM**

, the sensitivity of τ in the visible band to ω_0 is lower over dark surfaces (Kaufman et al., 1997), while

Page 8: [73] Formatted **Sun ji** **6/11/18 1:55:00 PM**

Font: 10 pt, English (US)

Page 8: [73] Formatted **Sun ji** **6/11/18 1:55:00 PM**

Font: 10 pt, English (US)

Page 8: [74] Formatted **Sun ji** **6/11/18 1:55:00 PM**

Font: 10 pt, English (US)

Page 8: [75] Formatted **Sun ji** **6/11/18 1:55:00 PM**

Font: 10 pt, English (US)

Page 8: [76] Formatted **Sun ji** **6/11/18 1:55:00 PM**

Font: 10 pt, English (US)

Page 8: [76] Formatted **Sun ji** **6/11/18 1:55:00 PM**

Font: 10 pt, English (US)

Page 8: [77] Deleted **Sun ji** **4/23/18 3:58:00 PM**

Empirical models were also developed to build connections between the AAI and parameters it depends on. Hsu et al. (1999) found a linear relation between the TOMS retrieved AAI and Sun-photometer measured τ over regions with biomass burning and regions covered by African dust. Ginoux and Torres (2003) implemented an empirical relation between the AAI retrieved from TOMS with τ, ω_0 and surface pressure (P_s) to characterize the dust aerosols. Although requiring less computational cost, applying these empirical models is either limited by specific conditions or subject to large errors. Thus, these methods have not been widely used.

Page 8: [77] Deleted **Sun ji** **4/23/18 3:58:00 PM**

Empirical models were also developed to build connections between the AAI and parameters it depends on. Hsu et al. (1999) found a linear relation between the TOMS retrieved AAI and Sun-photometer measured τ over regions with biomass burning and regions covered by African dust. Ginoux and Torres (2003) implemented an empirical relation between the AAI retrieved from TOMS with τ, ω_0 and surface pressure (P_s) to characterize the dust aerosols. Although requiring less computational cost, applying these empirical models is either limited by specific conditions or subject to large errors. Thus, these methods have not been widely used.

Page 8: [78] Formatted **Sun ji** **6/11/18 1:55:00 PM**

English (US)

Page 8: [78] Formatted **Sun ji** **6/11/18 1:55:00 PM**

English (US)

Page 8: [79] Deleted **Sun ji** **5/8/18 12:19:00 PM**

, that

Page 8: [79] Deleted **Sun ji** **5/8/18 12:19:00 PM**

, that

Page 8: [79] Deleted **Sun ji** **5/8/18 12:19:00 PM**

, that

Page 8: [80] Formatted **Sun ji** **6/11/18 1:55:00 PM**

Font: 10 pt, English (US)

Page 8: [80] Formatted **Sun ji** **6/11/18 1:55:00 PM**

Font: 10 pt, English (US)

Page 8: [80] Formatted **Sun ji** **6/11/18 1:55:00 PM**

Font: 10 pt, English (US)

Page 8: [81] Formatted **Sun ji** **6/11/18 1:55:00 PM**

Font: 10 pt, English (US)

Page 8: [82] Deleted **Sun ji** **8/2/18 10:20:00 AM**

, this series of fires occurring in central Chile (Pichilemu 34.39˚S 72.00˚W and Consititución 35.33˚S, 72.42˚W) was

Page 8: [83] Formatted **Sun ji** **6/11/18 1:55:00 PM**

Font: 10 pt, English (US)

Page 8: [83] Formatted **Sun ji** **6/11/18 1:55:00 PM**

Font: 10 pt, English (US)

Page 8: [83] Formatted **Sun ji** **6/11/18 1:55:00 PM**

Font: 10 pt, English (US)

Page 8: [83] Formatted **Sun ji** **6/11/18 1:55:00 PM**

Font: 10 pt, English (US)

Page 8: [84] Formatted **Sun ji** **6/11/18 1:55:00 PM**

Font: 10 pt, English (US)

Page 8: [85] Deleted **Sun ji** **6/17/18 10:17:00 AM**

the MODerate-resolution Imaging Spectroradiometer (

Page 8: [85] Deleted **Sun ji** **6/17/18 10:17:00 AM**

the MODerate-resolution Imaging Spectroradiometer (

Page 8: [85] Deleted **Sun ji** **6/17/18 10:17:00 AM**

the MODerate-resolution Imaging Spectroradiometer (

Page 8: [86] Formatted **Sun ji** **6/11/18 1:55:00 PM**

Font: 10 pt, English (US)

Page 9: [87] Formatted **Sun ji** **5/15/18 10:32:00 PM**

Heading 2

Page 9: [88] Formatted **Sun ji** **5/15/18 10:32:00 PM**

Left

Page 9: [89] Formatted **Sun ji** **6/11/18 1:55:00 PM**

Font: 10 pt, English (US)

Page 9: [89] Formatted **Sun ji** **6/11/18 1:55:00 PM**

Font: 10 pt, English (US)

Page 9: [90] Deleted	Sun ji	4/23/18 11:42:00 AM

for

Page 9: [90] Deleted	Sun ji	4/23/18 11:42:00 AM

for

Page 9: [90] Deleted	Sun ji	4/23/18 11:42:00 AM

for

Page 9: [90] Deleted	Sun ji	4/23/18 11:42:00 AM

for

Page 9: [90] Deleted	Sun ji	4/23/18 11:42:00 AM

for

Page 9: [91] Formatted	Sun ji	6/11/18 1:55:00 PM

Font: 10 pt, English (US)

Page 9: [92] Formatted	Sun ji	6/11/18 1:55:00 PM

Font: 10 pt, English (US)

Page 9: [92] Formatted	Sun ji	6/11/18 1:55:00 PM

Font: 10 pt, English (US)

Page 9: [92] Formatted	Sun ji	6/11/18 1:55:00 PM

Font: 10 pt, English (US)

Page 9: [93] Formatted	Sun ji	6/11/18 1:55:00 PM

Font: 10 pt, English (US)

Page 9: [93] Formatted	Sun ji	6/11/18 1:55:00 PM

Font: 10 pt, English (US)

Page 9: [93] Formatted	Sun ji	6/11/18 1:55:00 PM

Font: 10 pt, English (US)

Page 9: [93] Formatted	Sun ji	6/11/18 1:55:00 PM

Font: 10 pt, English (US)

Page 9: [93] Formatted	Sun ji	6/11/18 1:55:00 PM

Font: 10 pt, English (US)

Page 9: [93] Formatted	Sun ji	6/11/18 1:55:00 PM

Font: 10 pt, English (US)

Page 9: [93] Formatted	Sun ji	6/11/18 1:55:00 PM

Font: 10 pt, English (US)

Page 9: [93] Formatted	Sun ji	6/11/18 1:55:00 PM

Font: 10 pt, English (US)

Page 9: [93] Formatted	Sun ji	6/11/18 1:55:00 PM

Font: 10 pt, English (US)

Page 9: [93] Formatted	Sun ji	6/11/18 1:55:00 PM

Font: 10 pt, English (US)

Page 9: [93] Formatted	Sun ji	6/11/18 1:55:00 PM

Font: 10 pt, English (US)

Page 9: [93] Formatted	Sun ji	6/11/18 1:55:00 PM

Font: 10 pt, English (US)

Page 9: [93] Formatted	Sun ji	6/11/18 1:55:00 PM

Font: 10 pt, English (US)

Page 9: [93] Formatted	Sun ji	6/11/18 1:55:00 PM

Font: 10 pt, English (US)

Page 9: [93] Formatted	Sun ji	6/11/18 1:55:00 PM

Font: 10 pt, English (US)

Page 9: [93] Formatted	Sun ji	6/11/18 1:55:00 PM

Font: 10 pt, English (US)

Page 9: [94] Formatted	Sun ji	6/11/18 1:55:00 PM

Font: 10 pt, English (US)

Page 9: [95] Deleted	JP Veefkind	5/14/18 12:25:00 PM

the model

Page 9: [95] Deleted	JP Veefkind	5/14/18 12:25:00 PM

the model

Page 9: [96] Formatted	Sun ji	6/11/18 1:55:00 PM

Font: 10 pt, English (US)

Page 9: [97] Formatted	Sun ji	6/11/18 1:55:00 PM

Font: 10 pt, English (US)

Page 9: [97] Formatted	Sun ji	6/11/18 1:55:00 PM

Font: 10 pt, English (US)

Page 9: [97] Formatted	Sun ji	6/11/18 1:55:00 PM

Font: 10 pt, English (US)

Page 9: [97] Formatted	Sun ji	6/11/18 1:55:00 PM

Font: 10 pt, English (US)

Page 9: [97] Formatted	Sun ji	6/11/18 1:55:00 PM

Font: 10 pt, English (US)

Page 9: [97] Formatted	Sun ji	6/11/18 1:55:00 PM

Font: 10 pt, English (US)

Page 9: [97] Formatted	Sun ji	6/11/18 1:55:00 PM

Font: 10 pt, English (US)

Page 9: [97] Formatted	Sun ji	6/11/18 1:55:00 PM

Font: 10 pt, English (US)

Page 9: [97] Formatted	Sun ji	6/11/18 1:55:00 PM

Font: 10 pt, English (US)

Page 9: [97] Formatted	Sun ji	6/11/18 1:55:00 PM

Font: 10 pt, English (US)

Page 9: [97] Formatted	Sun ji	6/11/18 1:55:00 PM

Font: 10 pt, English (US)

Page 9: [98] Formatted	Sun ji	6/11/18 1:55:00 PM

Font: 10 pt, English (US)

Page 9: [98] Formatted	Sun ji	6/11/18 1:55:00 PM

Font: 10 pt, English (US)

Page 9: [98] Formatted	Sun ji	6/11/18 1:55:00 PM

Font: 10 pt, English (US)

Page 9: [98] Formatted	Sun ji	6/11/18 1:55:00 PM

Font: 10 pt, English (US)

Page 9: [99] Deleted	JP Veefkind	5/14/18 12:15:00 PM

The aerosol effect is assumed at λ_2 is negligible, so that the assumption of a Rayleigh atmosphere at this wavelength is valid. This The way the longer wavelength λ_2 is treated as reference wavelength where the surface albedo (a_s) is determined by fitting the observed radiance, i.e. $I_{\lambda 2}^{Ray}(a_s) = I_{\lambda 2}^{obs}$. This a_s is also assumed used at λ_1 to compute $I_{\lambda 1}^{Ray}$.

Page 9: [100] Formatted	Sun ji	6/11/18 1:55:00 PM

Font: 10 pt, English (US)

Page 9: [100] Formatted	Sun ji	6/11/18 1:55:00 PM

Font: 10 pt, English (US)

Page 9: [100] Formatted	Sun ji	6/11/18 1:55:00 PM

Font: 10 pt, English (US)

Page 9: [100] Formatted	Sun ji	6/11/18 1:55:00 PM

Font: 10 pt, English (US)

Page 9: [100] Formatted	Sun ji	6/11/18 1:55:00 PM

Font: 10 pt, English (US)

Page 9: [100] Formatted	Sun ji	6/11/18 1:55:00 PM

Font: 10 pt, English (US)

Page 9: [100] Formatted	Sun ji	6/11/18 1:55:00 PM

Font: 10 pt, English (US)

Page 9: [100] Formatted	Sun ji	6/11/18 1:55:00 PM

Font: 10 pt, English (US)

Page 9: [100] Formatted	Sun ji	6/11/18 1:55:00 PM

Font: 10 pt, English (US)

Page 9: [100] Formatted	Sun ji	6/11/18 1:55:00 PM

Font: 10 pt, English (US)

Page 9: [100] Formatted	Sun ji	6/11/18 1:55:00 PM

Font: 10 pt, English (US)

Page 9: [101] Formatted	Sun ji	6/11/18 1:55:00 PM

Font: 10 pt, English (US)

Page 9: [101] Formatted	Sun ji	6/11/18 1:55:00 PM

Font: 10 pt, English (US)

Page 9: [101] Formatted	Sun ji	6/11/18 1:55:00 PM

Font: 10 pt, English (US)

Page 9: [101] Formatted **Sun ji** **6/11/18 1:55:00 PM**

Font: 10 pt, English (US)

Page 9: [102] Formatted **Sun ji** **6/11/18 1:55:00 PM**

Font: 10 pt, English (US)

Page 9: [102] Formatted **Sun ji** **6/11/18 1:55:00 PM**

Font: 10 pt, English (US)

Page 9: [102] Formatted **Sun ji** **6/11/18 1:55:00 PM**

Font: 10 pt, English (US)

Page 9: [102] Formatted **Sun ji** **6/11/18 1:55:00 PM**

Font: 10 pt, English (US)

Page 9: [102] Formatted **Sun ji** **6/11/18 1:55:00 PM**

Font: 10 pt, English (US)

Page 9: [102] Formatted **Sun ji** **6/11/18 1:55:00 PM**

Font: 10 pt, English (US)

Page 9: [102] Formatted **Sun ji** **6/11/18 1:55:00 PM**

Font: 10 pt, English (US)

Page 9: [102] Formatted **Sun ji** **6/11/18 1:55:00 PM**

Font: 10 pt, English (US)

Page 9: [102] Formatted **Sun ji** **6/11/18 1:55:00 PM**

Font: 10 pt, English (US)

Page 9: [102] Formatted **Sun ji** **6/11/18 1:55:00 PM**

Font: 10 pt, English (US)

Page 9: [103] Deleted **Sun ji** **5/8/18 11:15:00 AM**

Consequently,

Page 9: [103] Deleted **Sun ji** **5/8/18 11:15:00 AM**

Consequently,

Page 9: [103] Deleted **Sun ji** **5/8/18 11:15:00 AM**

Consequently,

Page 9: [104] Deleted **Sun ji** **4/23/18 4:08:00 PM**

the difference between $I_{\lambda 1}^{obs}$ and $I_{\lambda 1}^{Ray}$ normalized by the measured radiance $I_{\lambda 1}^{obs}$:

Page 9: [105] Formatted Sun ji 6/11/18 1:55:00 PM
Font: 10 pt, English (US)

Page 9: [105] Formatted Sun ji 6/11/18 1:55:00 PM
Font: 10 pt, English (US)

Page 9: [105] Formatted Sun ji 6/11/18 1:55:00 PM
Font: 10 pt, English (US)

Page 9: [105] Formatted Sun ji 6/11/18 1:55:00 PM
Font: 10 pt, English (US)

Page 9: [106] Formatted Sun ji 6/11/18 1:55:00 PM
Font: 10 pt, English (US)

Page 9: [106] Formatted Sun ji 6/11/18 1:55:00 PM
Font: 10 pt, English (US)

Page 9: [106] Formatted Sun ji 6/11/18 1:55:00 PM
Font: 10 pt, English (US)

Page 9: [106] Formatted Sun ji 6/11/18 1:55:00 PM
Font: 10 pt, English (US)

Page 9: [107] Formatted Sun ji 6/11/18 1:55:00 PM
Font: 10 pt, English (US)

Page 9: [107] Formatted Sun ji 6/11/18 1:55:00 PM
Font: 10 pt, English (US)

Page 9: [107] Formatted Sun ji 6/11/18 1:55:00 PM
Font: 10 pt, English (US)

Page 9: [107] Formatted Sun ji 6/11/18 1:55:00 PM
Font: 10 pt, English (US)

Page 9: [108] Formatted Sun ji 6/11/18 1:55:00 PM
Font: 10 pt, English (US)

Page 9: [108] Formatted Sun ji 6/11/18 1:55:00 PM
Font: 10 pt, English (US)

Page 9: [108] Formatted Sun ji 6/11/18 1:55:00 PM

Font: 10 pt, English (US)

Page 9: [108] Formatted **Sun ji** **6/11/18 1:55:00 PM**

Font: 10 pt, English (US)

Page 9: [108] Formatted **Sun ji** **6/11/18 1:55:00 PM**

Font: 10 pt, English (US)

Page 9: [108] Formatted **Sun ji** **6/11/18 1:55:00 PM**

Font: 10 pt, English (US)

Page 9: [108] Formatted **Sun ji** **6/11/18 1:55:00 PM**

Font: 10 pt, English (US)

Page 9: [108] Formatted **Sun ji** **6/11/18 1:55:00 PM**

Font: 10 pt, English (US)

Page 9: [108] Formatted **Sun ji** **6/11/18 1:55:00 PM**

Font: 10 pt, English (US)

Page 9: [108] Formatted **Sun ji** **6/11/18 1:55:00 PM**

Font: 10 pt, English (US)

Page 9: [109] Formatted **Sun ji** **6/11/18 1:55:00 PM**

Font: 10 pt, English (US), Not Highlight

Page 9: [110] Formatted **Sun ji** **6/11/18 1:55:00 PM**

Font: 10 pt, English (US)

Page 9: [110] Formatted **Sun ji** **6/11/18 1:55:00 PM**

Font: 10 pt, English (US)

Page 9: [111] Formatted **Sun ji** **6/11/18 1:55:00 PM**

Font: 10 pt, English (US)

Page 9: [111] Formatted **Sun ji** **6/11/18 1:55:00 PM**

Font: 10 pt, English (US)

Page 9: [111] Formatted **Sun ji** **6/11/18 1:55:00 PM**

Font: 10 pt, English (US)

Page 9: [111] Formatted **Sun ji** **6/11/18 1:55:00 PM**

Font: 10 pt, English (US)

Page 9: [111] Formatted **Sun ji** **6/11/18 1:55:00 PM**

Font: 10 pt, English (US)

Page 9: [111] Formatted **Sun ji** **6/11/18 1:55:00 PM**

Font: 10 pt, English (US)

Page 9: [112] Formatted **Sun ji** **6/11/18 1:55:00 PM**

Font: 10 pt, English (US), Highlight

Page 9: [112] Formatted **Sun ji** **6/11/18 1:55:00 PM**

Font: 10 pt, English (US), Highlight

Page 9: [113] Formatted **Sun ji** **6/11/18 1:55:00 PM**

English (US)

Page 9: [113] Formatted **Sun ji** **6/11/18 1:55:00 PM**

English (US)

Page 9: [114] Formatted **Sun ji** **6/11/18 1:55:00 PM**

Font: 10 pt, English (US)

Page 9: [115] Deleted **JP Veefkind** **5/14/18 12:41:00 PM**

It

Page 9: [115] Deleted **JP Veefkind** **5/14/18 12:41:00 PM**

It

Page 9: [115] Deleted **JP Veefkind** **5/14/18 12:41:00 PM**

It

Page 9: [115] Deleted **JP Veefkind** **5/14/18 12:41:00 PM**

It

Page 9: [115] Deleted **JP Veefkind** **5/14/18 12:41:00 PM**

It

Page 9: [115] Deleted **JP Veefkind** **5/14/18 12:41:00 PM**

It

Page 9: [115] Deleted **JP Veefkind** **5/14/18 12:41:00 PM**

It

Page 9: [116] Deleted **JP Veefkind** **5/14/18 12:40:00 PM**

various

Page 9: [116] Deleted **JP Veefkind** **5/14/18 12:40:00 PM**

various

Page 9: [116] Deleted **JP Veefkind** **5/14/18 12:40:00 PM**

various

Page 9: [116] Deleted **JP Veefkind** **5/14/18 12:40:00 PM**

various

Page 9: [116] Deleted **JP Veefkind** **5/14/18 12:40:00 PM**

various

Page 9: [116] Deleted **JP Veefkind** **5/14/18 12:40:00 PM**

various

Page 9: [117] Formatted **Sun ji** **6/11/18 1:55:00 PM**

Font: 10 pt, English (US)

Page 9: [117] Formatted **Sun ji** **6/11/18 1:55:00 PM**

Font: 10 pt, English (US)

Page 9: [118] Deleted **JP Veefkind** **5/14/18 12:41:00 PM**

DISAMAR

Page 9: [118] Deleted **JP Veefkind** **5/14/18 12:41:00 PM**

DISAMAR

Page 9: [118] Deleted **JP Veefkind** **5/14/18 12:41:00 PM**

DISAMAR

Page 9: [119] Formatted **Sun ji** **6/11/18 1:55:00 PM**

Font: 10 pt, English (US)

Page 9: [119] Formatted **Sun ji** **6/11/18 1:55:00 PM**

Font: 10 pt, English (US)

Page 9: [119] Formatted **Sun ji** **6/11/18 1:55:00 PM**

Font: 10 pt, English (US)

Page 9: [120] Formatted **Sun ji** **5/15/18 10:32:00 PM**

Left, Don't add space between paragraphs of the same style

Page 9: [121] Deleted **Sun ji** **4/23/18 11:54:00 AM**

Given size distribution function (r_g), complex refractive index (n_r and n_i) at specific wavelengths and a certain wavelength interpolation method, DISAMAR calculates the spectrally dependent optical properties (e.g. ω_0 and phase function $P(\Theta)$) within the specified wavelength range. In this study, we use the linear interpolation and the spectrum coverage from 340 to 675 nm.

Page 9: [122] Deleted **JP Veefkind** **5/14/18 12:43:00 PM**

that

Page 9: [122] Deleted **JP Veefkind** **5/14/18 12:43:00 PM**

that

Page 9: [123] Deleted **Sun ji** **8/2/18 10:21:00 AM**

ly

Page 9: [123] Deleted **Sun ji** **8/2/18 10:21:00 AM**

ly

Page 9: [124] Formatted **Sun ji** **6/11/18 1:55:00 PM**

Font: 10 pt, English (US)

Page 9: [125] Formatted **Sun ji** **6/11/18 1:55:00 PM**

Font: 5.5 pt

Page 9: [126] Formatted **Sun ji** **6/11/18 1:55:00 PM**

English (US)

Page 9: [126] Formatted **Sun ji** **6/11/18 1:55:00 PM**

English (US)

Page 9: [127] Formatted **Sun ji** **6/11/18 1:55:00 PM**

Font: 10 pt, English (US)

Page 9: [127] Formatted **Sun ji** **6/11/18 1:55:00 PM**

Font: 10 pt, English (US)

Page 9: [127] Formatted **Sun ji** **6/11/18 1:55:00 PM**

Font: 10 pt, English (US)

Page 9: [127] Formatted **Sun ji** **6/11/18 1:55:00 PM**

Font: 10 pt, English (US)

Page 9: [128] Formatted **Sun ji** **6/11/18 1:55:00 PM**

Font: 10 pt, English (US)

Page 9: [128] Formatted **Sun ji** **6/11/18 1:55:00 PM**

Font: 10 pt, English (US)

Page 9: [128] Formatted **Sun ji** **6/11/18 1:55:00 PM**

Font: 10 pt, English (US)

Page 9: [129] Formatted **Sun ji** **6/11/18 1:55:00 PM**

Font: 10 pt, English (US)

Page 9: [129] Formatted **Sun ji** **6/11/18 1:55:00 PM**

Font: 10 pt, English (US)

Page 9: [130] Formatted **Sun ji** **6/11/18 1:55:00 PM**

English (US)

Page 9: [130] Formatted **Sun ji** **6/11/18 1:55:00 PM**

English (US)

Page 10: [131] Formatted **Sun ji** **6/11/18 1:55:00 PM**

Font: 10 pt, English (US)

Page 10: [132] Formatted **Sun ji** **6/11/18 1:55:00 PM**

Font: 10 pt, English (US)

Page 10: [133] Deleted **Sun ji** **8/10/18 2:45:00 PM**

each

Page 10: [133] Deleted **Sun ji** **8/10/18 2:45:00 PM**

each

Page 10: [133] Deleted **Sun ji** **8/10/18 2:45:00 PM**

each

Page 10: [134] Formatted **Sun ji** **6/11/18 1:55:00 PM**

Font: 10 pt, English (US)

Page 10: [135] Formatted **Sun ji** **6/11/18 1:55:00 PM**

Font: 10 pt, English (US)

Page 10: [136] Formatted **Sun ji** **5/15/18 10:32:00 PM**

Left

Page 10: [137] Formatted **Sun ji** **6/11/18 1:55:00 PM**

Font: 10 pt, English (US)

Page 10: [137] Formatted **Sun ji** **6/11/18 1:55:00 PM**

Font: 10 pt, English (US)

Page 10: [138] Formatted **Sun ji** **6/11/18 1:55:00 PM**

Font: 10 pt, English (US)

Page 10: [138] Formatted **Sun ji** **6/11/18 1:55:00 PM**

Font: 10 pt, English (US)

Page 10: [138] Formatted **Sun ji** **6/11/18 1:55:00 PM**

Font: 10 pt, English (US)

Page 10: [139] Formatted **Sun ji** **6/11/18 1:55:00 PM**

Font: 10 pt, English (US)

Page 10: [139] Formatted **Sun ji** **6/11/18 1:55:00 PM**

Font: 10 pt, English (US)

Page 10: [139] Formatted **Sun ji** **6/11/18 1:55:00 PM**

Font: 10 pt, English (US)

Page 10: [139] Formatted **Sun ji** **6/11/18 1:55:00 PM**

Font: 10 pt, English (US)

Page 10: [139] Formatted **Sun ji** **6/11/18 1:55:00 PM**

Font: 10 pt, English (US)

Page 10: [140] Formatted **Sun ji** **6/11/18 1:55:00 PM**

Font: 10 pt, English (US)

Page 10: [141] Formatted **Sun ji** **6/11/18 1:55:00 PM**

English (US)

Page 10: [142] Formatted **Sun ji** **6/11/18 1:55:00 PM**

Font: 10 pt, English (US)

Page 10: [142] Formatted **Sun ji** **6/11/18 1:55:00 PM**

Font: 10 pt, English (US)

Page 10: [142] Formatted **Sun ji** **6/11/18 1:55:00 PM**

Font: 10 pt, English (US)

Page 10: [143] Formatted **Sun ji** **6/11/18 1:55:00 PM**

Font: 10 pt, English (US)

Page 10: [143] Formatted **Sun ji** **6/11/18 1:55:00 PM**

Font: 10 pt, English (US)

Page 10: [143] Formatted **Sun ji** **6/11/18 1:55:00 PM**

Font: 10 pt, English (US)

Page 10: [143] Formatted **Sun ji** **6/11/18 1:55:00 PM**

Font: 10 pt, English (US)

Page 10: [144] Formatted	Sun ji	6/11/18 1:55:00 PM

Font: 10 pt, English (US)

Page 10: [144] Formatted	Sun ji	6/11/18 1:55:00 PM

Font: 10 pt, English (US)

Page 10: [144] Formatted	Sun ji	6/11/18 1:55:00 PM

Font: 10 pt, English (US)

Page 10: [145] Formatted	Sun ji	6/11/18 1:55:00 PM

Font: 10 pt, English (US)

Page 10: [146] Deleted	JP Veefkind	5/14/18 1:04:00 PM

The asymmetry factor g is the averaged cosine of the scattering angle Θ, weighted by P(Θ).

Page 10: [147] Formatted	Sun ji	6/11/18 1:55:00 PM

English (US)

Page 10: [148] Formatted	Sun ji	6/11/18 1:55:00 PM

Font: 10 pt, English (US)

Page 10: [149] Formatted	Sun ji	6/11/18 1:55:00 PM

English (US)

Page 10: [149] Formatted	Sun ji	6/11/18 1:55:00 PM

English (US)

Page 10: [150] Formatted	Sun ji	6/11/18 1:55:00 PM

Font: 10 pt, English (US)

Page 10: [150] Formatted	Sun ji	6/11/18 1:55:00 PM

Font: 10 pt, English (US)

Page 10: [150] Formatted	Sun ji	6/11/18 1:55:00 PM

Font: 10 pt, English (US)

Page 10: [150] Formatted	Sun ji	6/11/18 1:55:00 PM

Font: 10 pt, English (US)

Page 10: [150] Formatted	Sun ji	6/11/18 1:55:00 PM

Font: 10 pt, English (US)

Page 10: [150] Formatted	Sun ji	6/11/18 1:55:00 PM

Font: 10 pt, English (US)

Page 10: [151] Deleted **JP Veefkind** **5/14/18 1:05:00 PM**

(

Page 10: [151] Deleted **JP Veefkind** **5/14/18 1:05:00 PM**

(

Page 10: [151] Deleted **JP Veefkind** **5/14/18 1:05:00 PM**

(

Page 10: [152] Formatted **Sun ji** **6/11/18 1:55:00 PM**

Font: 10 pt, English (US)

Page 10: [153] Formatted **Sun ji** **6/11/18 1:55:00 PM**

Font: 10 pt, English (US)

Page 10: [153] Formatted **Sun ji** **6/11/18 1:55:00 PM**

Font: 10 pt, English (US)

Page 10: [153] Formatted **Sun ji** **6/11/18 1:55:00 PM**

Font: 10 pt, English (US)

Page 10: [154] Deleted **JP Veefkind** **5/14/18 3:56:00 PM**

As shown in Fig.3 (e) and (f), even with a decreasing ω_0 and an increasing g, or alternatively a decreasing $I_{\lambda 1}^{obs}$, the AAI primarily follows the behaviour of $\Delta I_{\lambda 1}$. The significant reduction in the spectral dependency of I_λ overwhelms the high reflectivity for small particles (r_g=0.1μm).

Page 10: [155] Formatted **Sun ji** **6/11/18 1:55:00 PM**

Font: 10 pt, English (US)

Page 10: [155] Formatted **Sun ji** **6/11/18 1:55:00 PM**

Font: 10 pt, English (US)

Page 10: [155] Formatted **Sun ji** **6/11/18 1:55:00 PM**

Font: 10 pt, English (US)

Page 10: [155] Formatted **Sun ji** **6/11/18 1:55:00 PM**

Font: 10 pt, English (US)

Page 10: [156] Formatted **Sun ji** **6/11/18 1:55:00 PM**

Font: 10 pt, English (US)

Page 10: [156] Formatted **Sun ji** **6/11/18 1:55:00 PM**

Font: 10 pt, English (US)

Page 10: [156] Formatted **Sun ji** **6/11/18 1:55:00 PM**

Font: 10 pt, English (US)

Page 10: [157] Formatted	Sun ji	6/11/18 1:55:00 PM

Font: 10 pt, English (US)

Page 10: [158] Formatted	Sun ji	6/11/18 1:55:00 PM

Font: 10 pt, English (US)

Page 10: [158] Formatted	Sun ji	6/11/18 1:55:00 PM

Font: 10 pt, English (US)

Page 10: [158] Formatted	Sun ji	6/11/18 1:55:00 PM

Font: 10 pt, English (US)

Page 10: [159] Formatted	Sun ji	6/11/18 1:55:00 PM

Font: 10 pt, English (US), Highlight

Page 10: [159] Formatted	Sun ji	6/11/18 1:55:00 PM

Font: 10 pt, English (US), Highlight

Page 10: [159] Formatted	Sun ji	6/11/18 1:55:00 PM

Font: 10 pt, English (US), Highlight

Page 10: [159] Formatted	Sun ji	6/11/18 1:55:00 PM

Font: 10 pt, English (US), Highlight

Page 10: [159] Formatted	Sun ji	6/11/18 1:55:00 PM

Font: 10 pt, English (US), Highlight

Page 10: [159] Formatted	Sun ji	6/11/18 1:55:00 PM

Font: 10 pt, English (US), Highlight

Page 10: [159] Formatted	Sun ji	6/11/18 1:55:00 PM

Font: 10 pt, English (US), Highlight

Page 10: [159] Formatted	Sun ji	6/11/18 1:55:00 PM

Font: 10 pt, English (US), Highlight

Page 10: [159] Formatted	Sun ji	6/11/18 1:55:00 PM

Font: 10 pt, English (US), Highlight

Page 10: [159] Formatted	Sun ji	6/11/18 1:55:00 PM

Font: 10 pt, English (US), Highlight

Page 10: [160] Formatted	Sun ji	6/11/18 1:55:00 PM

Font: 10 pt, English (US)

Page 10: [160] Formatted **Sun ji** **6/11/18 1:55:00 PM**

Font: 10 pt, English (US)

Page 10: [160] Formatted **Sun ji** **6/11/18 1:55:00 PM**

Font: 10 pt, English (US)

Page 10: [160] Formatted **Sun ji** **6/11/18 1:55:00 PM**

Font: 10 pt, English (US)

Page 10: [161] Formatted **Sun ji** **6/11/18 1:55:00 PM**

Font: 10 pt, English (US)

Page 10: [161] Formatted **Sun ji** **6/11/18 1:55:00 PM**

Font: 10 pt, English (US)

Page 10: [161] Formatted **Sun ji** **6/11/18 1:55:00 PM**

Font: 10 pt, English (US)

Page 10: [162] Deleted **Sun ji** **5/25/18 10:59:00 AM**

possible

Page 10: [162] Deleted **Sun ji** **5/25/18 10:59:00 AM**

possible

Page 10: [163] Formatted **Sun ji** **6/11/18 1:55:00 PM**

English (US)

Page 10: [164] Formatted **Sun ji** **6/11/18 1:55:00 PM**

Font: 10 pt, English (US)

Page 10: [164] Formatted **Sun ji** **6/11/18 1:55:00 PM**

Font: 10 pt, English (US)

Page 10: [164] Formatted **Sun ji** **6/11/18 1:55:00 PM**

Font: 10 pt, English (US)

Page 10: [165] Formatted **Sun ji** **6/11/18 1:55:00 PM**

Font: 10 pt, English (US)

Page 10: [165] Formatted **Sun ji** **6/11/18 1:55:00 PM**

Font: 10 pt, English (US)

Page 10: [165] Formatted **Sun ji** **6/11/18 1:55:00 PM**

Font: 10 pt, English (US)

Page 10: [166] Deleted **Sun ji** **8/10/18 2:53:00 PM**

of the aerosol layer

Page 10: [166] Deleted **Sun ji** **8/10/18 2:53:00 PM**

of the aerosol layer

Page 10: [167] Formatted **Sun ji** **6/11/18 1:55:00 PM**

Font: 10 pt, English (US)

Page 10: [168] Formatted **Sun ji** **6/11/18 1:55:00 PM**

Font: 10 pt, English (US)

Page 10: [168] Formatted **Sun ji** **6/11/18 1:55:00 PM**

Font: 10 pt, English (US)

Page 10: [169] Formatted **Sun ji** **6/11/18 1:55:00 PM**

Font: 10 pt, English (US)

Page 10: [169] Formatted **Sun ji** **6/11/18 1:55:00 PM**

Font: 10 pt, English (US)

Page 10: [170] Formatted **Sun ji** **6/11/18 1:55:00 PM**

English (US)

Page 10: [171] Formatted **Sun ji** **6/11/18 1:55:00 PM**

Font: 10 pt, English (US)

Page 10: [171] Formatted **Sun ji** **6/11/18 1:55:00 PM**

Font: 10 pt, English (US)

Page 10: [172] Formatted **Sun ji** **6/11/18 1:55:00 PM**

Font: 10 pt, English (US)

Page 10: [173] Formatted **Sun ji** **6/11/18 1:55:00 PM**

Font: 10 pt, English (US)

Page 10: [173] Formatted **Sun ji** **6/11/18 1:55:00 PM**

Font: 10 pt, English (US)

Page 10: [173] Formatted **Sun ji** **6/11/18 1:55:00 PM**

Font: 10 pt, English (US)

Page 10: [174] Formatted **Sun ji** **6/11/18 1:55:00 PM**

Font: 10 pt, English (US)

Page 10: [175] Deleted **JP Veefkind** **5/14/18 4:04:00 PM**

, where it was found that the retrieved AAI could be highly overestimated without correction for terrain height

Page 10: [176] Formatted **Sun ji** **6/11/18 1:55:00 PM**

Font: 10 pt, English (US)

Page 10: [177] Formatted **Sun ji** **6/11/18 1:55:00 PM**

Font: 10 pt, English (US)

Page 10: [177] Formatted **Sun ji** **6/11/18 1:55:00 PM**

Font: 10 pt, English (US)

Page 10: [177] Formatted **Sun ji** **6/11/18 1:55:00 PM**

Font: 10 pt, English (US)

Page 10: [177] Formatted **Sun ji** **6/11/18 1:55:00 PM**

Font: 10 pt, English (US)

Page 10: [178] Formatted **Sun ji** **6/11/18 1:55:00 PM**

Font: 10 pt, English (US)

Page 10: [178] Formatted **Sun ji** **6/11/18 1:55:00 PM**

Font: 10 pt, English (US)

Page 10: [178] Formatted **Sun ji** **6/11/18 1:55:00 PM**

Font: 10 pt, English (US)

Page 10: [179] Formatted **Sun ji** **6/11/18 1:55:00 PM**

Font: 10 pt, English (US)

Page 10: [180] Formatted **Sun ji** **6/11/18 1:55:00 PM**

Font: 10 pt, English (US)

Page 10: [181] Deleted **Sun ji** **8/10/18 2:57:00 PM**

also

Page 10: [181] Deleted **Sun ji** **8/10/18 2:57:00 PM**

also

Page 10: [182] Formatted **Sun ji** **6/11/18 1:55:00 PM**

Font: 10 pt, English (US)

Page 10: [182] Formatted **Sun ji** **6/11/18 1:55:00 PM**

Font: 10 pt, English (US)

Page 10: [182] Formatted **Sun ji** **6/11/18 1:55:00 PM**

Font: 10 pt, English (US)

Page 10: [182] Formatted **Sun ji** **6/11/18 1:55:00 PM**

Font: 10 pt, English (US)

Page 10: [182] Formatted **Sun ji** **6/11/18 1:55:00 PM**

Font: 10 pt, English (US)

Page 10: [182] Formatted **Sun ji** **6/11/18 1:55:00 PM**

Font: 10 pt, English (US)

Page 10: [182] Formatted **Sun ji** **6/11/18 1:55:00 PM**

Font: 10 pt, English (US)

Page 10: [183] Formatted **Sun ji** **6/11/18 1:55:00 PM**

Font: 10 pt, English (US)

Page 10: [184] Formatted **Sun ji** **6/11/18 1:55:00 PM**

Font: 10 pt, English (US)

Page 10: [185] Formatted **Sun ji** **6/11/18 1:55:00 PM**

Font: 10 pt, English (US)

Page 10: [185] Formatted **Sun ji** **6/11/18 1:55:00 PM**

Font: 10 pt, English (US)

Page 10: [185] Formatted **Sun ji** **6/11/18 1:55:00 PM**

Font: 10 pt, English (US)

Page 10: [185] Formatted **Sun ji** **6/11/18 1:55:00 PM**

Font: 10 pt, English (US)

Page 10: [186] Formatted **Sun ji** **6/11/18 1:55:00 PM**

Font: 10 pt, English (US)

Page 10: [186] Formatted **Sun ji** **6/11/18 1:55:00 PM**

Font: 10 pt, English (US)

Page 10: [186] Formatted **Sun ji** **6/11/18 1:55:00 PM**

Font: 10 pt, English (US)

Page 10: [186] Formatted **Sun ji** **6/11/18 1:55:00 PM**

Font: 10 pt, English (US)

Page 10: [186] Formatted	Sun ji	6/11/18 1:55:00 PM

Font: 10 pt, English (US)

Page 11: [187] Formatted	Sun ji	6/11/18 1:55:00 PM

Font: 10 pt, English (US)

Page 11: [187] Formatted	Sun ji	6/11/18 1:55:00 PM

Font: 10 pt, English (US)

Page 11: [187] Formatted	Sun ji	6/11/18 1:55:00 PM

Font: 10 pt, English (US)

Page 11: [187] Formatted	Sun ji	6/11/18 1:55:00 PM

Font: 10 pt, English (US)

Page 11: [187] Formatted	Sun ji	6/11/18 1:55:00 PM

Font: 10 pt, English (US)

Page 11: [187] Formatted	Sun ji	6/11/18 1:55:00 PM

Font: 10 pt, English (US)

Page 11: [187] Formatted	Sun ji	6/11/18 1:55:00 PM

Font: 10 pt, English (US)

Page 11: [187] Formatted	Sun ji	6/11/18 1:55:00 PM

Font: 10 pt, English (US)

Page 11: [188] Deleted	Sun ji	5/16/18 5:25:00 PM

corresponding to the selected Θ does not strictly follow the changes in P(Θ)

Page 11: [189] Formatted	Sun ji	6/11/18 1:55:00 PM

Font: 10 pt, English (US)

Page 11: [190] Formatted	Sun ji	6/11/18 1:55:00 PM

English (US), Not Highlight

Page 11: [190] Formatted	Sun ji	6/11/18 1:55:00 PM

English (US), Not Highlight

Page 11: [191] Deleted	Sun ji	5/16/18 3:18:00 PM

the reason that the length of the light path through the aerosol layer also varies with the measurement geometry. Although the overall change in P(Θ) with an increasing Θ is negative, the light path within the aerosol layer also

decreases. Less absorption occurring in the aerosol layer overwhelms the decrease in reflectivity for larger Θ, resulting in an increase in $I_{\lambda 1}^{obs}$ with Θ. [Sj1]

Page 11: [192] Formatted **Sun ji** **6/11/18 1:55:00 PM**

Font: 10 pt, English (US)

Page 11: [192] Formatted **Sun ji** **6/11/18 1:55:00 PM**

Font: 10 pt, English (US)

Page 11: [192] Formatted **Sun ji** **6/11/18 1:55:00 PM**

Font: 10 pt, English (US)

Page 11: [192] Formatted **Sun ji** **6/11/18 1:55:00 PM**

Font: 10 pt, English (US)

Page 11: [193] Commented [Sj9] **Sun ji** **5/16/18 12:11:00 PM**

I reconsider the reason, and also set up a simulation under the same condition but without aerosol (not included in the manuscript). It turns out the Rayleigh scattering at forward and backward direction is strong.

Page 11: [194] Formatted **Sun ji** **6/11/18 1:55:00 PM**

English (US), Not Highlight

Page 11: [194] Formatted **Sun ji** **6/11/18 1:55:00 PM**

English (US), Not Highlight

Page 11: [195] Formatted **Sun ji** **6/11/18 1:55:00 PM**

English (US), Not Highlight

Page 11: [195] Formatted **Sun ji** **6/11/18 1:55:00 PM**

English (US), Not Highlight

Page 11: [196] Formatted **Sun ji** **6/11/18 1:55:00 PM**

Font: 10 pt, English (US)

Page 11: [197] Deleted **Sun ji** **5/15/18 4:41:00 PM**

Although the DISAMAR can calculate wavelength dependent, ω_0 at 550 nm is used as retrieved value for the consistent comparison with AERONET measurements. [JV2][Sj3]

Page 11: [198] Formatted **Sun ji** **6/11/18 1:55:00 PM**

Font: 5.5 pt

Page 11: [199] Formatted **Sun ji** **6/11/18 1:55:00 PM**

Font: 10 pt, English (US)

Page 11: [200] Formatted **Sun ji** **6/11/18 1:55:00 PM**

English (US)

Page 11: [200] Formatted **Sun ji** **6/11/18 1:55:00 PM**

English (US)

Page 11: [201] Formatted **Sun ji** **6/11/18 1:55:00 PM**

Font: 10 pt, English (US)

Page 11: [201] Formatted **Sun ji** **6/11/18 1:55:00 PM**

Font: 10 pt, English (US)

Page 11: [202] Formatted **Sun ji** **6/11/18 1:55:00 PM**

Font: 10 pt, English (US)

Page 11: [202] Formatted **Sun ji** **6/11/18 1:55:00 PM**

Font: 10 pt, English (US)

Page 11: [202] Formatted **Sun ji** **6/11/18 1:55:00 PM**

Font: 10 pt, English (US)

Page 11: [203] Formatted **Sun ji** **6/11/18 1:55:00 PM**

English (US)

Page 11: [204] Formatted **Sun ji** **6/11/18 1:55:00 PM**

Font: 10 pt, English (US)

Page 11: [205] Formatted **Sun ji** **6/11/18 1:55:00 PM**

Font: 10 pt, English (US)

Page 11: [206] Formatted **Sun ji** **6/11/18 1:55:00 PM**

English (US)

Page 11: [206] Formatted **Sun ji** **6/11/18 1:55:00 PM**

English (US)

Page 11: [207] Formatted **Sun ji** **6/11/18 1:55:00 PM**

Font: 10 pt, English (US)

Page 11: [208] Formatted **Sun ji** **6/11/18 1:55:00 PM**

Font: 10 pt, (Asian) Chinese (China), (Other) English (US)

Page 11: [209] Deleted **JP Veefkind** **5/14/18 4:13:00 PM**

plume

Page 11: [209] Deleted **JP Veefkind** **5/14/18 4:13:00 PM**

plume

Page 11: [210] Formatted **Sun ji** **6/11/18 1:55:00 PM**

Font: 10 pt, English (US)

Page 11: [211] Deleted **Sun ji** **8/10/18 3:11:00 PM**

,

Page 11: [211] Deleted **Sun ji** **8/10/18 3:11:00 PM**

,

Page 11: [212] Formatted **Sun ji** **6/11/18 1:55:00 PM**

Font: 10 pt, English (US)

Page 11: [213] Formatted **Sun ji** **6/11/18 1:55:00 PM**

English (US)

Page 11: [213] Formatted **Sun ji** **6/11/18 1:55:00 PM**

English (US)

Page 11: [214] Deleted **JP Veefkind** **5/14/18 4:15:00 PM**

a

Page 11: [214] Deleted **JP Veefkind** **5/14/18 4:15:00 PM**

a

Page 11: [214] Deleted **JP Veefkind** **5/14/18 4:15:00 PM**

a

Page 11: [215] Formatted **Sun ji** **6/11/18 1:55:00 PM**

Font: 10 pt, English (US), Highlight

Page 11: [215] Formatted **Sun ji** **6/11/18 1:55:00 PM**

Font: 10 pt, English (US), Highlight

Page 11: [215] Formatted **Sun ji** **6/11/18 1:55:00 PM**

Font: 10 pt, English (US), Highlight

Page 11: [216] Deleted **JP Veefkind** **5/14/18 4:17:00 PM**

the spectrum ranges from

Page 11: [216] Deleted **JP Veefkind** **5/14/18 4:17:00 PM**

the spectrum ranges from

Page 11: [216] Deleted **JP Veefkind** **5/14/18 4:17:00 PM**

the spectrum ranges from

Page 11: [217] Formatted	Sun ji	6/11/18 1:55:00 PM

Font: 10 pt, English (US)

Page 11: [217] Formatted	Sun ji	6/11/18 1:55:00 PM

Font: 10 pt, English (US)

Page 11: [218] Formatted	Sun ji	6/11/18 1:55:00 PM

Font: 10 pt, English (US)

Page 11: [218] Formatted	Sun ji	6/11/18 1:55:00 PM

Font: 10 pt, English (US)

Page 11: [218] Formatted	Sun ji	6/11/18 1:55:00 PM

Font: 10 pt, English (US)

Page 11: [218] Formatted	Sun ji	6/11/18 1:55:00 PM

Font: 10 pt, English (US)

Page 11: [218] Formatted	Sun ji	6/11/18 1:55:00 PM

Font: 10 pt, English (US)

Page 11: [218] Formatted	Sun ji	6/11/18 1:55:00 PM

Font: 10 pt, English (US)

Page 11: [218] Formatted	Sun ji	6/11/18 1:55:00 PM

Font: 10 pt, English (US)

Page 11: [218] Formatted	Sun ji	6/11/18 1:55:00 PM

Font: 10 pt, English (US)

Page 11: [218] Formatted	Sun ji	6/11/18 1:55:00 PM

Font: 10 pt, English (US)

Page 11: [219] Formatted	Sun ji	6/11/18 1:55:00 PM

Font: 10 pt, English (US)

Page 11: [219] Formatted	Sun ji	6/11/18 1:55:00 PM

Font: 10 pt, English (US)

Page 11: [219] Formatted	Sun ji	6/11/18 1:55:00 PM

Font: 10 pt, English (US)

Page 11: [220] Formatted	Sun ji	6/11/18 1:55:00 PM

Font: 5.5 pt

Page 11: [221] Formatted **Sun ji** **6/11/18 1:55:00 PM**

Font: 10 pt, English (US)

Page 11: [221] Formatted **Sun ji** **6/11/18 1:55:00 PM**

Font: 10 pt, English (US)

Page 11: [221] Formatted **Sun ji** **6/11/18 1:55:00 PM**

Font: 10 pt, English (US)

Page 11: [222] Deleted **Sun ji** **8/7/18 9:16:00 AM**

treated as a reference dataset to evaluate potential biases in

Page 11: [223] Formatted **Sun ji** **6/11/18 1:55:00 PM**

Font: 10 pt, English (US)

Page 11: [223] Formatted **Sun ji** **6/11/18 1:55:00 PM**

Font: 10 pt, English (US)

Page 11: [223] Formatted **Sun ji** **6/11/18 1:55:00 PM**

Font: 10 pt, English (US)

Page 12: [224] Formatted **Sun ji** **6/11/18 1:55:00 PM**

Font: 10 pt, English (US)

Page 12: [224] Formatted **Sun ji** **6/11/18 1:55:00 PM**

Font: 10 pt, English (US)

Page 12: [224] Formatted **Sun ji** **6/11/18 1:55:00 PM**

Font: 10 pt, English (US)

Page 12: [224] Formatted **Sun ji** **6/11/18 1:55:00 PM**

Font: 10 pt, English (US)

Page 12: [225] Formatted **Sun ji** **6/11/18 1:55:00 PM**

English (US)

Page 12: [225] Formatted **Sun ji** **6/11/18 1:55:00 PM**

English (US)

Page 12: [225] Formatted **Sun ji** **6/11/18 1:55:00 PM**

English (US)

Page 12: [226] Formatted **Sun ji** **6/11/18 1:55:00 PM**

Font: 10 pt, English (US)

Page 12: [226] Formatted	Sun ji	6/11/18 1:55:00 PM

Font: 10 pt, English (US)

Page 12: [227] Formatted	Sun ji	6/11/18 1:55:00 PM

Font: 10 pt, English (US), Highlight

Page 12: [227] Formatted	Sun ji	6/11/18 1:55:00 PM

Font: 10 pt, English (US), Highlight

Page 12: [227] Formatted	Sun ji	6/11/18 1:55:00 PM

Font: 10 pt, English (US), Highlight

Page 12: [227] Formatted	Sun ji	6/11/18 1:55:00 PM

Font: 10 pt, English (US), Highlight

Page 12: [228] Formatted	Sun ji	6/11/18 1:55:00 PM

English (US)

Page 12: [228] Formatted	Sun ji	6/11/18 1:55:00 PM

English (US)

Page 12: [229] Formatted	Sun ji	6/11/18 1:55:00 PM

Font: 10 pt, English (US)

Page 12: [229] Formatted	Sun ji	6/11/18 1:55:00 PM

Font: 10 pt, English (US)

Page 12: [229] Formatted	Sun ji	6/11/18 1:55:00 PM

Font: 10 pt, English (US)

Page 12: [229] Formatted	Sun ji	6/11/18 1:55:00 PM

Font: 10 pt, English (US)

Page 12: [229] Formatted	Sun ji	6/11/18 1:55:00 PM

Font: 10 pt, English (US)

Page 12: [229] Formatted	Sun ji	6/11/18 1:55:00 PM

Font: 10 pt, English (US)

Page 12: [229] Formatted	Sun ji	6/11/18 1:55:00 PM

Font: 10 pt, English (US)

Page 12: [229] Formatted	Sun ji	6/11/18 1:55:00 PM

Font: 10 pt, English (US)

Page 12: [229] Formatted **Sun ji** **6/11/18 1:55:00 PM**

Font: 10 pt, English (US)

Page 12: [230] Formatted **Sun ji** **6/11/18 1:55:00 PM**

English (US)

Page 12: [230] Formatted **Sun ji** **6/11/18 1:55:00 PM**

English (US)

Page 12: [231] Formatted **Sun ji** **6/11/18 1:55:00 PM**

English (US)

Page 12: [231] Formatted **Sun ji** **6/11/18 1:55:00 PM**

English (US)

Page 12: [232] Formatted **Sun ji** **6/11/18 1:55:00 PM**

Font: 10 pt, English (US)

Page 12: [232] Formatted **Sun ji** **6/11/18 1:55:00 PM**

Font: 10 pt, English (US)

Page 12: [232] Formatted **Sun ji** **6/11/18 1:55:00 PM**

Font: 10 pt, English (US)

Page 12: [233] Deleted **Sun ji** **5/16/18 11:16:00 AM**

inversion

Page 12: [233] Deleted **Sun ji** **5/16/18 11:16:00 AM**

inversion

Page 12: [233] Deleted **Sun ji** **5/16/18 11:16:00 AM**

inversion

Page 12: [233] Deleted **Sun ji** **5/16/18 11:16:00 AM**

inversion

Page 12: [234] Formatted **Sun ji** **6/11/18 1:55:00 PM**

Font: 10 pt, English (US)

Page 12: [234] Formatted **Sun ji** **6/11/18 1:55:00 PM**

Font: 10 pt, English (US)

Page 12: [235] Deleted **JP Veefkind** **5/14/18 4:20:00 PM**

when

Page 12: [235] Deleted	JP Veefkind	5/14/18 4:20:00 PM

when

Page 12: [236] Formatted	Sun ji	6/11/18 1:55:00 PM

English (US)

Page 12: [236] Formatted	Sun ji	6/11/18 1:55:00 PM

English (US)

Page 12: [236] Formatted	Sun ji	6/11/18 1:55:00 PM

English (US)

Page 12: [237] Formatted	Sun ji	6/11/18 1:55:00 PM

Font: 10 pt, English (US)

Page 12: [237] Formatted	Sun ji	6/11/18 1:55:00 PM

Font: 10 pt, English (US)

Page 12: [238] Formatted	Sun ji	6/11/18 1:55:00 PM

English (US)

Page 12: [238] Formatted	Sun ji	6/11/18 1:55:00 PM

English (US)

Page 12: [238] Formatted	Sun ji	6/11/18 1:55:00 PM

English (US)

Page 12: [238] Formatted	Sun ji	6/11/18 1:55:00 PM

English (US)

Page 12: [238] Formatted	Sun ji	6/11/18 1:55:00 PM

English (US)

Page 12: [239] Formatted	Sun ji	6/11/18 1:55:00 PM

Font: 10 pt, English (US)

Page 12: [239] Formatted	Sun ji	6/11/18 1:55:00 PM

Font: 10 pt, English (US)

Page 12: [240] Formatted	Sun ji	6/11/18 1:55:00 PM

Font: 10 pt, English (US)

Page 12: [240] Formatted	Sun ji	6/11/18 1:55:00 PM

Font: 10 pt, English (US)

Page 12: [240] Formatted **Sun ji** **6/11/18 1:55:00 PM**

Font: 10 pt, English (US)

Page 12: [240] Formatted **Sun ji** **6/11/18 1:55:00 PM**

Font: 10 pt, English (US)

Page 12: [240] Formatted **Sun ji** **6/11/18 1:55:00 PM**

Font: 10 pt, English (US)

Page 12: [240] Formatted **Sun ji** **6/11/18 1:55:00 PM**

Font: 10 pt, English (US)

Page 12: [240] Formatted **Sun ji** **6/11/18 1:55:00 PM**

Font: 10 pt, English (US)

Page 12: [240] Formatted **Sun ji** **6/11/18 1:55:00 PM**

Font: 10 pt, English (US)

Page 12: [240] Formatted **Sun ji** **6/11/18 1:55:00 PM**

Font: 10 pt, English (US)

Page 12: [240] Formatted **Sun ji** **6/11/18 1:55:00 PM**

Font: 10 pt, English (US)

Page 12: [240] Formatted **Sun ji** **6/11/18 1:55:00 PM**

Font: 10 pt, English (US)

Page 12: [240] Formatted **Sun ji** **6/11/18 1:55:00 PM**

Font: 10 pt, English (US)

Page 12: [240] Formatted **Sun ji** **6/11/18 1:55:00 PM**

Font: 10 pt, English (US)

Page 12: [240] Formatted **Sun ji** **6/11/18 1:55:00 PM**

Font: 10 pt, English (US)

Page 12: [240] Formatted **Sun ji** **6/11/18 1:55:00 PM**

Font: 10 pt, English (US)

Page 12: [240] Formatted **Sun ji** **6/11/18 1:55:00 PM**

Font: 10 pt, English (US)

Page 12: [240] Formatted **Sun ji** **6/11/18 1:55:00 PM**

Font: 10 pt, English (US)

Page 12: [240] Formatted	Sun ji	6/11/18 1:55:00 PM

Font: 10 pt, English (US)

Page 12: [240] Formatted	Sun ji	6/11/18 1:55:00 PM

Font: 10 pt, English (US)

Page 12: [240] Formatted	Sun ji	6/11/18 1:55:00 PM

Font: 10 pt, English (US)

Page 12: [240] Formatted	Sun ji	6/11/18 1:55:00 PM

Font: 10 pt, English (US)

Page 12: [240] Formatted	Sun ji	6/11/18 1:55:00 PM

Font: 10 pt, English (US)

Page 12: [241] Formatted	Sun ji	6/11/18 1:55:00 PM

Font: 10 pt, English (US)

Page 12: [241] Formatted	Sun ji	6/11/18 1:55:00 PM

Font: 10 pt, English (US)

Page 12: [241] Formatted	Sun ji	6/11/18 1:55:00 PM

Font: 10 pt, English (US)

Page 12: [241] Formatted	Sun ji	6/11/18 1:55:00 PM

Font: 10 pt, English (US)

Page 12: [241] Formatted	Sun ji	6/11/18 1:55:00 PM

Font: 10 pt, English (US)

Page 12: [241] Formatted	Sun ji	6/11/18 1:55:00 PM

Font: 10 pt, English (US)

Page 12: [241] Formatted	Sun ji	6/11/18 1:55:00 PM

Font: 10 pt, English (US)

Page 12: [241] Formatted	Sun ji	6/11/18 1:55:00 PM

Font: 10 pt, English (US)

Page 12: [241] Formatted	Sun ji	6/11/18 1:55:00 PM

Font: 10 pt, English (US)

Page 12: [241] Formatted	Sun ji	6/11/18 1:55:00 PM

Font: 10 pt, English (US)

Page 12: [241] Formatted Sun ji 6/11/18 1:55:00 PM

Font: 10 pt, English (US)

Page 12: [242] Formatted Sun ji 6/11/18 1:55:00 PM

Font: 10 pt, English (US)

Page 12: [242] Formatted Sun ji 6/11/18 1:55:00 PM

Font: 10 pt, English (US)

Page 12: [242] Formatted Sun ji 6/11/18 1:55:00 PM

Font: 10 pt, English (US)

Page 12: [242] Formatted Sun ji 6/11/18 1:55:00 PM

Font: 10 pt, English (US)

Page 12: [242] Formatted Sun ji 6/11/18 1:55:00 PM

Font: 10 pt, English (US)

Page 12: [242] Formatted Sun ji 6/11/18 1:55:00 PM

Font: 10 pt, English (US)

Page 12: [243] Deleted JP Veefkind 5/14/18 4:22:00 PM

.

Page 12: [243] Deleted JP Veefkind 5/14/18 4:22:00 PM

.

Page 12: [243] Deleted JP Veefkind 5/14/18 4:22:00 PM

.

Page 12: [244] Deleted Sun ji 4/23/18 7:24:00 PM

, and the optical properties of

Page 12: [244] Deleted Sun ji 4/23/18 7:24:00 PM

, and the optical properties of

Page 12: [244] Deleted Sun ji 4/23/18 7:24:00 PM

, and the optical properties of

Page 12: [245] Formatted Sun ji 6/11/18 1:55:00 PM

Font: 10 pt, English (US)

Page 12: [245] Formatted Sun ji 6/11/18 1:55:00 PM

Font: 10 pt, English (US)

Page 12: [245] Formatted Sun ji 6/11/18 1:55:00 PM

Font: 10 pt, English (US)

Page 12: [245] Formatted	Sun ji	6/11/18 1:55:00 PM

Font: 10 pt, English (US)

Page 12: [245] Formatted	Sun ji	6/11/18 1:55:00 PM

Font: 10 pt, English (US)

Page 12: [245] Formatted	Sun ji	6/11/18 1:55:00 PM

Font: 10 pt, English (US)

Page 12: [245] Formatted	Sun ji	6/11/18 1:55:00 PM

Font: 10 pt, English (US)

Page 12: [245] Formatted	Sun ji	6/11/18 1:55:00 PM

Font: 10 pt, English (US)

Page 12: [245] Formatted	Sun ji	6/11/18 1:55:00 PM

Font: 10 pt, English (US)

Page 12: [245] Formatted	Sun ji	6/11/18 1:55:00 PM

Font: 10 pt, English (US)

Page 12: [245] Formatted	Sun ji	6/11/18 1:55:00 PM

Font: 10 pt, English (US)

Page 12: [245] Formatted	Sun ji	6/11/18 1:55:00 PM

Font: 10 pt, English (US)

Page 12: [245] Formatted	Sun ji	6/11/18 1:55:00 PM

Font: 10 pt, English (US)

Page 12: [245] Formatted	Sun ji	6/11/18 1:55:00 PM

Font: 10 pt, English (US)

Page 12: [245] Formatted	Sun ji	6/11/18 1:55:00 PM

Font: 10 pt, English (US)

Page 12: [245] Formatted	Sun ji	6/11/18 1:55:00 PM

Font: 10 pt, English (US)

Page 12: [245] Formatted	Sun ji	6/11/18 1:55:00 PM

Font: 10 pt, English (US)

Page 12: [245] Formatted	Sun ji	6/11/18 1:55:00 PM

Font: 10 pt, English (US)

Page 12: [245] Formatted	Sun ji	6/11/18 1:55:00 PM

Font: 10 pt, English (US)

Page 12: [245] Formatted	Sun ji	6/11/18 1:55:00 PM

Font: 10 pt, English (US)

Page 12: [245] Formatted	Sun ji	6/11/18 1:55:00 PM

Font: 10 pt, English (US)

Page 12: [245] Formatted	Sun ji	6/11/18 1:55:00 PM

Font: 10 pt, English (US)

Page 12: [245] Formatted	Sun ji	6/11/18 1:55:00 PM

Font: 10 pt, English (US)

Page 12: [245] Formatted	Sun ji	6/11/18 1:55:00 PM

Font: 10 pt, English (US)

Page 12: [245] Formatted	Sun ji	6/11/18 1:55:00 PM

Font: 10 pt, English (US)

Page 12: [245] Formatted	Sun ji	6/11/18 1:55:00 PM

Font: 10 pt, English (US)

Page 12: [245] Formatted	Sun ji	6/11/18 1:55:00 PM

Font: 10 pt, English (US)

Page 12: [245] Formatted	Sun ji	6/11/18 1:55:00 PM

Font: 10 pt, English (US)

Page 12: [245] Formatted	Sun ji	6/11/18 1:55:00 PM

Font: 10 pt, English (US)

Page 12: [245] Formatted	Sun ji	6/11/18 1:55:00 PM

Font: 10 pt, English (US)

Page 12: [246] Formatted	Sun ji	6/11/18 1:55:00 PM

Font: 10 pt, English (US)

Page 12: [246] Formatted	Sun ji	6/11/18 1:55:00 PM

Font: 10 pt, English (US)

Page 12: [246] Formatted	Sun ji	6/11/18 1:55:00 PM

Font: 10 pt, English (US)

Page 12: [246] Formatted	Sun ji	6/11/18 1:55:00 PM

Font: 10 pt, English (US)

Page 12: [246] Formatted	Sun ji	6/11/18 1:55:00 PM

Font: 10 pt, English (US)

Page 12: [246] Formatted	Sun ji	6/11/18 1:55:00 PM

Font: 10 pt, English (US)

Page 12: [247] Formatted	Sun ji	6/11/18 1:55:00 PM

Font: 10 pt, English (US)

Page 12: [247] Formatted	Sun ji	6/11/18 1:55:00 PM

Font: 10 pt, English (US)

Page 12: [247] Formatted	Sun ji	6/11/18 1:55:00 PM

Font: 10 pt, English (US)

Page 12: [248] Formatted	Sun ji	6/11/18 1:55:00 PM

Font: 10 pt, English (US)

Page 12: [248] Formatted	Sun ji	6/11/18 1:55:00 PM

Font: 10 pt, English (US)

Page 12: [248] Formatted	Sun ji	6/11/18 1:55:00 PM

Font: 10 pt, English (US)

Page 12: [248] Formatted	Sun ji	6/11/18 1:55:00 PM

Font: 10 pt, English (US)

Page 12: [248] Formatted	Sun ji	6/11/18 1:55:00 PM

Font: 10 pt, English (US)

Page 12: [248] Formatted	Sun ji	6/11/18 1:55:00 PM

Font: 10 pt, English (US)

Page 12: [248] Formatted	Sun ji	6/11/18 1:55:00 PM

Font: 10 pt, English (US)

Page 12: [248] Formatted	Sun ji	6/11/18 1:55:00 PM

Font: 10 pt, English (US)

Page 12: [248] Formatted	Sun ji	6/11/18 1:55:00 PM

Font: 10 pt, English (US)

Page 12: [248] Formatted	Sun ji	6/11/18 1:55:00 PM

Font: 10 pt, English (US)

Page 12: [248] Formatted	Sun ji	6/11/18 1:55:00 PM

Font: 10 pt, English (US)

Page 12: [248] Formatted	Sun ji	6/11/18 1:55:00 PM

Font: 10 pt, English (US)

Page 12: [248] Formatted	Sun ji	6/11/18 1:55:00 PM

Font: 10 pt, English (US)

Page 12: [248] Formatted	Sun ji	6/11/18 1:55:00 PM

Font: 10 pt, English (US)

Page 12: [248] Formatted	Sun ji	6/11/18 1:55:00 PM

Font: 10 pt, English (US)

Page 12: [248] Formatted	Sun ji	6/11/18 1:55:00 PM

Font: 10 pt, English (US)

Page 12: [248] Formatted	Sun ji	6/11/18 1:55:00 PM

Font: 10 pt, English (US)

Page 13: [249] Formatted	Sun ji	6/11/18 1:55:00 PM

Font: 10 pt, English (US)

Page 13: [249] Formatted	Sun ji	6/11/18 1:55:00 PM

Font: 10 pt, English (US)

Page 13: [249] Formatted	Sun ji	6/11/18 1:55:00 PM

Font: 10 pt, English (US)

Page 13: [249] Formatted	Sun ji	6/11/18 1:55:00 PM

Font: 10 pt, English (US)

Page 13: [249] Formatted	Sun ji	6/11/18 1:55:00 PM

Font: 10 pt, English (US)

Page 13: [249] Formatted	Sun ji	6/11/18 1:55:00 PM

Font: 10 pt, English (US)

Page 13: [250] Formatted	Sun ji	6/11/18 1:55:00 PM

Font: 10 pt, English (US)

Page 13: [250] Formatted	Sun ji	6/11/18 1:55:00 PM

Font: 10 pt, English (US)

Page 13: [250] Formatted	Sun ji	6/11/18 1:55:00 PM

Font: 10 pt, English (US)

Page 13: [250] Formatted	Sun ji	6/11/18 1:55:00 PM

Font: 10 pt, English (US)

Page 13: [250] Formatted	Sun ji	6/11/18 1:55:00 PM

Font: 10 pt, English (US)

Page 13: [250] Formatted	Sun ji	6/11/18 1:55:00 PM

Font: 10 pt, English (US)

Page 13: [250] Formatted	Sun ji	6/11/18 1:55:00 PM

Font: 10 pt, English (US)

Page 13: [250] Formatted	Sun ji	6/11/18 1:55:00 PM

Font: 10 pt, English (US)

Page 13: [250] Formatted	Sun ji	6/11/18 1:55:00 PM

Font: 10 pt, English (US)

Page 13: [250] Formatted	Sun ji	6/11/18 1:55:00 PM

Font: 10 pt, English (US)

Page 13: [250] Formatted	Sun ji	6/11/18 1:55:00 PM

Font: 10 pt, English (US)

Page 13: [250] Formatted	Sun ji	6/11/18 1:55:00 PM

Font: 10 pt, English (US)

Page 13: [250] Formatted	Sun ji	6/11/18 1:55:00 PM

Font: 10 pt, English (US)

Page 13: [250] Formatted	Sun ji	6/11/18 1:55:00 PM

Font: 10 pt, English (US)

Page 13: [250] Formatted	Sun ji	6/11/18 1:55:00 PM

Font: 10 pt, English (US)

Page 13: [250] Formatted	Sun ji	6/11/18 1:55:00 PM

Font: 10 pt, English (US)

Page 13: [250] Formatted **Sun ji** **6/11/18 1:55:00 PM**

Font: 10 pt, English (US)

Page 13: [250] Formatted **Sun ji** **6/11/18 1:55:00 PM**

Font: 10 pt, English (US)

Page 13: [250] Formatted **Sun ji** **6/11/18 1:55:00 PM**

Font: 10 pt, English (US)

Page 13: [250] Formatted **Sun ji** **6/11/18 1:55:00 PM**

Font: 10 pt, English (US)

Page 13: [250] Formatted **Sun ji** **6/11/18 1:55:00 PM**

Font: 10 pt, English (US)

Page 13: [250] Formatted **Sun ji** **6/11/18 1:55:00 PM**

Font: 10 pt, English (US)

Page 13: [250] Formatted **Sun ji** **6/11/18 1:55:00 PM**

Font: 10 pt, English (US)

Page 13: [250] Formatted **Sun ji** **6/11/18 1:55:00 PM**

Font: 10 pt, English (US)

Page 13: [250] Formatted **Sun ji** **6/11/18 1:55:00 PM**

Font: 10 pt, English (US)

Page 13: [251] Formatted **Sun ji** **6/11/18 1:55:00 PM**

Font: 10 pt, English (US)

Page 13: [251] Formatted **Sun ji** **6/11/18 1:55:00 PM**

Font: 10 pt, English (US)

Page 13: [251] Formatted **Sun ji** **6/11/18 1:55:00 PM**

Font: 10 pt, English (US)

Page 13: [251] Formatted **Sun ji** **6/11/18 1:55:00 PM**

Font: 10 pt, English (US)

Page 13: [251] Formatted **Sun ji** **6/11/18 1:55:00 PM**

Font: 10 pt, English (US)

Page 13: [251] Formatted **Sun ji** **6/11/18 1:55:00 PM**

Font: 10 pt, English (US)

Page 13: [251] Formatted	Sun ji	6/11/18 1:55:00 PM

Font: 10 pt, English (US)

Page 13: [251] Formatted	Sun ji	6/11/18 1:55:00 PM

Font: 10 pt, English (US)

Page 13: [251] Formatted	Sun ji	6/11/18 1:55:00 PM

Font: 10 pt, English (US)

Page 13: [251] Formatted	Sun ji	6/11/18 1:55:00 PM

Font: 10 pt, English (US)

Page 13: [252] Formatted	Sun ji	6/17/18 9:26:00 PM

Font color: Text 1

Page 13: [252] Formatted	Sun ji	6/17/18 9:26:00 PM

Font color: Text 1

Page 13: [252] Formatted	Sun ji	6/17/18 9:26:00 PM

Font color: Text 1

Page 13: [252] Formatted	Sun ji	6/17/18 9:26:00 PM

Font color: Text 1

Page 13: [252] Formatted	Sun ji	6/17/18 9:26:00 PM

Font color: Text 1

Page 13: [252] Formatted	Sun ji	6/17/18 9:26:00 PM

Font color: Text 1

Page 13: [252] Formatted	Sun ji	6/17/18 9:26:00 PM

Font color: Text 1

Page 13: [253] Formatted	Sun ji	6/11/18 1:55:00 PM

Font: 10 pt, English (US)

Page 13: [253] Formatted	Sun ji	6/11/18 1:55:00 PM

Font: 10 pt, English (US)

Page 13: [254] Formatted	Sun ji	6/11/18 1:55:00 PM

Font: 10 pt, English (US)

Page 13: [254] Formatted	Sun ji	6/11/18 1:55:00 PM

Font: 10 pt, English (US)

Page 13: [254] Formatted	Sun ji	6/11/18 1:55:00 PM

Font: 10 pt, English (US)

Page 13: [255] Formatted	Sun ji	6/11/18 1:55:00 PM

English (US)

Page 13: [255] Formatted	Sun ji	6/11/18 1:55:00 PM

English (US)

Page 13: [255] Formatted	Sun ji	6/11/18 1:55:00 PM

English (US)

Page 13: [256] Formatted	Sun ji	6/11/18 1:55:00 PM

Font: 10 pt, English (US)

Page 13: [256] Formatted	Sun ji	6/11/18 1:55:00 PM

Font: 10 pt, English (US)

Page 13: [257] Formatted	Sun ji	6/11/18 1:55:00 PM

Font: 10 pt, English (US)

Page 13: [257] Formatted	Sun ji	6/11/18 1:55:00 PM

Font: 10 pt, English (US)

Page 13: [257] Formatted	Sun ji	6/11/18 1:55:00 PM

Font: 10 pt, English (US)

Page 13: [257] Formatted	Sun ji	6/11/18 1:55:00 PM

Font: 10 pt, English (US)

Page 14: [258] Formatted	Sun ji	6/11/18 1:55:00 PM

Font: 10 pt, English (US)

Page 14: [259] Formatted	Sun ji	6/11/18 1:55:00 PM

Font: 10 pt, English (US)

Page 14: [260] Formatted	Sun ji	6/11/18 1:55:00 PM

Font: 10 pt, English (US)

Page 14: [260] Formatted	Sun ji	6/11/18 1:55:00 PM

Font: 10 pt, English (US)

Page 14: [260] Formatted	Sun ji	6/11/18 1:55:00 PM

Font: 10 pt, English (US)

Page 14: [261] Deleted **Sun ji** **8/2/18 2:05:00 PM**

ground

Page 14: [261] Deleted **Sun ji** **8/2/18 2:05:00 PM**

ground

Page 14: [262] Formatted **Sun ji** **6/11/18 1:55:00 PM**

Font: 10 pt, English (US)

Page 14: [262] Formatted **Sun ji** **6/11/18 1:55:00 PM**

Font: 10 pt, English (US)

Page 14: [263] Formatted **Sun ji** **6/11/18 1:55:00 PM**

English (US)

Page 14: [263] Formatted **Sun ji** **6/11/18 1:55:00 PM**

English (US)

Page 14: [264] Formatted **Sun ji** **6/11/18 1:55:00 PM**

English (US)

Page 14: [264] Formatted **Sun ji** **6/11/18 1:55:00 PM**

English (US)

Page 14: [265] Deleted **Sun ji** **5/22/18 5:29:00 PM**

is relatively small and the sample distribution

Page 14: [265] Deleted **Sun ji** **5/22/18 5:29:00 PM**

is relatively small and the sample distribution

Page 14: [266] Formatted **Sun ji** **6/11/18 1:55:00 PM**

English (US)

Page 14: [266] Formatted **Sun ji** **6/11/18 1:55:00 PM**

English (US)

Page 14: [267] Formatted **Sun ji** **6/11/18 1:55:00 PM**

Font: 10 pt, English (US)

Page 14: [267] Formatted **Sun ji** **6/11/18 1:55:00 PM**

Font: 10 pt, English (US)

Page 14: [267] Formatted **Sun ji** **6/11/18 1:55:00 PM**

Font: 10 pt, English (US)

Page 14: [267] Formatted **Sun ji** **6/11/18 1:55:00 PM**

Font: 10 pt, English (US)

Page 14: [268] Formatted **Sun ji** **6/11/18 1:55:00 PM**

Font: 5.5 pt

Page 14: [269] Commented [Sj19R18] **Sun ji** **5/15/18 7:11:00 PM**

It means the number of observations is limited so that the dataset is sensitive to outliers. I rephrased this sentence.

Page 14: [270] Formatted **Sun ji** **6/11/18 1:55:00 PM**

Font: 10 pt, English (US)

Page 14: [271] Formatted **Sun ji** **6/11/18 1:55:00 PM**

English (US)

Page 14: [271] Formatted **Sun ji** **6/11/18 1:55:00 PM**

English (US)

Page 14: [271] Formatted **Sun ji** **6/11/18 1:55:00 PM**

English (US)

Page 14: [272] Formatted **Sun ji** **6/11/18 1:55:00 PM**

Font: 10 pt, English (US)

Page 14: [272] Formatted **Sun ji** **6/11/18 1:55:00 PM**

Font: 10 pt, English (US)

Page 14: [273] Commented [JV20] **JP Veefkind** **5/14/18 5:19:00 PM**

We first fit, then apply the outlier, then we fit again

Page 14: [274] Formatted **Sun ji** **6/11/18 1:55:00 PM**

Font: 5.5 pt

Page 14: [275] Commented [Sj21R20] **Sun ji** **5/16/18 11:41:00 AM**

I implied that by the scatter plots in Fig.8, but I did not provide the fitting results (AAI, SSA, etc.) calculated by the whole data (including outliers).

Page 14: [276] Formatted **Sun ji** **6/11/18 1:55:00 PM**

Font: 10 pt, English (US)

Page 14: [277] Formatted **Sun ji** **6/11/18 1:55:00 PM**

Font: 10 pt, English (US)

Page 14: [277] Formatted **Sun ji** **6/11/18 1:55:00 PM**

Font: 10 pt, English (US)

Page 14: [277] Formatted	Sun ji	6/11/18 1:55:00 PM

Font: 10 pt, English (US)

Page 14: [277] Formatted	Sun ji	6/11/18 1:55:00 PM

Font: 10 pt, English (US)

Page 14: [277] Formatted	Sun ji	6/11/18 1:55:00 PM

Font: 10 pt, English (US)

Page 14: [277] Formatted	Sun ji	6/11/18 1:55:00 PM

Font: 10 pt, English (US)

Page 14: [277] Formatted	Sun ji	6/11/18 1:55:00 PM

Font: 10 pt, English (US)

Page 14: [277] Formatted	Sun ji	6/11/18 1:55:00 PM

Font: 10 pt, English (US)

Page 14: [277] Formatted	Sun ji	6/11/18 1:55:00 PM

Font: 10 pt, English (US)

Page 14: [277] Formatted	Sun ji	6/11/18 1:55:00 PM

Font: 10 pt, English (US)

Page 14: [277] Formatted	Sun ji	6/11/18 1:55:00 PM

Font: 10 pt, English (US)

Page 14: [277] Formatted	Sun ji	6/11/18 1:55:00 PM

Font: 10 pt, English (US)

Page 14: [278] Formatted	Sun ji	6/11/18 1:55:00 PM

Font: 10 pt, English (US)

Page 14: [279] Deleted	Sun ji	8/10/18 3:47:00 PM

on MetOp-A/B

Page 14: [279] Deleted	Sun ji	8/10/18 3:47:00 PM

on MetOp-A/B

Page 14: [280] Formatted	Sun ji	6/11/18 1:55:00 PM

English (US)

Page 14: [280] Formatted	Sun ji	6/11/18 1:55:00 PM

English (US)

Page 14: [281] Formatted **Sun ji** **6/11/18 1:55:00 PM**

Font: 10 pt, English (US)

Page 14: [282] Formatted **Sun ji** **6/11/18 1:55:00 PM**

English (US)

Page 14: [282] Formatted **Sun ji** **6/11/18 1:55:00 PM**

English (US)

Page 14: [283] Formatted **Sun ji** **6/11/18 1:55:00 PM**

English (US)

Page 14: [283] Formatted **Sun ji** **6/11/18 1:55:00 PM**

English (US)

Page 14: [284] Formatted **Sun ji** **6/11/18 1:55:00 PM**

Font: 10 pt, English (US)

Page 14: [284] Formatted **Sun ji** **6/11/18 1:55:00 PM**

Font: 10 pt, English (US)

Page 14: [285] Formatted **Sun ji** **6/11/18 1:55:00 PM**

Font: 10 pt, English (US)

Page 14: [285] Formatted **Sun ji** **6/11/18 1:55:00 PM**

Font: 10 pt, English (US)

Page 14: [286] Formatted **Sun ji** **6/11/18 1:55:00 PM**

Font: 10 pt, English (US)

Page 14: [287] Deleted **JP Veefkind** **5/14/18 5:31:00 PM**

from

Page 14: [287] Deleted **JP Veefkind** **5/14/18 5:31:00 PM**

from

Page 14: [287] Deleted **JP Veefkind** **5/14/18 5:31:00 PM**

from

Page 14: [287] Deleted **JP Veefkind** **5/14/18 5:31:00 PM**

from

Page 14: [287] Deleted **JP Veefkind** **5/14/18 5:31:00 PM**

from

Page 14: [288] Formatted **Sun ji** **6/11/18 1:55:00 PM**

English (US)

Page 14: [288] Formatted	Sun ji	6/11/18 1:55:00 PM

English (US)

Page 14: [288] Formatted	Sun ji	6/11/18 1:55:00 PM

English (US)

Page 14: [288] Formatted	Sun ji	6/11/18 1:55:00 PM

English (US)

Page 14: [289] Formatted	Sun ji	6/11/18 1:55:00 PM

Font: 10 pt, English (US)

Page 14: [290] Deleted	Sun ji	6/12/18 8:57:00 AM

probably did not always measure the plume feature, and may even fail to capture the elevated

Page 14: [291] Formatted	Sun ji	6/11/18 1:55:00 PM

Font: 10 pt, English (US)

Page 14: [292] Formatted	Sun ji	6/11/18 1:55:00 PM

Font: 10 pt, English (US)

Page 14: [293] Formatted	Sun ji	6/11/18 1:55:00 PM

Font: 10 pt, English (US)

Page 15: [294] Formatted	Sun ji	6/11/18 1:55:00 PM

Font: 10 pt, English (US)

Page 15: [294] Formatted	Sun ji	6/11/18 1:55:00 PM

Font: 10 pt, English (US)

Page 15: [295] Formatted	Sun ji	6/11/18 1:55:00 PM

Font: 10 pt, English (US)

Page 15: [296] Formatted	Sun ji	6/11/18 1:55:00 PM

Font: 10 pt, English (US)

Page 15: [297] Deleted	Sun ji	8/3/18 11:31:00 AM

low

Page 15: [297] Deleted	Sun ji	8/3/18 11:31:00 AM

low

Page 15: [298] Formatted	Sun ji	6/11/18 1:55:00 PM

Font: 10 pt, English (US)

Page 15: [299] Formatted **Sun ji** **6/11/18 1:55:00 PM**

Font: 10 pt, English (US)

Page 15: [300] Formatted **Sun ji** **6/11/18 1:55:00 PM**

English (US)

Page 15: [301] Deleted **Sun ji** **5/25/18 12:25:00 PM**

, which reflects is in correspondence with the smoke ageing process (Reid et al., 2004)

Page 15: [302] Formatted **Sun ji** **6/11/18 1:55:00 PM**

Font: 10 pt, English (US)

Page 15: [303] Formatted **Sun ji** **6/11/18 1:55:00 PM**

Font: 10 pt, English (US)

Page 15: [304] Formatted **Sun ji** **6/11/18 1:55:00 PM**

Font: 10 pt, English (US)

Page 15: [304] Formatted **Sun ji** **6/11/18 1:55:00 PM**

Font: 10 pt, English (US)

Page 15: [305] Formatted **Sun ji** **6/11/18 1:55:00 PM**

Font: 10 pt, English (US)

Page 15: [306] Formatted **Sun ji** **6/11/18 1:55:00 PM**

Font: 10 pt, English (US)

Page 15: [306] Formatted **Sun ji** **6/11/18 1:55:00 PM**

Font: 10 pt, English (US)

Page 15: [307] Formatted **Sun ji** **6/17/18 5:26:00 PM**

Font color: Text 1

Page 15: [307] Formatted **Sun ji** **6/17/18 5:26:00 PM**

Font color: Text 1

Page 15: [307] Formatted **Sun ji** **6/17/18 5:26:00 PM**

Font color: Text 1

Page 15: [307] Formatted **Sun ji** **6/17/18 5:26:00 PM**

Font color: Text 1

Page 15: [307] Formatted **Sun ji** **6/17/18 5:26:00 PM**

Font color: Text 1

Page 15: [307] Formatted **Sun ji** **6/17/18 5:26:00 PM**

Font color: Text 1

Page 15: [307] Formatted **Sun ji** **6/17/18 5:26:00 PM**

Font color: Text 1

Page 15: [307] Formatted **Sun ji** **6/17/18 5:26:00 PM**

Font color: Text 1

Page 15: [307] Formatted **Sun ji** **6/17/18 5:26:00 PM**

Font color: Text 1

Page 15: [307] Formatted **Sun ji** **6/17/18 5:26:00 PM**

Font color: Text 1

Page 15: [307] Formatted **Sun ji** **6/17/18 5:26:00 PM**

Font color: Text 1

Page 15: [308] Formatted **Sun ji** **6/17/18 5:26:00 PM**

Font color: Text 1

Page 15: [308] Formatted **Sun ji** **6/17/18 5:26:00 PM**

Font color: Text 1

Page 15: [308] Formatted **Sun ji** **6/17/18 5:26:00 PM**

Font color: Text 1

Page 15: [308] Formatted **Sun ji** **6/17/18 5:26:00 PM**

Font color: Text 1

Page 15: [309] Deleted **Sun ji** **6/12/18 9:06:00 AM**

. This difference might be due to the fact that the selected AERONET site is not exactly at the primary biomass burning regions as mentioned in section 3.1.3. The ω_0 measured by AERONET could increase as the result of aerosol ageing. Specifically, the location of the AERONET site is in the downtown, where the more reflective urban or industrial aerosols may mix with the smoke and enhance the measured ω_0. Besides

Page 15: [310] Formatted **Sun ji** **6/11/18 1:55:00 PM**

Font: 10 pt, English (US)

Page 15: [310] Formatted **Sun ji** **6/11/18 1:55:00 PM**

Font: 10 pt, English (US)

Page 15: [311] Formatted **Sun ji** **6/11/18 1:55:00 PM**

English (US), Not Highlight

Page 15: [311] Formatted **Sun ji** **6/11/18 1:55:00 PM**

English (US), Not Highlight

Page 15: [312] Deleted **Sun ji** **6/12/18 10:09:00 AM**

micro-physics parameters retrieved from

Page 15: [312] Deleted **Sun ji** **6/12/18 10:09:00 AM**

micro-physics parameters retrieved from

Page 15: [313] Formatted **Sun ji** **6/11/18 1:55:00 PM**

Font: 10 pt, English (US)

Page 15: [314] Formatted **Sun ji** **6/11/18 1:55:00 PM**

Font: 10 pt, English (US)

Page 15: [315] Commented [JV22] **JP Veefkind** **5/14/18 5:56:00 PM**

Should these be left in? The AERONET product is much better established…

Page 15: [316] Formatted **Sun ji** **6/11/18 1:55:00 PM**

Font: 5.5 pt

Page 15: [317] Commented [Sj23R22] **Sun ji** **5/15/18 10:45:00 PM**

Just mention that AERONET measurements is not perfect also. The input size distribution functions may not be the major error source in our case, but the refractive index is not, which may bias the forward simulation. The SSA, as the parameter to validate, is also with uncertainty of 0.03.

Page 15: [318] Formatted **Sun ji** **6/11/18 1:55:00 PM**

Font: 10 pt, English (US)

Page 15: [318] Formatted **Sun ji** **6/11/18 1:55:00 PM**

Font: 10 pt, English (US)

Page 15: [318] Formatted **Sun ji** **6/11/18 1:55:00 PM**

Font: 10 pt, English (US)

Page 15: [319] Deleted **Sun ji** **6/11/18 7:22:00 PM**

i

Page 15: [319] Deleted **Sun ji** **6/11/18 7:22:00 PM**

i

Page 15: [320] Formatted **Sun ji** **6/11/18 1:55:00 PM**

Font: 10 pt, English (US)

Page 15: [320] Formatted **Sun ji** **6/11/18 1:55:00 PM**

Font: 10 pt, English (US)

Page 15: [320] Formatted **Sun ji** **6/11/18 1:55:00 PM**

Font: 10 pt, English (US)

Page 15: [321] Formatted **Sun ji** **8/10/18 5:24:00 PM**

Font color: Text 1

Page 15: [321] Formatted **Sun ji** **8/10/18 5:24:00 PM**

Font color: Text 1

Page 15: [322] Formatted **Sun ji** **6/12/18 10:30:00 AM**

Font: 10 pt, English (US), Highlight

Page 15: [322] Formatted **Sun ji** **6/12/18 10:30:00 AM**

Font: 10 pt, English (US), Highlight

Page 15: [323] Formatted **Sun ji** **6/11/18 1:55:00 PM**

Font: 10 pt, English (US)

Page 15: [323] Formatted **Sun ji** **6/11/18 1:55:00 PM**

Font: 10 pt, English (US)

Page 15: [324] Formatted **Sun ji** **6/11/18 1:55:00 PM**

Font: 10 pt, English (US)

Page 15: [325] Formatted **Sun ji** **6/11/18 1:55:00 PM**

English (US)

Page 15: [326] Formatted **Sun ji** **6/11/18 1:55:00 PM**

English (US)

Page 15: [326] Formatted **Sun ji** **6/11/18 1:55:00 PM**

English (US)

Page 15: [327] Deleted **Sun ji** **5/25/18 12:06:00 PM**

s

Page 15: [327] Deleted **Sun ji** **5/25/18 12:06:00 PM**

s

Page 15: [328] Formatted **Sun ji** **6/11/18 1:55:00 PM**

Font: 10 pt, English (US)

Page 16: [329] Formatted **Sun ji** **6/11/18 1:55:00 PM**

Font: 10 pt, English (US)

Page 16: [330] Formatted **Sun ji** **6/11/18 1:55:00 PM**

Font: 10 pt, English (US)

Page 16: [331] Formatted **Sun ji** **6/11/18 1:55:00 PM**

Font: 10 pt, English (US)

Page 16: [332] Formatted **Sun ji** **6/11/18 1:55:00 PM**

Font: 10 pt, English (US)

Page 16: [332] Formatted **Sun ji** **6/11/18 1:55:00 PM**

Font: 10 pt, English (US)

Page 16: [333] Formatted **Sun ji** **6/11/18 1:55:00 PM**

Font: 10 pt, English (US)

Page 16: [334] Formatted **Sun ji** **6/11/18 1:55:00 PM**

Font: 10 pt, English (US)

Page 16: [335] Formatted **Sun ji** **6/11/18 1:55:00 PM**

English (US)

Page 16: [335] Formatted **Sun ji** **6/11/18 1:55:00 PM**

English (US)

Page 16: [336] Deleted **Sun ji** **5/16/18 4:43:00 PM**

for the

Page 16: [336] Deleted **Sun ji** **5/16/18 4:43:00 PM**

for the

Page 16: [337] Formatted **Sun ji** **6/11/18 1:55:00 PM**

English (US)

Page 16: [338] Formatted **Sun ji** **6/11/18 1:55:00 PM**

Font: 10 pt, English (US)

Page 16: [339] Formatted **Sun ji** **6/11/18 1:55:00 PM**

Font: 10 pt, English (US)

Page 16: [340] Deleted **JP Veefkind** **5/14/18 6:01:00 PM**

However, even with relative reasonable retrieval of z_{aer}, it is noted that the ω_0 retrieved on 27 January is significantly underestimated and biased from the mean level of other cases. This implies the existence of other error sources, such as the observational errors from the input τ of MODIS and the AAI of OMI to be fit.

Page 16: [341] Formatted **Sun ji** **6/11/18 1:55:00 PM**
Font: 10 pt, English (US)

Page 16: [342] Formatted **Sun ji** **6/11/18 1:55:00 PM**
Font: 10 pt, English (US)

Page 16: [342] Formatted **Sun ji** **6/11/18 1:55:00 PM**
Font: 10 pt, English (US)

Page 16: [342] Formatted **Sun ji** **6/11/18 1:55:00 PM**
Font: 10 pt, English (US)

Page 16: [343] Deleted **Sun ji** **5/25/18 12:21:00 PM**
However

Page 16: [343] Deleted **Sun ji** **5/25/18 12:21:00 PM**
However

Page 16: [343] Deleted **Sun ji** **5/25/18 12:21:00 PM**
However

Page 16: [343] Deleted **Sun ji** **5/25/18 12:21:00 PM**
However

Page 16: [344] Formatted **Sun ji** **6/11/18 1:55:00 PM**
English (US)

Page 16: [345] Formatted **Sun ji** **6/11/18 1:55:00 PM**
English (US)

Page 16: [346] Deleted **Sun ji** **5/25/18 12:22:00 PM**
. E

Page 16: [346] Deleted **Sun ji** **5/25/18 12:22:00 PM**
. E

Page 16: [347] Formatted **Sun ji** **6/11/18 1:55:00 PM**
Font: 10 pt, English (US)

Page 16: [347] Formatted **Sun ji** **6/11/18 1:55:00 PM**
Font: 10 pt, English (US)

Page 16: [348] Formatted **Sun ji** **6/11/18 1:55:00 PM**

Font: 10 pt, English (US)

Page 16: [348] Formatted **Sun ji** **6/11/18 1:55:00 PM**

Font: 10 pt, English (US)

Page 16: [349] Formatted **Sun ji** **6/11/18 1:55:00 PM**

Font: 10 pt, English (US)

Page 16: [350] Formatted **Sun ji** **6/11/18 1:55:00 PM**

Font: 10 pt, English (US)

Page 16: [351] Formatted **Sun ji** **6/11/18 1:55:00 PM**

Font: 10 pt, English (US)

Page 16: [352] Formatted **Sun ji** **6/11/18 1:55:00 PM**

Font: 10 pt, (Asian) Chinese (China), (Other) English (US)

Page 16: [353] Formatted **Sun ji** **6/11/18 1:55:00 PM**

Font: 10 pt, English (US)

Page 16: [354] Formatted **Sun ji** **6/11/18 1:55:00 PM**

English (US)

Page 16: [354] Formatted **Sun ji** **6/11/18 1:55:00 PM**

English (US)

Page 16: [355] Formatted **Sun ji** **6/11/18 1:55:00 PM**

English (US)

Page 16: [355] Formatted **Sun ji** **6/11/18 1:55:00 PM**

English (US)

Page 16: [356] Formatted **Sun ji** **6/11/18 1:55:00 PM**

Font: 10 pt, English (US)

Page 16: [357] Formatted **Sun ji** **6/11/18 1:55:00 PM**

English (US)

Page 16: [358] Formatted **Sun ji** **6/11/18 1:55:00 PM**

Font: 10 pt, English (US)

Page 16: [358] Formatted **Sun ji** **6/11/18 1:55:00 PM**

Font: 10 pt, English (US)

Page 16: [358] Formatted **Sun ji** **6/11/18 1:55:00 PM**

Font: 10 pt, English (US)

Page 16: [359] Formatted **Sun ji** **6/11/18 1:55:00 PM**

English (US)

Page 16: [359] Formatted **Sun ji** **6/11/18 1:55:00 PM**

English (US)

Page 16: [360] Formatted **Sun ji** **6/11/18 1:55:00 PM**

Font: 10 pt, English (US)

Page 16: [361] Formatted **Sun ji** **6/11/18 1:55:00 PM**

Font: 10 pt, English (US)

Page 16: [362] Formatted **Sun ji** **6/11/18 1:55:00 PM**

Font: 10 pt, English (US)

Page 16: [363] Formatted **Sun ji** **6/11/18 1:55:00 PM**

English (US)

Page 16: [364] Formatted **Sun ji** **6/11/18 1:55:00 PM**

Font: 10 pt, English (US)

Page 16: [365] Formatted **Sun ji** **6/11/18 1:55:00 PM**

English (US)

Page 16: [365] Formatted **Sun ji** **6/11/18 1:55:00 PM**

English (US)

Page 16: [366] Formatted **Sun ji** **6/11/18 1:55:00 PM**

English (US)

Page 16: [366] Formatted **Sun ji** **6/11/18 1:55:00 PM**

English (US)

Page 16: [366] Formatted **Sun ji** **6/11/18 1:55:00 PM**

English (US)

Page 16: [367] Deleted **Sun ji** **6/12/18 10:52:00 AM**

proves its usefulness and effectiveness

Page 16: [367] Deleted **Sun ji** **6/12/18 10:52:00 AM**

proves its usefulness and effectiveness

Page 16: [368] Formatted **Sun ji** **6/11/18 1:55:00 PM**

Font: 10 pt, English (US)

Page 16: [369] Formatted **Sun ji** **6/11/18 1:55:00 PM**

English (US)

Page 16: [369] Formatted **Sun ji** **6/11/18 1:55:00 PM**

English (US)

Page 16: [370] Deleted **Sun ji** **8/2/18 4:15:00 PM**

The retrieved ω_0 is reasonable, taking into account the typical uncertainty in the ω_0 retrieved from AERONET ($\pm$0.03).

Page 16: [371] Formatted **Sun ji** **6/11/18 1:55:00 PM**

Font: 10 pt, English (US)

Page 16: [372] Formatted **Sun ji** **6/11/18 1:55:00 PM**

Font: 10 pt, English (US)

Page 16: [373] Formatted **Sun ji** **6/11/18 1:55:00 PM**

Font: 10 pt, English (US)

Page 16: [374] Deleted **Sun ji** **6/12/18 11:00:00 AM**

the assumption of homogeneous and static plume properties, which ignores the plume evolution over space and time;

Page 16: [375] Formatted **Sun ji** **6/11/18 1:55:00 PM**

Font: 10 pt, English (US)

Page 16: [375] Formatted **Sun ji** **6/11/18 1:55:00 PM**

Font: 10 pt, English (US)

Page 17: [376] Deleted **Sun ji** **6/17/18 5:37:00 PM**

This study proves the potential of utilizing OMI measured AAI to quantitatively characterize aerosol optical properties like ω_0. Even without direct observation of aerosol profiles, this parameter can also be retrieved with quite good confidence. However, apart from the observational uncertainties, the current study is probably somewhat limited by the necessary assumptions of homogeneous and static plume properties, whose impact on retrieved ω_0 is difficult to quantify. In the future planned

Page 17: [377] Deleted **Sun ji** **6/12/18 11:45:00 AM**

work, a chemistry transport model is needed to describe the evolution of the plume properties in space and time. Moreover, also clouds should be taken into consideration in order to use the AAI observations over clouds, thus making the maximum use of the near-UV observations.

Page 17: [378] Formatted **Sun ji** **8/3/18 9:17:00 AM**

Font: Not Bold, English (US), Do not check spelling or grammar

Page 17: [379] Deleted **Sun ji** **4/23/18 2:30:00 PM**

Adler, G., Flores, J. M., Abo Riziq, A., Borrmann, S. and Rudich, Y.: Chemical, physical, and optical evolution of biomass burning aerosols: A case study, Atmos. Chem. Phys., 11, 1491–1503, doi:10.5194/acp-11-1491-2011, 2011.

Bäumer, D., Vogel, B., Versick, S., Rinke, R., Möhler, O. and Schnaiter, M.: Relationship of visibility, aerosol optical thicknss and aerosol size distribution in an ageing air mass over South-West Germany, Atmos. Environ., 42, 989–998, doi:10.1016/j.atmosenv.2007.10.017, 2008.

Page 17: [380] Formatted **Sun ji** **8/7/18 10:25:00 AM**

Font: Not Bold, Font color: Auto, English (US), Do not check spelling or grammar, Not Highlight

Page 31: [381] Formatted **Sun ji** **6/11/18 1:55:00 PM**

English (US)

Page 31: [382] Formatted **Sun ji** **6/11/18 1:55:00 PM**

English (US)

Page 31: [383] Formatted **Sun ji** **6/11/18 1:55:00 PM**

Font: 9 pt, English (US)

Page 31: [384] Formatted **Sun ji** **5/15/18 10:32:00 PM**

Left

Page 31: [385] Formatted **Sun ji** **6/11/18 1:55:00 PM**

Font: 7.5 pt, English (US)

Page 31: [386] Formatted **Sun ji** **6/11/18 1:55:00 PM**

Font: 9 pt, English (US)

Page 31: [386] Formatted **Sun ji** **6/11/18 1:55:00 PM**

Font: 9 pt, English (US)

Page 31: [387] Formatted **Sun ji** **6/11/18 1:55:00 PM**

Font: 9 pt, English (US)

Page 31: [387] Formatted **Sun ji** **6/11/18 1:55:00 PM**

Font: 9 pt, English (US)

Page 31: [388] Formatted **Sun ji** **6/11/18 1:55:00 PM**

Font: 9 pt, English (US)

Page 31: [388] Formatted **Sun ji** **6/11/18 1:55:00 PM**

Font: 9 pt, English (US)

Page 31: [389] Formatted **Sun ji** **6/11/18 1:55:00 PM**

Font: 9 pt, English (US)

Page 31: [390] Formatted **Sun ji** **5/15/18 10:32:00 PM**

Left

Page 31: [391] Formatted **Sun ji** **6/11/18 1:55:00 PM**

Font: 7.5 pt, English (US)

Page 31: [392] Formatted **Sun ji** **6/11/18 1:55:00 PM**

Font: 9 pt, English (US)

Page 31: [392] Formatted **Sun ji** **6/11/18 1:55:00 PM**

Font: 9 pt, English (US)

Page 31: [393] Formatted **Sun ji** **6/11/18 1:55:00 PM**

Font: 9 pt, English (US)

Page 31: [393] Formatted **Sun ji** **6/11/18 1:55:00 PM**

Font: 9 pt, English (US)

Page 31: [394] Formatted **Sun ji** **6/11/18 1:55:00 PM**

Font: 9 pt, English (US)

Page 31: [394] Formatted **Sun ji** **6/11/18 1:55:00 PM**

Font: 9 pt, English (US)

Page 31: [395] Formatted **Sun ji** **6/11/18 1:55:00 PM**

Font: 9 pt, English (US)

Page 31: [396] Formatted **Sun ji** **5/15/18 10:32:00 PM**

Left

Page 31: [397] Formatted **Sun ji** **6/11/18 1:55:00 PM**

Font: 7.5 pt, English (US)

Page 31: [398] Formatted **Sun ji** **6/11/18 1:55:00 PM**

Font: 9 pt, English (US)

Page 31: [398] Formatted **Sun ji** **6/11/18 1:55:00 PM**

Font: 9 pt, English (US)

Page 31: [399] Formatted **Sun ji** **6/11/18 1:55:00 PM**

Font: 9 pt, English (US)

Page 31: [399] Formatted	Sun ji	6/11/18 1:55:00 PM

Font: 9 pt, English (US)

Page 31: [400] Formatted	Sun ji	6/11/18 1:55:00 PM

Font: 9 pt, English (US)

Page 31: [400] Formatted	Sun ji	6/11/18 1:55:00 PM

Font: 9 pt, English (US)

Page 31: [401] Formatted	Sun ji	6/11/18 1:55:00 PM

Font: 9 pt, English (US)

Page 31: [402] Formatted	Sun ji	5/15/18 10:32:00 PM

Left

Page 31: [403] Formatted	Sun ji	6/11/18 1:55:00 PM

Font: 7.5 pt, English (US)

Page 31: [404] Formatted	Sun ji	6/11/18 1:55:00 PM

Font: 9 pt, English (US)

Page 31: [404] Formatted	Sun ji	6/11/18 1:55:00 PM

Font: 9 pt, English (US)

Page 31: [405] Formatted	Sun ji	6/11/18 1:55:00 PM

Font: 9 pt, English (US)

Page 31: [405] Formatted	Sun ji	6/11/18 1:55:00 PM

Font: 9 pt, English (US)

Page 31: [406] Formatted	Sun ji	6/11/18 1:55:00 PM

Font: 9 pt, English (US)

Page 31: [406] Formatted	Sun ji	6/11/18 1:55:00 PM

Font: 9 pt, English (US)

Page 31: [407] Formatted	Sun ji	6/11/18 1:55:00 PM

Font: 9 pt, English (US)

Page 31: [408] Formatted	Sun ji	5/15/18 10:32:00 PM

Left

Page 31: [409] Formatted	Sun ji	6/11/18 1:55:00 PM

Font: 7.5 pt, English (US)

Page 31: [410] Formatted	Sun ji	6/11/18 1:55:00 PM

Font: 9 pt, English (US)

Page 31: [410] Formatted	Sun ji	6/11/18 1:55:00 PM

Font: 9 pt, English (US)

Page 31: [411] Formatted	Sun ji	6/11/18 1:55:00 PM

Font: 9 pt, English (US)

Page 31: [411] Formatted	Sun ji	6/11/18 1:55:00 PM

Font: 9 pt, English (US)

Page 31: [412] Formatted	Sun ji	6/11/18 1:55:00 PM

Font: 9 pt, English (US)

Page 31: [412] Formatted	Sun ji	6/11/18 1:55:00 PM

Font: 9 pt, English (US)

Page 31: [413] Formatted	Sun ji	6/11/18 1:55:00 PM

Font: 9 pt, English (US)

Page 31: [414] Formatted	Sun ji	5/15/18 10:32:00 PM

Left

Page 31: [415] Formatted	Sun ji	6/11/18 1:55:00 PM

Font: 9 pt, English (US)

Page 31: [416] Formatted	Sun ji	5/15/18 10:32:00 PM

Left

Page 31: [417] Formatted	Sun ji	6/11/18 1:55:00 PM

Font: 9 pt, English (US)

Page 31: [418] Formatted	Sun ji	6/11/18 1:55:00 PM

Font: 9 pt, English (US)

Page 31: [419] Formatted	Sun ji	5/15/18 10:32:00 PM

Left

Page 31: [420] Formatted Table	ji Sun	2/7/18 10:45:00 AM

Formatted Table

Page 31: [421] Formatted	Sun ji	6/11/18 1:55:00 PM

Font: 7.5 pt, English (US)

Page 31: [422] Formatted **Sun ji** **6/11/18 1:55:00 PM**

Font: 9 pt, English (US)

Page 31: [422] Formatted **Sun ji** **6/11/18 1:55:00 PM**

Font: 9 pt, English (US)

Page 31: [423] Formatted **Sun ji** **6/11/18 1:55:00 PM**

Font: 9 pt, English (US)

Page 31: [423] Formatted **Sun ji** **6/11/18 1:55:00 PM**

Font: 9 pt, English (US)

Page 31: [424] Formatted **Sun ji** **6/11/18 1:55:00 PM**

Font: 9 pt, English (US)

Page 31: [424] Formatted **Sun ji** **6/11/18 1:55:00 PM**

Font: 9 pt, English (US)

Page 31: [425] Formatted **Sun ji** **6/11/18 1:55:00 PM**

Font: 9 pt, English (US)

Page 31: [426] Formatted **Sun ji** **5/15/18 10:32:00 PM**

Left

Page 31: [427] Formatted **Sun ji** **6/11/18 1:55:00 PM**

Font: 9 pt, English (US)

Page 31: [428] Formatted **Sun ji** **5/15/18 10:32:00 PM**

Left

Page 31: [429] Formatted **Sun ji** **6/11/18 1:55:00 PM**

Font: 9 pt, English (US)

Page 31: [430] Formatted **Sun ji** **5/15/18 10:32:00 PM**

Left

Page 31: [431] Formatted **Sun ji** **6/11/18 1:55:00 PM**

Font: 7.5 pt, English (US)

Page 31: [432] Formatted **Sun ji** **6/11/18 1:55:00 PM**

Font: 9 pt, English (US)

Page 31: [432] Formatted **Sun ji** **6/11/18 1:55:00 PM**

Font: 9 pt, English (US)

Page 31: [433] Formatted **Sun ji** **6/11/18 1:55:00 PM**

Font: 9 pt, English (US)

Page 31: [433] Formatted **Sun ji** **6/11/18 1:55:00 PM**

Font: 9 pt, English (US)

Page 31: [434] Formatted **Sun ji** **6/11/18 1:55:00 PM**

Font: 9 pt, English (US)

Page 31: [434] Formatted **Sun ji** **6/11/18 1:55:00 PM**

Font: 9 pt, English (US)

Page 31: [435] Formatted **Sun ji** **6/11/18 1:55:00 PM**

Font: 9 pt, English (US)

Page 31: [436] Formatted **Sun ji** **5/15/18 10:32:00 PM**

Left

Page 31: [437] Formatted **Sun ji** **6/11/18 1:55:00 PM**

Font: 7.5 pt, English (US)

Page 31: [438] Formatted **Sun ji** **6/11/18 1:55:00 PM**

Font: 9 pt, English (US)

Page 31: [438] Formatted **Sun ji** **6/11/18 1:55:00 PM**

Font: 9 pt, English (US)

Page 31: [439] Formatted **Sun ji** **6/11/18 1:55:00 PM**

Font: 9 pt, English (US)

Page 31: [439] Formatted **Sun ji** **6/11/18 1:55:00 PM**

Font: 9 pt, English (US)

Page 31: [440] Formatted **Sun ji** **6/11/18 1:55:00 PM**

Font: 9 pt, English (US)

Page 31: [440] Formatted **Sun ji** **6/11/18 1:55:00 PM**

Font: 9 pt, English (US)

Page 31: [441] Formatted **Sun ji** **6/11/18 1:55:00 PM**

Font: 9 pt, English (US)

Page 31: [442] Formatted **Sun ji** **5/15/18 10:32:00 PM**

Left

Page 31: [443] Formatted **Sun ji** **6/11/18 1:55:00 PM**

Font: 9 pt, English (US)

Page 31: [443] Formatted **Sun ji** **6/11/18 1:55:00 PM**

Font: 9 pt, English (US)

Page 31: [443] Formatted **Sun ji** **6/11/18 1:55:00 PM**

Font: 9 pt, English (US)

Page 31: [444] Formatted **Sun ji** **6/11/18 1:55:00 PM**

Font: 7.5 pt, English (US)

Page 31: [445] Formatted **Sun ji** **6/11/18 1:55:00 PM**

Font: 9 pt, English (US)

Page 31: [445] Formatted **Sun ji** **6/11/18 1:55:00 PM**

Font: 9 pt, English (US)

Page 31: [446] Formatted **Sun ji** **6/11/18 1:55:00 PM**

Font: 9 pt, English (US)

Page 31: [447] Formatted **Sun ji** **6/11/18 1:55:00 PM**

Font: 7.5 pt, English (US)

Page 31: [448] Formatted **Sun ji** **6/11/18 1:55:00 PM**

Font: 9 pt, English (US)

Page 31: [448] Formatted **Sun ji** **6/11/18 1:55:00 PM**

Font: 9 pt, English (US)

Page 31: [449] Formatted **Sun ji** **6/11/18 1:55:00 PM**

Font: 6.5 pt, English (US)

Page 31: [450] Formatted **Sun ji** **6/11/18 1:55:00 PM**

Font: 10 pt, English (US)

Page 31: [451] Formatted **Sun ji** **5/15/18 10:32:00 PM**

Left

Page 31: [452] Formatted **Sun ji** **6/11/18 1:55:00 PM**

English (US)

Page 31: [453] Formatted **Sun ji** **5/25/18 2:00:00 PM**

Normal

Page 31: [454] Formatted **Sun ji** **6/11/18 1:55:00 PM**

Font: 6.5 pt, English (US)

Page 32: [455] Formatted **Sun ji** **6/11/18 1:55:00 PM**

English (US)

Page 32: [456] Formatted **Sun ji** **6/11/18 1:55:00 PM**

English (US)

Page 32: [456] Formatted **Sun ji** **6/11/18 1:55:00 PM**

English (US)

Page 32: [457] Formatted **Sun ji** **6/11/18 1:55:00 PM**

Font: 9 pt, English (US)

Page 32: [457] Formatted **Sun ji** **6/11/18 1:55:00 PM**

Font: 9 pt, English (US)

Page 32: [458] Formatted **Sun ji** **6/11/18 1:55:00 PM**

Font: 9 pt, English (US)

Page 32: [459] Formatted **Sun ji** **5/15/18 10:32:00 PM**

Left

Page 32: [460] Formatted **Sun ji** **6/11/18 1:55:00 PM**

Font: 7.5 pt, English (US)

Page 32: [461] Formatted **Sun ji** **6/11/18 1:55:00 PM**

Font: 9 pt, English (US)

Page 32: [461] Formatted **Sun ji** **6/11/18 1:55:00 PM**

Font: 9 pt, English (US)

Page 32: [462] Formatted **Sun ji** **6/11/18 1:55:00 PM**

Font: 9 pt, English (US)

Page 32: [462] Formatted **Sun ji** **6/11/18 1:55:00 PM**

Font: 9 pt, English (US)

Page 32: [463] Formatted **Sun ji** **6/11/18 1:55:00 PM**

Font: 9 pt, English (US)

Page 32: [463] Formatted **Sun ji** **6/11/18 1:55:00 PM**

Font: 9 pt, English (US)

Page 32: [464] Formatted **Sun ji** **8/2/18 4:26:00 PM**

Font: 9 pt

Page 32: [465] Formatted **Sun ji** **6/11/18 1:55:00 PM**

Font: 9 pt, English (US)

Page 32: [466] Formatted **Sun ji** **5/15/18 10:32:00 PM**

Left

Page 32: [467] Formatted **Sun ji** **6/11/18 1:55:00 PM**

Font: 7.5 pt, English (US)

Page 32: [468] Formatted **Sun ji** **6/11/18 1:55:00 PM**

Font: 9 pt, English (US)

Page 32: [468] Formatted **Sun ji** **6/11/18 1:55:00 PM**

Font: 9 pt, English (US)

Page 32: [469] Formatted **Sun ji** **6/11/18 1:55:00 PM**

Font: 9 pt, English (US)

Page 32: [469] Formatted **Sun ji** **6/11/18 1:55:00 PM**

Font: 9 pt, English (US)

Page 32: [470] Formatted **Sun ji** **6/11/18 1:55:00 PM**

Font: 9 pt, English (US)

Page 32: [470] Formatted **Sun ji** **6/11/18 1:55:00 PM**

Font: 9 pt, English (US)

Page 32: [471] Formatted **Sun ji** **6/11/18 1:55:00 PM**

Font: 9 pt, English (US)

Page 32: [471] Formatted **Sun ji** **6/11/18 1:55:00 PM**

Font: 9 pt, English (US)

Page 32: [472] Formatted **Sun ji** **6/11/18 1:55:00 PM**

Font: 9 pt, English (US)

Page 32: [472] Formatted **Sun ji** **6/11/18 1:55:00 PM**

Font: 9 pt, English (US)

Page 32: [473] Formatted **Sun ji** **6/11/18 1:55:00 PM**

Font: 9 pt, English (US)

Page 32: [473] Formatted	Sun ji	6/11/18 1:55:00 PM

Font: 9 pt, English (US)

Page 32: [474] Formatted	Sun ji	6/11/18 1:55:00 PM

Font: 9 pt, English (US)

Page 32: [474] Formatted	Sun ji	6/11/18 1:55:00 PM

Font: 9 pt, English (US)

Page 32: [475] Formatted	Sun ji	6/11/18 1:55:00 PM

Font: 9 pt, English (US)

Page 32: [475] Formatted	Sun ji	6/11/18 1:55:00 PM

Font: 9 pt, English (US)

Page 32: [476] Formatted	Sun ji	6/11/18 1:55:00 PM

Font: 9 pt, English (US)

Page 32: [476] Formatted	Sun ji	6/11/18 1:55:00 PM

Font: 9 pt, English (US)

Page 32: [477] Formatted	Sun ji	6/11/18 1:55:00 PM

Font: 9 pt, English (US)

Page 32: [477] Formatted	Sun ji	6/11/18 1:55:00 PM

Font: 9 pt, English (US)

Page 32: [478] Formatted	Sun ji	6/11/18 1:55:00 PM

Font: 9 pt, English (US)

Page 32: [478] Formatted	Sun ji	6/11/18 1:55:00 PM

Font: 9 pt, English (US)

Page 32: [479] Formatted	Sun ji	6/11/18 1:55:00 PM

Font: 9 pt, English (US)

Page 32: [479] Formatted	Sun ji	6/11/18 1:55:00 PM

Font: 9 pt, English (US)

Page 32: [480] Formatted	Sun ji	6/11/18 1:55:00 PM

Font: 9 pt, English (US)

Page 32: [480] Formatted	Sun ji	6/11/18 1:55:00 PM

Font: 9 pt, English (US)

Page 32: [481] Formatted	Sun ji	6/11/18 1:55:00 PM

Font: 9 pt, English (US)

Page 32: [481] Formatted	Sun ji	6/11/18 1:55:00 PM

Font: 9 pt, English (US)

Page 32: [482] Formatted	Sun ji	6/11/18 1:55:00 PM

Font: 9 pt, English (US)

Page 32: [482] Formatted	Sun ji	6/11/18 1:55:00 PM

Font: 9 pt, English (US)

Page 32: [483] Formatted	Sun ji	6/11/18 1:55:00 PM

Font: 9 pt, English (US)

Page 32: [483] Formatted	Sun ji	6/11/18 1:55:00 PM

Font: 9 pt, English (US)

Page 32: [484] Formatted	Sun ji	6/11/18 1:55:00 PM

Font: 9 pt, English (US)

Page 32: [484] Formatted	Sun ji	6/11/18 1:55:00 PM

Font: 9 pt, English (US)

Page 32: [485] Formatted	Sun ji	6/11/18 1:55:00 PM

Font: 9 pt, English (US)

Page 32: [485] Formatted	Sun ji	6/11/18 1:55:00 PM

Font: 9 pt, English (US)

Page 32: [486] Formatted	Sun ji	6/11/18 1:55:00 PM

Font: 9 pt, English (US)

Page 32: [486] Formatted	Sun ji	6/11/18 1:55:00 PM

Font: 9 pt, English (US)

Page 32: [487] Formatted	Sun ji	6/11/18 1:55:00 PM

Font: 9 pt, English (US)

Page 32: [487] Formatted	Sun ji	6/11/18 1:55:00 PM

Font: 9 pt, English (US)

Page 32: [488] Formatted	Sun ji	6/11/18 1:55:00 PM

Font: 9 pt, English (US)

Page 32: [489] Formatted **Sun ji** **5/15/18 10:32:00 PM**

Left

Page 32: [490] Formatted **Sun ji** **6/11/18 1:55:00 PM**

Font: 7.5 pt, English (US)

Page 32: [491] Formatted **Sun ji** **6/11/18 1:55:00 PM**

Font: 9 pt, English (US)

Page 32: [491] Formatted **Sun ji** **6/11/18 1:55:00 PM**

Font: 9 pt, English (US)

Page 32: [492] Formatted **Sun ji** **6/11/18 1:55:00 PM**

Font: 9 pt, English (US)

Page 32: [492] Formatted **Sun ji** **6/11/18 1:55:00 PM**

Font: 9 pt, English (US)

Page 32: [493] Formatted **Sun ji** **6/11/18 1:55:00 PM**

Font: 9 pt, English (US)

Page 32: [493] Formatted **Sun ji** **6/11/18 1:55:00 PM**

Font: 9 pt, English (US)

Page 32: [494] Formatted **Sun ji** **6/11/18 1:55:00 PM**

Font: 9 pt, English (US)

Page 32: [494] Formatted **Sun ji** **6/11/18 1:55:00 PM**

Font: 9 pt, English (US)

Page 32: [495] Formatted **Sun ji** **6/11/18 1:55:00 PM**

Font: 9 pt, English (US)

Page 32: [495] Formatted **Sun ji** **6/11/18 1:55:00 PM**

Font: 9 pt, English (US)

Page 32: [496] Formatted **Sun ji** **6/11/18 1:55:00 PM**

Font: 9 pt, English (US)

Page 32: [496] Formatted **Sun ji** **6/11/18 1:55:00 PM**

Font: 9 pt, English (US)

Page 32: [497] Formatted **Sun ji** **6/11/18 1:55:00 PM**

Font: 9 pt, English (US)

Page 32: [497] Formatted **Sun ji** **6/11/18 1:55:00 PM**

Font: 9 pt, English (US)

Page 32: [498] Formatted **Sun ji** **6/11/18 1:55:00 PM**

Font: 9 pt, English (US), Not Superscript/ Subscript

Page 32: [499] Formatted **Sun ji** **6/11/18 1:55:00 PM**

English (US)

Page 32: [500] Formatted **Sun ji** **6/11/18 1:55:00 PM**

English (US)

Page 32: [501] Formatted **Sun ji** **6/11/18 1:55:00 PM**

English (US)

Page 32: [502] Formatted **Sun ji** **6/11/18 1:55:00 PM**

English (US)

Page 32: [503] Formatted **Sun ji** **6/11/18 1:55:00 PM**

English (US)

Page 32: [504] Formatted **Sun ji** **6/11/18 1:55:00 PM**

English (US)

Page 32: [505] Formatted **Sun ji** **6/11/18 1:55:00 PM**

Font: 9 pt, English (US)

Page 32: [506] Formatted **Sun ji** **5/15/18 10:32:00 PM**

Left

Page 32: [507] Formatted **Sun ji** **6/11/18 1:55:00 PM**

Font: 7.5 pt, English (US)

Page 32: [508] Formatted **Sun ji** **6/11/18 1:55:00 PM**

Font: 9 pt, English (US)

Page 32: [508] Formatted **Sun ji** **6/11/18 1:55:00 PM**

Font: 9 pt, English (US)

Page 32: [509] Formatted **Sun ji** **6/11/18 1:55:00 PM**

Font: 9 pt, English (US)

Page 32: [509] Formatted **Sun ji** **6/11/18 1:55:00 PM**

Font: 9 pt, English (US)

Page 32: [510] Formatted	Sun ji	6/11/18 1:55:00 PM

Font: 9 pt, English (US)

Page 32: [510] Formatted	Sun ji	6/11/18 1:55:00 PM

Font: 9 pt, English (US)

Page 32: [511] Formatted	Sun ji	6/11/18 1:55:00 PM

Font: 9 pt, English (US)

Page 32: [511] Formatted	Sun ji	6/11/18 1:55:00 PM

Font: 9 pt, English (US)

Page 32: [512] Formatted	Sun ji	6/11/18 1:55:00 PM

Font: 9 pt, English (US)

Page 32: [512] Formatted	Sun ji	6/11/18 1:55:00 PM

Font: 9 pt, English (US)

Page 32: [513] Formatted	Sun ji	6/11/18 1:55:00 PM

Font: 9 pt, English (US)

Page 32: [513] Formatted	Sun ji	6/11/18 1:55:00 PM

Font: 9 pt, English (US)

Page 32: [514] Formatted	Sun ji	6/11/18 1:55:00 PM

Font: 9 pt, English (US)

Page 32: [514] Formatted	Sun ji	6/11/18 1:55:00 PM

Font: 9 pt, English (US)

Page 32: [515] Formatted	Sun ji	6/11/18 1:55:00 PM

Font: 9 pt, English (US)

Page 32: [515] Formatted	Sun ji	6/11/18 1:55:00 PM

Font: 9 pt, English (US)

Page 32: [516] Formatted	Sun ji	6/11/18 1:55:00 PM

Font: 9 pt, English (US)

Page 32: [516] Formatted	Sun ji	6/11/18 1:55:00 PM

Font: 9 pt, English (US)

Page 32: [517] Formatted	Sun ji	6/11/18 1:55:00 PM

Font: 9 pt, English (US)

Page 32: [517] Formatted	Sun ji	6/11/18 1:55:00 PM

Font: 9 pt, English (US)

Page 32: [518] Formatted	Sun ji	6/11/18 1:55:00 PM

Font: 9 pt, English (US)

Page 32: [518] Formatted	Sun ji	6/11/18 1:55:00 PM

Font: 9 pt, English (US)

Page 32: [519] Formatted	Sun ji	6/11/18 1:55:00 PM

Font: 9 pt, English (US)

Page 32: [519] Formatted	Sun ji	6/11/18 1:55:00 PM

Font: 9 pt, English (US)

Page 32: [520] Formatted	Sun ji	6/11/18 1:55:00 PM

Font: 9 pt, English (US)

Page 32: [520] Formatted	Sun ji	6/11/18 1:55:00 PM

Font: 9 pt, English (US)

Page 32: [521] Formatted	Sun ji	6/11/18 1:55:00 PM

Font: 9 pt, English (US)

Page 32: [521] Formatted	Sun ji	6/11/18 1:55:00 PM

Font: 9 pt, English (US)

Page 32: [522] Formatted	Sun ji	6/11/18 1:55:00 PM

Font: 9 pt, English (US)

Page 32: [522] Formatted	Sun ji	6/11/18 1:55:00 PM

Font: 9 pt, English (US)

Page 32: [523] Formatted	Sun ji	6/11/18 1:55:00 PM

English (US)

Page 32: [524] Formatted	Sun ji	5/15/18 10:32:00 PM

Left

Page 32: [525] Formatted	Sun ji	6/11/18 1:50:00 PM

Justified